BOUNDARY INTEGRAL EQUATION METHODS

FOR PROBLEMS IN NON-LINEAR MAGNETOSTATICS

by

JANET LOINES

A thesis submitted for the degree of
Doctor of Philosophy
of the University of London
and
Diploma of Membership of the Imperial College

Numerical Analysis Section
Department of Mathematics
Imperial College of Science & Technology
London SW7

October 1984

Nil desperandum.

Motto of House Seven,
Christ's Hospital Girls' School
Hertford.

TO THE MEN IN MY LIFE:

Mike 'The Boss' Bernal

Charlie Elliott

John Barrett

Dan Moore

Jeff Cash

Ken Pitman

Frank Warren

Ian Walton

Neil Readwin

Thomas Sippel-Dau

Mike Nock

Graham Dipple

Tom Goldrick

Geoff Reason

Reg Perera

.....

ABSTRACT

The major part of this thesis concerns a problem which was presented at a meeting of the University Consortium for Industrial Numerical Analysis. The objective is to determine the screening effect of a thin plate of non-linear magnetic material when the source field is due to a powerful electromagnet, of the kind used in scanning equipment in hospitals.

The problem is formulated as a non-linear integral equation in the scalar magnetic potential, ψ, and the susceptibility, χ, in the plate. Using finite element techniques and collocation one obtains a system of non-linear algebraic equations for the unknown values of ψ and χ at the nodes. The calculation involves the evaluation of integrals over the surface and/or volume elements describing the plate. The calculation of these integrals by an analytic method has proved unsatisfactory due to the thinness of the plate, and to overcome this difficulty a scheme combining analytic and quadrature techniques has been devised. The resulting system of non-linear equations is solved by the Powell hybrid method; a scheme for calculating an initial approximation to the Jacobian which exploits the structure of the system is presented.

The symmetries occurring in the problem are fully exploited. In addition, a non-standard assembly process is used which ensures that integrals are not repeatedly calculated.

The results of these calculations are discussed.

The final chapter of this thesis concerns an application of the boundary integral equation method to a moving boundary problem arising from a study of percolation in gently sloping beaches.

ACKNOWLEDGEMENTS

I would like to thank my supervisor, Dr. M.J.M. Bernal, for his help, encouragement and, above all, his unfailing good humour throughout the preparation of this thesis. The problem discussed in Chapter 5 was suggested by Dr. C.M. Elliott and I would like to thank him for his help on this topic. (My only regret is that I did not get sent on a field trip to investigate 'percolation in gently sloping beaches'.)

A BIG thankyou is due to the lads at the Imperial College Program Advisory - Thomas Sippel-Dau, Mike Nock, Graham Dipple and Tom Goldrick - who have helped with my numerous computational problems. There were times when I believed that Thomas purposely took his tea breaks when I walked into the Advisory Office; however, it did not take me long to learn the way to the tea room....

Of my friends in the department I would particularly like to thank Neil Readwin, whose advice on programming and use/abuse of the CDC Cyber 855, Amdahl 470V/8 and Cray 1-S computers has been invaluable.

I am grateful to Mrs. H. Hodgson for her excellent typing.

Finally, the financial support of the Science and Engineering Research Council is gratefully acknowledged.

CONTENTS

Page

CHAPTER 1: INTRODUCTION AND OUTLINE OF THESIS

1.1 The University Consortium for Industrial Numerical Analysis 8

1.2 Description of the Problem 8

1.3 Outline of Thesis 9

1.4 The Rationalized mks System of Units 11

CHAPTER 2: AN INTEGRAL EQUATION FORMULATION

2.1 Magnetic Scanners 13

2.2 Statement of the Problem 14

2.3 Fundamental Equations of Magnetostatics 17

2.4 Differential and Integral Operators 19

2.5 Choice of Potential 20

2.6 Integral Equation Formulations 21

2.7 χ-H Relation 30

2.8 Mathematical Model 31

CHAPTER 3: NUMERICAL SOLUTION OF THE INTEGRAL EQUATION

3.1 Discretization and Choice of Shape Functions 33

3.2 Solution Methods 37

3.3 Discretized Integral Equation 39

3.4 Complete System of Equations 42

3.5 Solution of the Non-linear System 43

3.6 Evaluation of the Integrals 46

3.7 Calculation of the Source Potential 52

3.8 Recovery of Fields 56

3.9 Evaluation of the Field Integral Equation 58

Page

3.10 Economy 60

3.11 Some Computational Aspects 65

3.12 Approximation of the Jacobian 67

Appendix A.3: Evaluation of the Volume Integrals by Analytic and Quadrature Techniques 72

CHAPTER 4: RESULTS AND CONCLUDING REMARKS

4.1 (ψ,χ) Calculation 79

4.2 Recovery of Fields 89

4.3 Conclusion 94

CHAPTER 5: PERCOLATION IN GENTLY SLOPING BEACHES

5.1 Introduction 99

5.2 The Model Problem 99

5.3 An Asymptotic Formulation 100

5.4 An Explicit Scheme 102

5.5 The Boundary Integral Equation 103

5.6 Discretization and Solution Methods 107

5.7 Choice of Approximating Functions 110

5.8 Final System of Equations 111

5.9 Evaluation of the Integrals 112

5.10 Time-Stepping Algorithm 115

5.11 Results 116

5.12 Conclusion 116

Appendix A.5: Derivation of Green's 3rd Identity 119

REFERENCES 120

CHAPTER 1: INTRODUCTION AND OUTLINE OF THESIS

1.1 The University Consortium for Industrial Numerical Analysis

The major part of this thesis concerns a problem which was presented at a meeting of the University Consortium for Industrial Numerical Analysis (UCINA) in May 1982. UCINA was set up in 1979, originally with SERC support and now Department of Industry support,

(i) to make available to industry and government research laboratories and similar organizations the expertise in numerical analysis which exists within the universities;

(ii) to bring industrial problems to the attention of university staff and research students working in the area of numerical analysis and to encourage direct contacts with industry in their research programmes.

The numerical analysis groups participating in the Consortium are those from Bath, Brunel, Imperial College, Reading and Oxford, together with numerical analysts from the National Physical Laboratory. Each year the Consortium has held well-attended symposia at which applied mathematicians and engineers from industry present problems to which they seek practical (usually numerical) solutions.

1.2 Description of the Problem

The problem discussed in this thesis relates to the shielding of magnetic scanning equipment in hospitals. A magnetic scanner

is essentially just a large electromagnet, and although the field is generally thought to be harmless to both patient and observer, it could nevertheless stop a mechanical wrist watch or, more seriously, affect an observer's pacemaker. It was therefore decided to see whether some sort of metal screening was possible, which would reduce the field in the room above, say, to a given tolerance. This is not only an expensive solution; it may be unfeasible if the metal plate is too heavy for the existing structure, in which case a special room would have to be constructed.

An integral equation method was proposed for the solution of this problem and so it was of particular interest to us because of our related work on two- and three-dimensional boundary integral equation methods. Of course, although the major part of this thesis is orientated towards the solution of a particular problem, the numerical techniques discussed could be applied to a wide range of linear and non-linear problems both in magnetostatics and in other areas of applied mathematics.

1.3 Outline of Thesis

In the next chapter we give a formal description of the magnetic screening problem. Two- and three-dimensional linear and non-linear problems in magnetostatics have been studied by many authors (for example, Simkin and Trowbridge [1976], [1979], [1980]) and both differential and integral operator formulations have been considered; a brief discussion on the relative advantages and disadvantages of the two approaches is given.

A summary of the various choices of dependent variable is given in the paper by Simkin and Trowbridge [1979]. We show how the magnetic screening problem can be formulated as a non-linear integral equation for the total scalar potential ψ, whose gradient represents the total field. Three possible formulations of the integral equation are derived, and we conclude Chapter 2 by presenting our mathematical model for the magnetic screening problem.

In Chapter 3 the numerical solution techniques for the problem are discussed. The plate is discretized into a regular grid of elements and finite element approximations are chosen for the unknowns in the usual way. Substituting the finite element approximations into the integral equation and collocating gives rise to a system of non-linear algebraic equations for which we have investigated two possible solution methods. The first is based on a simple iterative scheme, proposed by Armstrong et al. [1978]. This worked well for coarse grids, but its performance deteriorated as the mesh was refined. This led us to consider an alternative non-linear solver, the Powell hybrid method [1970]. For this method an initial approximation to the Jacobian is required, which at first sight would appear to be very expensive computationally. We show how the structure of the system can be exploited to reduce this cost.

Much of the success of the boundary integral equation method depends, in our case, on the evaluation of integrals over volume elements (and thus, strictly, the term 'boundary' should not be used to describe the method). We have devised an integration scheme which uses a combination of analytic and quadrature techniques

to overcome difficulties induced by the thinness of the plate.

The fact that we have chosen to work with a regular grid allows us to make further economies. If a standard finite element assembly process was used, many of the integrals would be repeatedly calculated; to avoid this we have proposed a non-standard assembly structure. Furthermore, the integrals themselves are independent of the iterations of the non-linear solver. Hence, by the use of a FORTRAN direct access file the integrals can be calculated once and for all before the non-linear solver is called.

In Chapter 4 the results of these calculations are discussed.

In the final chapter of this thesis we consider a moving boundary problem relating to a study of percolation in gently sloping beaches. An asymptotic formulation of this problem is given in the paper by Aitchison, Elliott and Ockendon [1983]. We show how this problem may be solved using the boundary integral equation method and compare our results with those obtained by Aitchison, Elliott and Ockendon using the finite element method. We have used an explicit time-stepping algorithm for this problem; a stability criterion for this scheme, which has been determined by experiment, is given.

1.4 The Rationalized mks System of Units

Considerable confusion can arise in magnetostatic problems over the system of units adopted - cgs, Gaussian or mks. For a brief history of the development of these systems the reader is referred to Chapter 1 of the book by Pugh and Pugh [1970].

In this thesis we have used rationalized mks units throughout. The magnetostatic quantities we shall encounter and the corresponding units are given in Table 1.1. In addition, the permeability of free space, μ_0, is defined in the mks system as

$$\mu_0 = 4\pi \times 10^{-7} \text{ Hm}^{-1} \quad \text{(or wb/Am)}$$

Physical quantity	Symbol	Unit
Magnetic induction	$\underline{B}$	T (Tesla)
Magnetic field	$\underline{H}$	Am^{-1}
Magnetization	$\underline{M}$	Am^{-1}
Magnetostatic scalar potential	φ or ψ	A

Table 1.1: Magnetostatic quantities and corresponding mks units.

Validity of our results

The checks which we carried out on our calculations are not reported in this thesis. Nevertheless, extensive checks were made at all stages of the computation, for example:

(i) isoparametrics were originally built into the program to enable the numerical results to be compared with analytic solutions for linear problems (hollow or solid spheres in a uniform magnetic field);

(ii) the integration formulae we derived were checked against very high order Gaussian quadrature;

(iii) the source field was checked against the analytic solution at the magnet centre;

(iv) the program incorporating symmetry was checked against a version in which symmetry was not taken into account.

CHAPTER 2: AN INTEGRAL EQUATION FORMULATION

2.1 Magnetic Scanners

An article on magnetic scanners appeared in the Sunday Times magazine on June 19th 1983; in the following brief description of a magnetic scanner we refer essentially to that article.

The magnetic scanner is a relatively new British diagnostic instrument which is able to recognise disease in internal organs. Unlike the conventional X-ray scanner, the magnetic scanner causes no known side effects to either patient or observer.

The idea behind the magnetic scanner is based on a process called nuclear magnetic resonance (NMR) spectroscopy. The scanner is essentially just a large electromagnet. The patient lies inside the coils of the magnet and the scanner operates by switching the magnet on and off and recording the electromagnetic (e.m.) signals which emerge. The e.m. signals come from the hydrogen atoms which are present in all organs of the body (each organ is approximately 75% water). The nucleus of each hydrogen atom is a tiny magnet, and in the absence of a magnetic field these magnets point in random directions. When the electromagnet is turned on, the nuclei align. When it is switched off, the nuclei begin to move in different directions, and as they do so, each one emits a radio signal. Although the nuclei are identical the signals are not, since the nature of these signals depends on the position of the atom in the coil and on surrounding atoms. The e.m. signals are analysed by computer and sophisticated graphics enable a map of the organs to be produced. Since diseased organs emit different e.m. signals

from healthy organs, these differences show up clearly on the map.

Perhaps the greatest advantage of magnetic scanners is that all organs can be analysed, and thus tumours and dead patches on the brain, for example, can be detected without the introduction of a 'contrast medium' which is often needed by more conventional X-ray or brain scanners.

2.2 Statement of the Problem

The following "simple" problem will be considered:

The electromagnet consists of three solenoid sections which are aligned with the x-axis, the origin being taken at the magnet centre. The details of the magnet geometry are shown in figure 2.1. This configuration produces a magnetic intensity of 1.9 Tesla at the origin.

For simplicity the screen is chosen to be rectangular, approximately 10 metres square and of thickness h. It is placed at a distance of H metres from the magnet centre, parallel to the xy-plane (z = 0 plane). [See figure 2.2.]

The problem is to determine the minimum thickness h of the screen which will reduce the field beyond the plate to less than a given tolerance. As an initial 'guess' we took h = .01 metre.

In the next section we recall the fundamental equations of magnetostatics and then in the remainder of this chapter we discuss the mathematical formulation of the magnetic screening problem.

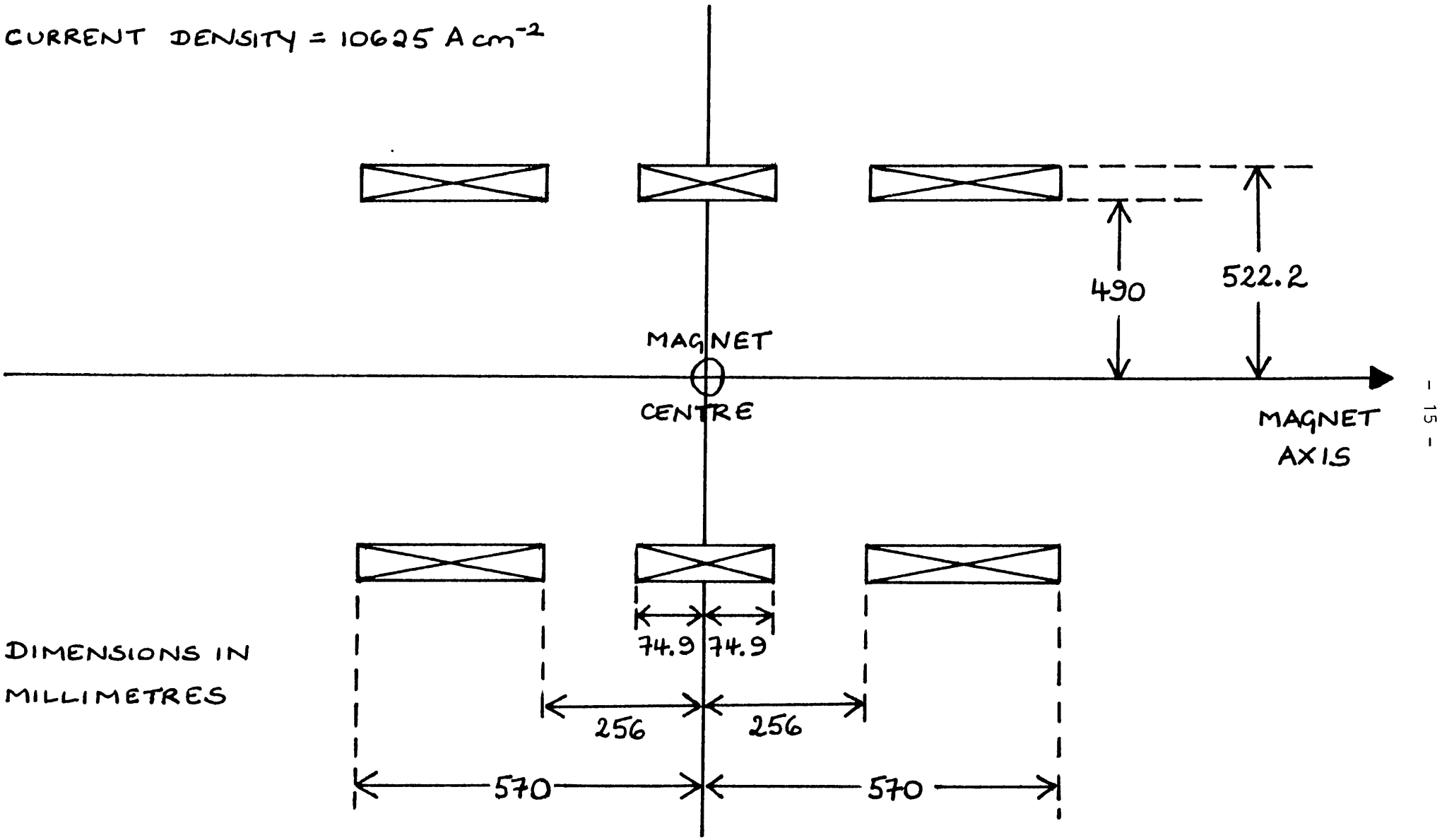


Fig. 2.1. Details of the magnet geometry (not to scale).

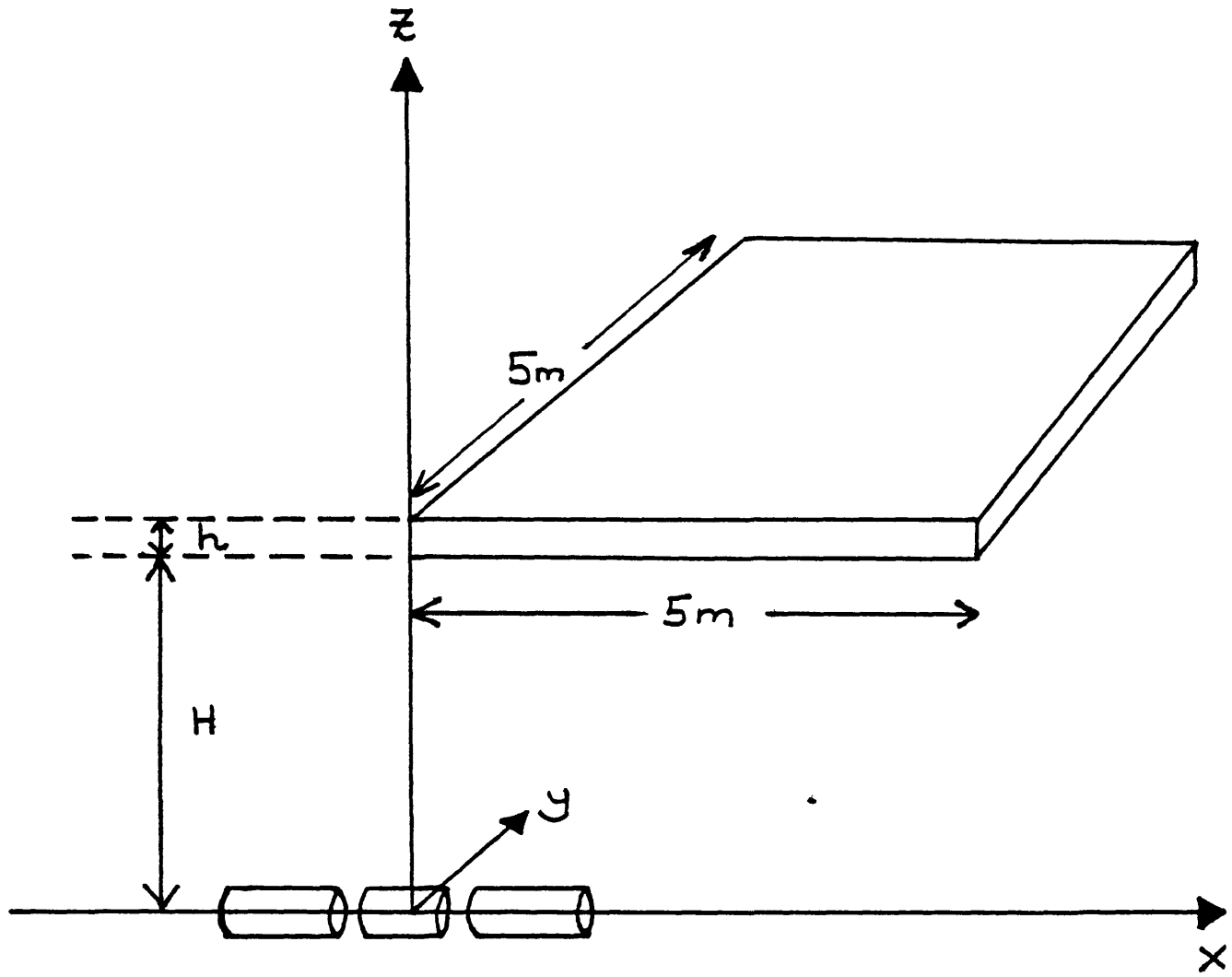


Fig. 2.2. Geometry of the problem (not to scale).

One quarter of the plate is shown; the plate is symmetric about x = 0 and y = 0.

2.3 Fundamental Equations of Magnetostatics

In magnetostatics the following vector fields are considered:

$\underline{B}$ magnetic induction

$\underline{H}$ magnetic field

$\underline{J}$ current density

$\underline{M}$ magnetization.

These vectors are functions of the point $\underline{r}$ in space only. In differential form the vectors satisfy

$$\text{curl } \underline{H} = \underline{J} \tag{2.3.1}$$

and

$$\nabla.\underline{B} = 0 \tag{2.3.2}$$

which form part of the set known as Maxwell's equations. (For a full discussion of Maxwell's equations see, for example, Reitz and Milford [1967] or Graffi [1980].) Furthermore, there are interface conditions between regions of different magnetic media, namely

$$[\underline{H}_t] = \underline{0}$$

$$[\underline{B}.\underline{n}] = 0.$$

Here we have used the notation $[\underline{u}_t]$ and $[\underline{u}.\underline{n}]$ to denote the discontinuity across the interface of the tangential and normal components

of a vector $\underline{u}$, with

$$[\underline{u}.\underline{n}] = [\underline{u}].\underline{n}$$

and

$$[\underline{u}_t] = [\underline{u}] - [\underline{u}.\underline{n}]\underline{n},$$

$\underline{n}$ being the unit normal vector.

In addition to the Maxwell equations and the interface conditions we also need a relationship between $\underline{B}$, $\underline{H}$ and $\underline{M}$. This is provided by the constitutive equations

$$\underline{B} = \mu\underline{H} = \mu_0(\underline{M} + \underline{H}) \tag{2.3.3}$$

and

$$\underline{M} = \chi\underline{H}, \tag{2.3.4}$$

where μ_0 is the permeability of free space and μ and χ are the permeability and susceptibility respectively of the magnetic material. From these equations we see that the relation between μ and χ is given by

$$\mu = \mu_0(1 + \chi).$$

We remark that in isotropic media μ and χ are scalar quantities, while in anisotropic media they are tensors of rank two. The relation between $\underline{M}$ and $\underline{H}$ depends on the nature of the material and is usually determined by experiment. In a large class of materials there exists an approximately linear relationship between $\underline{M}$ and $\underline{H}$, so

that μ and χ are constant. However, in this thesis we consider only ferromagnetic materials, which are not linear, and hence if we assume that hysteresis effects are neglected (so that μ is a single-valued function of $|\underline{H}|$) we have

$$\mu = \mu(H),$$

$$\chi = \chi(H),$$

where $H = |\underline{H}|$.

2.4 Differential and Integral Operators

Both differential and integral equation formulations have been used to solve 3-dimensional problems in magnetostatics (see, for example, Armstrong et al. [1975], [1978], Simkin and Trowbridge [1979], [1980]) and the question of which formulation to choose is not easy to answer. Integral operator formulations offer many advantages - for example:

(i) only the iron and coils need to be specified, with a mesh defined in the iron region only;

(ii) the external far field boundary condition is automatically taken into account by the formulation;

(iii) the jump condition across an interface is automatically satisfied.

However, there are also disadvantages. It is well known that integral equation methods lead, in general, to full, unsymmetric matrices

which are not only expensive to compute but also to solve. In comparison, differential (finite element or finite difference) methods yield sparse, symmetric matrices for which special solution techniques are available.

There is a third alternative, and that is the coupling of differential and integral operator techniques which is reported in the paper by Zienkiewicz et al. [1977], for example. In this method the differential operator is used for non-linear iron regions and the integral operator for external regions.

At the time of writing there seems to be no overriding reason for favouring one method over another. As more practical experience and theoretical understanding of the various methods is obtained one can hope that a clear case for choosing one method rather than another will emerge. It would certainly not be surprising if the choice of 'best' method was both problem- and computer-dependent. It is hoped that the work reported in this thesis, on an integral equation formulation, will contribute to a future assessment of the relative merits of the various methods.

2.5 Choice of Potential

In any numerical scheme the choice of dependent variable is important. A good discussion on the choice of potential is given in the paper by Simkin and Trowbridge [1979], where they also present comparative results for some 2-dimensional problems.

The Rutherford Laboratory package GFUN uses an integral equation in terms of the unknown magnetization $\underline{M}$ (see Trowbridge [1976],

Armstrong et al. [1975], for example). Another choice of dependent variable is the vector potential. However, the disadvantage of these methods in 3-dimensions is that there are, of course, three unknowns per element node. Thus a scalar potential is preferred for reasons of economy. The choice is then between formulations involving the reduced scalar potential, whose gradient is defined to be the field due to the induced magnetization, or formulations involving both the reduced and the total scalar potentials.

Simkin and Trowbridge [1979] have noted that using the reduced scalar potential alone gives low accuracy in the permeable regions. This is caused by cancellation between the known source field and the calculated potential field. It is therefore preferable to work in terms of a scalar potential which represents the total field, since in this way the difference quantity is calculated directly.

2.6 Integral Equation Formulation

Suppose the current density $\underline{J}$ of the source is known and occupies a region of the problem space Ω_J. Then from the Biot-Savart Law the field due to the source, $\underline{H}_s$, may be expressed in integral form as

$$\underline{H}_s(\underline{r}) = \frac{1}{4\pi} \int_{\Omega_J} \underline{J}(\underline{r}') \wedge \nabla\left(\frac{1}{R'}\right) \, d\,\Omega_{\underline{r}'} \, , \tag{2.6.1}$$

$$R' = |\underline{r}' - \underline{r}| .$$

The derivation of this result is given, for example, in Stratton [1941] or Reitz and Milford [1967]. Taking the curl of equation

(2.6.1) gives

$$\text{curl } \underline{H}_S = \underline{J} \ . \tag{2.6.2}$$

If we now write the total field $\underline{H}$ as the sum of the field due to the source and the field due to the induced magnetization $\underline{H}_M$, i.e.

$$\underline{H} = \underline{H}_M + \underline{H}_S \tag{2.6.3}$$

then this together with Maxwell's equation curl $\underline{H} = \underline{J}$ implies that

$$\text{curl } \underline{H}_M = \underline{0} \quad \text{everywhere.}$$

Therefore, $\underline{H}_M$ can be represented as the gradient of a scalar potential,

$$\underline{H}_M = - \nabla\varphi \ , \tag{2.6.4}$$

where φ is called the reduced scalar potential. It can be shown (Reitz and Milford, pp. 187-189, for example) that φ can be expressed in integral form as

$$\varphi(\underline{r}) = \frac{1}{4\pi} \int_{\Omega} \underline{M}(\underline{r}') \cdot \nabla\left(\frac{1}{R'}\right) \, d\Omega_{\underline{r}'}$$

where Ω is the region containing the magnetic material and $R' = |\underline{r}' - \underline{r}|$ is the distance from the source point $\underline{r}'$ to the field point $\underline{r}$.
It should be noted that the external boundary condition

$$\varphi(\underline{r}) \to 0 \quad \text{as } \underline{r} \to \infty$$

is automatically satisfied by this integral expression for φ.

In the region external to the current sources, which we shall denote by Ω_c,

$$\text{curl } \underline{H}_s = \underline{0}$$

and thus, provided Ω_c is simply connected, $\underline{H}_s$ can also be represented as the gradient of a scalar potential, i.e.

$$\underline{H}_s = - \nabla\psi_s \quad \text{in } \Omega_c. \tag{2.6.5}$$

The region Ω_c can always be made simply connected by the introduction of suitable 'cuts'. There are, of course, an infinite number of ways in which these imaginary cuts might be placed, but for our purpose it is simplest to think of them as surfaces spanning the cross-section of each solenoid.

The total field $\underline{H}$ can also be represented as the gradient of a scalar potential in the current-free regions, and hence

$$\underline{H} = - \nabla\psi \quad \text{in } \Omega_c. \tag{2.6.6}$$

ψ is called the total scalar potential.

Thus, from equations (2.6.3) - (2.6.6) we have

$$\psi = \varphi + \psi_s + \text{constant},$$

where for convenience we choose the constant to be zero, so that

$$\psi = \varphi + \psi_s . \tag{2.6.7}$$

Summary

In the iron region Ω, which is current free and has permeability $\mu(H)$, we have

$$\underline{H} = - \nabla\psi$$

and therefore

$$\underline{B} = \mu(H)\underline{H} = - \mu(H)\nabla\psi .$$

In free space,

$$\underline{H} = \underline{H}_S + \underline{H}_M = \underline{H}_S - \nabla\varphi$$

and

$$\underline{B} = \mu_0\underline{H} = \mu_0(\underline{H}_S - \nabla\varphi) .$$

If we now apply Maxwell's equation $\nabla.\underline{B} = 0$ to these equations, then we see that the governing partial differential equations are

$$\left.\begin{aligned} \nabla.(- \mu(H)\nabla\psi) &= 0 \quad \text{in } \Omega \\ \nabla^2\varphi &= 0 \quad \text{in free space.} \end{aligned}\right\}$$

Formulation I

Substituting the integral expression for φ into equation (2.6.7) gives

$$\psi(\underline{r}) = \frac{1}{4\pi}\int_{\Omega} \underline{M}(\underline{r}').\nabla(\frac{1}{R'})\, d\Omega_{\underline{r}'} + \psi_s(\underline{r}),$$

$$R' = |\underline{r}' - \underline{r}|, \ \underline{r} \in \Omega_c \qquad (2.6.8)$$

and since

$$\underline{M}(\underline{r}) = \chi(H)\underline{H}(\underline{r}) = -\chi(H)\nabla\psi(\underline{r}), \quad H = |\underline{H}(\underline{r})|$$

this gives immediately

$$\psi(\underline{r}) = -\frac{1}{4\pi}\int_{\Omega} \chi(H(\underline{r}'))\nabla\psi(\underline{r}').\nabla(\frac{1}{R'})\, d\Omega_{\underline{r}'} + \psi_s(\underline{r}). \qquad (I)$$

This integral equation for ψ has no boundary conditions, since they have already been taken into account, and hence it can be solved by numerical techniques by discretizing the iron region Ω. If ψ^* is the restriction of ψ to Ω, then if one can compute the solution of the integral equation for ψ^*, namely

$$\psi^*(\underline{r}) = -\frac{1}{4\pi}\int_{\Omega} \chi(H(\underline{r}'))\nabla\psi^*(\underline{r}').\nabla(\frac{1}{R'})\, d\Omega_{\underline{r}'} + \psi_s(\underline{r}), \quad \underline{r} \in \Omega.$$

(where $H(\underline{r}') = |-\nabla\psi^*(\underline{r}')|$), then ψ can be computed at all points $\underline{r} \in \Omega_c$ from

$$\psi(\underline{r}) = -\frac{1}{4\pi}\int_{\Omega} \chi(H(\underline{r}'))\nabla\psi^*(\underline{r}').\nabla(\frac{1}{R'})\, d\Omega_{\underline{r}'} + \psi_s(\underline{r}),$$

$$\underline{r} \in \Omega_c. \qquad (2.6.9)$$

We have used this formulation of the integral equation for ψ in most of our calculations. However, we also mention two other possible formulations. Simkin [1982] notes that formulation I limits to a Fredholm integral equation of the first kind for high susceptibility; however, we have not experienced any ill-conditioning problems by using this formulation.

Formulation II

Returning to the integral equation (2.6.8) and using the identity

$$\nabla.(\frac{1}{R'}\,\underline{M}) = \nabla(\frac{1}{R'}).\underline{M} + \frac{1}{R'}\,\nabla.\underline{M}$$

and the divergence theorem, one can derive an integral equation for ψ in terms of the magnetization $\underline{M}$, namely

$$\psi(\underline{r}) = \frac{1}{4\pi}\int_{\partial\Omega} \frac{\underline{M}(\underline{r}').\hat{\underline{n}}(\underline{r}')}{R'}\, dS_{\underline{r}'}$$

$$-\frac{1}{4\pi}\int_{\Omega} \frac{\nabla_{\underline{r}'}.\underline{M}(\underline{r}')}{R'}\, d\Omega_{\underline{r}'} + \psi_s(\underline{r}) \qquad (II)$$

where $\partial\Omega$ is the surface of the domain Ω and $\hat{\underline{n}}(\underline{r}')$ is the outward unit normal at $\underline{r}'$. This formulation of the integral equation is discussed in the book by Silvester and Ferrari [1983].

Note

The surface integral in (II) represents the potential of a simple layer, and the volume integral is the (Newtonian) volume potential. The properties of these potentials are derived in Vladimirov [1971], for example, and from these it is possible to show, subject to certain continuity conditions on the kernels of the integrals and smoothness conditions on the surface $\partial\Omega$ of the region,

(i) $\psi(\underline{r}) \to \psi_s(\underline{r})$ as $\underline{r} \to \infty$ (i.e. $\varphi(\underline{r}) \to 0$)

(ii) ψ is continuous across an interface.

Formulation III

The integral equation formulation I involves both ψ and its gradient. By using a simple identity and applying the divergence theorem it is possible to construct an integral equation for ψ alone. Consider

$$\varphi(\underline{r}) = -\frac{1}{4\pi}\int_{\Omega} \chi(\underline{r}')\nabla\psi(\underline{r}').\nabla\left(\frac{1}{R'}\right) d\Omega_{\underline{r}'}$$

and suppose $\underline{r} \in \Omega$, $\underline{r} \notin \partial\Omega$.

We recall the definition of convergence for integrals (see, for example, Kellogg [1953]):

Definition

If the integrand $f(\underline{r})$ becomes infinite at a single point $\underline{r}^*$ of the region Ω of integration, then the integral

$$I = \int_{\Omega} f(\underline{r})\, d\Omega_{\underline{r}}$$

is said to be convergent provided

$$\lim_{\varepsilon \to 0} \int_{\Omega - \Omega_{\varepsilon}} f(\underline{r})\, d\Omega_{\underline{r}}$$

exists, where Ω_{ε} is a variable regular region such that

(i) $\underline{r}^*$ is an interior point of Ω_{ε}, and

(ii) the maximum chord of Ω_{ε} is not greater than ε.

The value of the convergent integral is defined to be this limit.

Since the integral defining $\varphi(\underline{r})$ is convergent, we may surround the field point $\underline{r}$ by a sphere Ω_{ε}, radius ε, and write

$$\varphi(\underline{r}) = \lim_{\varepsilon \to 0} -\frac{1}{4\pi} \int_{\Omega - \Omega_{\varepsilon}} \chi(\underline{r}')\nabla\psi(\underline{r}').\nabla\left(\frac{1}{R'}\right) d\Omega_{\underline{r}'} .$$

Then, by noting the identity

$$\nabla.\left(\chi\psi\nabla\left(\frac{1}{R'}\right)\right) = \chi\psi\nabla^2\left(\frac{1}{R'}\right) + \chi\nabla\psi.\nabla\left(\frac{1}{R'}\right) + \psi\nabla\chi.\nabla\left(\frac{1}{R'}\right)$$

and using the fact that

$$\nabla^2\left(\frac{1}{R'}\right) = 0 \text{ for } \underline{r} \in \Omega - \Omega_{\varepsilon}$$

we obtain

$$\varphi(\underline{r}) = \lim_{\varepsilon\to 0} \; -\frac{1}{4\pi}\int_{\Omega-\Omega_\varepsilon} \nabla.\{\chi\psi\nabla(\frac{1}{R'},)\} \; d\Omega_{\underline{r}'},$$

$$+ \lim_{\varepsilon\to 0} \; \frac{1}{4\pi}\int_{\Omega-\Omega_\varepsilon} \psi\nabla\chi.\nabla(\frac{1}{R'},) \; d\Omega_{\underline{r}'}.$$

The first integral can be transformed to a surface integral by applying the Gauss divergence theorem and hence

$$\varphi(\underline{r}) = -\chi(\underline{r})\psi(\underline{r})c(\underline{r}) - \frac{1}{4\pi}\int_{\partial\Omega}\chi(\underline{r}')\psi(\underline{r}')\nabla(\frac{1}{R'},).\hat{\underline{n}}(\underline{r}') \; dS_{\underline{r}'},$$

$$+ \frac{1}{4\pi}\int_{\Omega}\psi(\underline{r}')\nabla\chi(\underline{r}').\nabla(\frac{1}{R'},) \; d\Omega_{\underline{r}'},$$

where

$$c(\underline{r}) = \lim_{\varepsilon\to 0}\frac{1}{4\pi}\int_{\partial\Omega_\varepsilon}\nabla(\frac{1}{R'},).\hat{\underline{n}}(\underline{r}') \; dS_{\underline{r}'},$$

($\partial\Omega_\varepsilon$ is the surface of the sphere)

and $\hat{\underline{n}}(\underline{r}')$ is the outward unit normal at $\underline{r}'$. $c(\underline{r})$ may be interpreted in terms of the solid angle subtended at $\underline{r}$ by the surface $\partial\Omega_\varepsilon$.

The case $\underline{r} \in \partial\Omega$ follows in an analogous way, with the region Ω_ε defined to be the intersection of the domain Ω with a sphere of radius ε centred at $\underline{r}$. The case $\underline{r} \notin \bar{\Omega}$ is straightforward, since the integrand in (2.6.8) is never singular.

Thus we have the following integral equation for ψ, which is valid for all $\underline{r}$ in Ω_c:

$$[1 + c(\underline{r})\chi(\underline{r})]\psi(\underline{r}) = -\frac{1}{4\pi}\int_{\partial\Omega}\chi(\underline{r}')\psi(\underline{r}')\nabla(\frac{1}{R'}).\hat{\underline{n}}(\underline{r}') \; dS_{\underline{r}'},$$

$$+ \frac{1}{4\pi}\int_{\Omega}\psi(\underline{r}')\nabla\chi(\underline{r}').\nabla(\frac{1}{R'},) \; d\Omega_{\underline{r}'} + \psi_s(\underline{r}) \qquad \text{(III)}$$

It should be noted that the values taken by $c(\underline{r})$ are particularly simple when the region Ω has a smooth boundary, since then $c(\underline{r})$ takes one of only three values:

$$c(\underline{r}) = \begin{cases} 0 & \underline{r} \text{ outside } (\underline{r} \notin \bar{\Omega}) \\ \frac{1}{2} & \underline{r} \in \partial\Omega \\ 1 & \underline{r} \text{ inside } (\underline{r} \in \Omega,\ \underline{r} \notin \partial\Omega) \end{cases}$$

However, it is possible to remove all references to $c(\underline{r})$ from the numerical algorithm. The details of this are given in the next chapter.

Note

For linear problems, that is when $\chi(\underline{r})$ is constant throughout Ω, we have

$$\nabla\chi = 0$$

and hence the volume integral in (III) is zero. Therefore, formulation III is particularly suitable for linear problems, since only surface integrals have to be evaluated.

2.7 χ-H Relation

The relation between the susceptibility, χ, and the field strength, H, depends on the nature of the magnetic material and is usually determined by experiment. In this work we have used

data for low carbon mild steel, which was provided in the form of $|\underline{B}|$ v. $|\underline{H}|$ readings. Using the relation

$$\chi = \frac{1}{\mu_0} \frac{|\underline{B}|}{|\underline{H}|} - 1$$

a cubic spline interpolate of the data was obtained which enables the susceptibility to be found for any H (fig. 2.3). We shall use the notation $\bar{\chi}(H)$ to denote this interpolating function, and hence our approximation to the χ-H relation is given by

$$\chi(\underline{r}) = \bar{\chi}(H(\underline{r})), \quad H = |-\nabla\psi(\underline{r})|.$$

2.8 Mathematical Model

The problem can now be written as

$$\left.\begin{aligned} I(\psi,\chi;\underline{r}) &= 0, \quad \underline{r} \in \Omega \qquad (2.8.1) \\ \chi &= \bar{\chi}(H), \quad H = |-\nabla\psi| \qquad (2.8.2) \end{aligned}\right\}$$

where (2.8.1) is the chosen integral equation formulation and (2.8.2) is the known relation between the susceptibility and the field strength. As mentioned earlier, we have mostly used formulation I of the integral equation in this work and hence we define

$$I(\psi,\chi;\underline{r}) \equiv \psi(\underline{r}) + \frac{1}{4\pi}\int_{\Omega} \chi(\underline{r}')\nabla\psi(\underline{r}').\nabla\left(\frac{1}{R'}\right) d\Omega_{\underline{r}'} - \psi_s(\underline{r}),$$

$$R' = |\underline{r}' - \underline{r}|$$

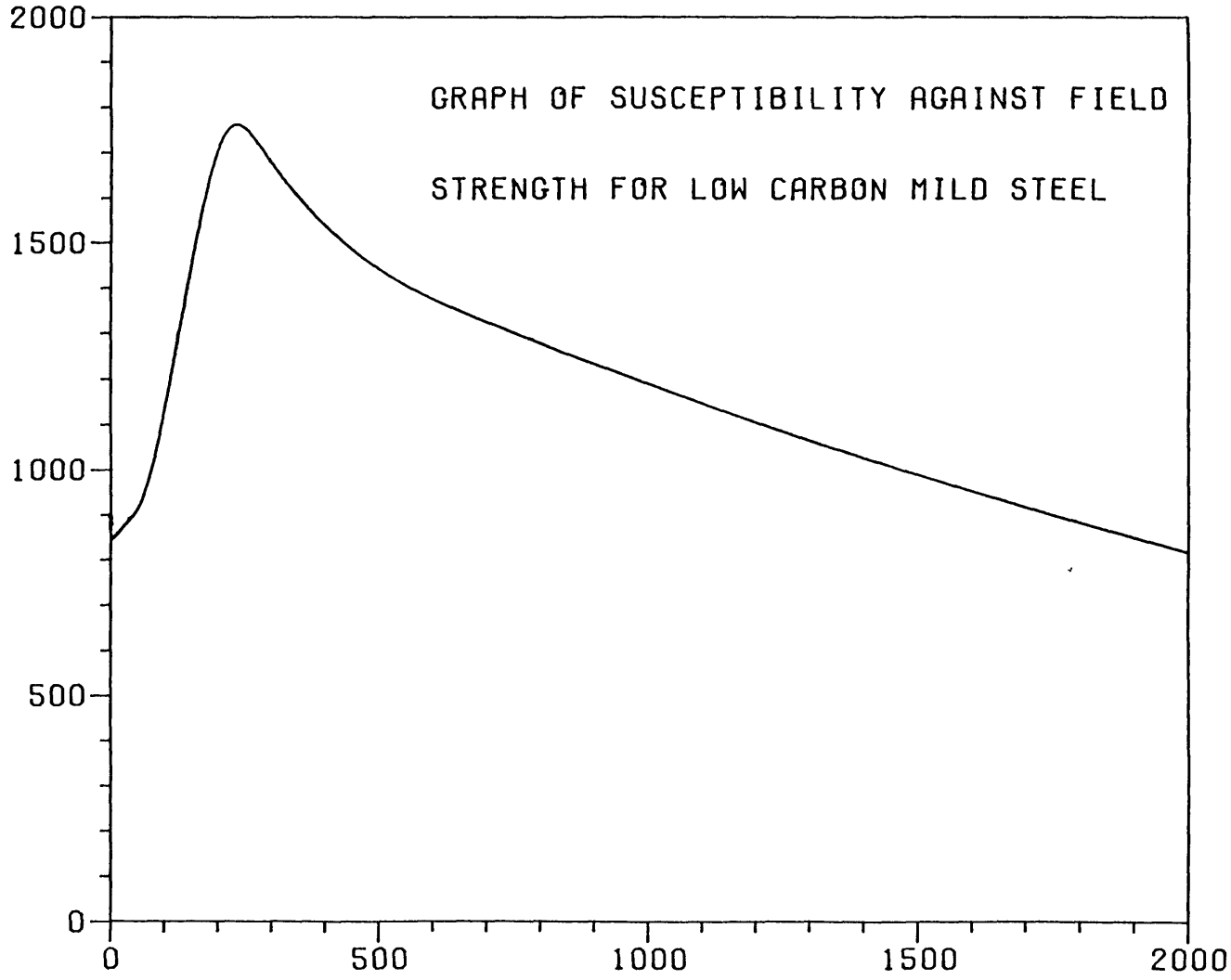


Fig. 2.3. Cubic spline interpolate of the χ-H data.

CHAPTER 3: NUMERICAL SOLUTION OF THE INTEGRAL EQUATION

3.1 Discretization and Choice of Shape Functions

In order to solve equations (2.8.1) and (2.8.2) numerically we must first divide the domain Ω into volume elements and then define finite element approximations for ψ and χ.

We have taken the rectangular brick element as our reference element, defined in the (ξ,η,ζ) coordinate system by

$$-1 \leqslant \xi,\eta,\zeta \leqslant 1.$$

If the domain Ω is subdivided into volume elements such that the sides of the elements are parallel to the coordinate planes and the nodes in a given direction (x, y or z) are equally spaced, then each volume element may be obtained by a linear transformation of the reference element. Moreover, this mapping is invertible. Thus, if the volume element e is defined by

$$e = \{(x,y,z) : a \leqslant x \leqslant b, \quad c \leqslant y \leqslant d, \quad e \leqslant z \leqslant f\}$$

then any point $\underline{r} = (x,y,z)$ of e may be written as

$$\underline{r} = (x^e(\xi,\eta,\zeta), \quad y^e(\xi,\eta,\zeta), \quad z^e(\xi,\eta,\zeta))$$

where, for example,

$$x^e(\xi,\eta,\zeta) = \left(\frac{b-a}{2}\right)\xi + \left(\frac{a+b}{2}\right) .$$

This can be written in matrix notation as

$$\underline{r} = \underline{r}^e(\underline{\xi}) = T\,\underline{\xi} + \underline{k}, \quad \underline{\xi} = (\xi,\eta,\zeta),$$

with

$$T = \frac{1}{2}\begin{bmatrix} b-a & 0 & 0 \\ 0 & d-c & 0 \\ 0 & 0 & f-e \end{bmatrix} \quad \text{and} \quad \underline{k} = \frac{1}{2}\begin{bmatrix} a+b \\ c+d \\ e+f \end{bmatrix}$$

The inverse mapping is, of course, given by

$$\underline{\xi} = \underline{\xi}^e(x,y,z) = T^{-1}(\underline{r} - \underline{k}).$$

In this work we have chosen to use quadratic (20 node) serendipity elements for ψ (see, for example, Zienkiewicz [1971]). The quadratic shape function associated with the corner node (ξ_i,η_i,ζ_i) is given by

$$Q_i(\xi,\eta,\zeta) = \frac{1}{8}(1+\bar{\xi}_i)(1+\bar{\eta}_i)(1+\bar{\zeta}_i)(\bar{\xi}_i+\bar{\eta}_i+\bar{\zeta}_i-2)$$

and a typical mid-side node ($\xi_i = 0, \eta_i = \pm 1, \zeta_i = \pm 1$) shape function is given by

$$Q_i(\xi,\eta,\zeta) = \frac{1}{4}(1-\xi^2)(1+\bar{\eta}_i)(1+\bar{\zeta}_i),$$

where

$$\bar{\xi}_i = \xi_i\xi, \quad \bar{\eta}_i = \eta_i\eta, \quad \bar{\zeta}_i = \zeta_i\zeta.$$

In the usual finite element manner the shape functions defined over a volume element can be used to generate basis functions $\{v_j\}$, such that the approximation to ψ is given by

$$\tilde{\psi}(\underline{r}) = \sum_{j=1}^{N} \psi_j v_j(\underline{r}) \qquad (3.1.1)$$

Thus, if j is the i-th node of volume element e, then

$$v_j(\underline{r}) = Q_i(\underline{\xi}^e(\underline{r})), \quad \underline{r} \in e.$$

The basis functions v_j are continuous, piece-wise polynomial and have compact support (that is, v_j is zero except on elements which contain the node j). Furthermore, they have the property that

$$v_j(\underline{r}_k) = \delta_{jk}$$

and hence

$$\tilde{\psi}(\underline{r}_k) = \sum_{j=1}^{N} \psi_j v_j(\underline{r}_k) = \psi_k.$$

The basis functions $\{\omega_k\}$ for χ may be defined in a similar way, to give

$$\tilde{\chi}(\underline{r}) = \sum_{k=1}^{M} \chi_k \omega_k(\underline{r}). \qquad (3.1.2)$$

Of course, we may choose different order approximations for ψ and χ, and hence, in general, $M \neq N$. We have mostly used linear (8 node)

serendipity elements for χ. The linear shape functions are defined by

$$L_i(\xi,\eta,\zeta) = \frac{1}{8}(1 + \bar{\xi}_i)(1 + \bar{\eta}_i)(1 + \bar{\zeta}_i)$$

where, as before,

$$\bar{\xi}_i = \xi_i\xi, \quad \bar{\eta}_i = \eta_i\eta, \quad \bar{\zeta}_i = \zeta_i\zeta.$$

In order to distinguish between the two sets of nodes, we shall use the notation $\underline{r}_j^{(\psi)}$, $1 \leq j \leq N$, and $\underline{r}_k^{(\chi)}$, $1 \leq k \leq M$, where appropriate, for the ψ and χ nodes respectively.

Note

We have considered two other possible representations of $\tilde{\chi}$:

a) $\tilde{\chi}$ is constant over each volume element (this scheme was proposed by Armstrong et al. [1978]);

b) $\tilde{\chi}$ is linear in each volume element but not continuous across inter-element boundaries.

In both these cases it is convenient to associate the χ-nodes with a (volume element, local node) pair, rather than using a global node numbering system. However, since we have used continuous linear basis functions for $\tilde{\chi}$ in most of our work, we only present the numerical details for this case.

3.2 Solution Methods

On substituting (3.1.1) and (3.1.2) into equation (2.8.1) one obtains an approximation to the integral equation of the form

$$I(\tilde{\psi},\tilde{\chi};\underline{r}) = e(\underline{r}) \tag{3.2.1}$$

where $e(\underline{r})$ is the error introduced by using $\tilde{\psi}$ and $\tilde{\chi}$ instead of the true solution ψ and χ. If we now collocate the integral equation at $\{\underline{r}_j^{(\psi)}\}$, i.e. demand that

$$e(\underline{r}_j^{(\psi)}) = 0 \qquad j = 1,2,\ldots,N$$

then we obtain N equations for the N unknowns $\{\psi_j\}$, namely

$$I(\tilde{\psi},\tilde{\chi};\underline{r}_j^{(\psi)}) = 0 \qquad j = 1,2,\ldots,N. \tag{3.2.2}$$

We need M further equations for the unknowns $\{\chi_k\}$. One idea would be to use

$$\underline{\tilde{H}}(\underline{r}) = -\nabla\tilde{\psi}(\underline{r}) \tag{3.2.3}$$

$$\chi(\underline{r}) = \bar{\chi}(|\underline{\tilde{H}}|) \tag{3.2.4}$$

to give an approximation to $\chi(\underline{r}_k^{(\chi)})$, $k = 1,2,\ldots,M$. However,

$$\nabla\tilde{\psi}(\underline{r}) = \sum_{j=1}^{N} \psi_j \nabla v_j(\underline{r})$$

is not properly defined at inter-element boundaries, since the

basis functions have discontinuous derivatives there. If we define $\underline{h}^e$ as the restriction of $\nabla\tilde{\psi}$ to volume element e, then

$$\underline{h}^e(\underline{r}) = \nabla\tilde{\psi}\big|_e = \sum_{i=1}^{20} \psi_{j(i)} \nabla_{\underline{r}} Q_i(\underline{\xi}^e(\underline{r})),$$

where j(i) is the global node corresponding to the i-th node of e, and we can define

$$h_k^e = |\underline{h}^e(\underline{r}_k^{(\chi)})|. \tag{3.2.5}$$

We have already noted that $\nabla\tilde{\psi}$ is discontinuous across element interfaces and hence equation (3.2.5) will generate as many approximations to the field at node k as there are volume elements having k as a node. To overcome this we used a simple averaging process: Define

$$H_k^{av} = \frac{1}{n} \sum_{e:k\in e} h_k^e$$

where n is the number of volume elements having k as a node, and then use the χ--H relation to obtain χ_k, i.e.

$$\chi_k = \bar{\chi}(H_k^{av}), \qquad k = 1,2,\ldots,M.$$

We also did limited experiments on an alternative averaging process, where

$$\chi_k := \frac{1}{n} \sum_{e:k\in e} \bar{\chi}(h_k^e).$$

However, this made no appreciable difference to our results. It may be worthwhile to consider other approaches for finding the M additional equations from the χ-H relation.

3.3 Discretized Integral Equation

In our calculations we have mostly used formulation I of the integral equation,

$$\psi(\underline{r}) = -\frac{1}{4\pi}\int_{\Omega}\chi(\underline{r}')\nabla\psi(\underline{r}').\nabla\left(\frac{1}{R'}\right)\,d\Omega_{\underline{r}'} + \psi_s(\underline{r}),$$

$$R' = |\underline{r}' - \underline{r}|. \qquad (3.3.1)$$

Substituting the finite element approximations for ψ and χ into equation (3.3.1) and collocating at $\underline{r}_i^{(\psi)}$, i = 1,2,...,N, gives

$$\psi_i + \frac{1}{4\pi}\sum_{j=1}^{N}\psi_j\int_{\Omega}\tilde{\chi}\nabla v_j.\nabla\left(\frac{1}{R_i'}\right)\,d\Omega_{\underline{r}'} = \psi_{s_i}, \qquad (3.3.2)$$

with the obvious notation

$$\psi_i = \psi(\underline{r}_i^{(\psi)}),$$

$$\psi_{s_i} = \psi_s(\underline{r}_i^{(\psi)}),$$

and

$$R_i' = |\underline{r}' - \underline{r}_i|.$$

We can rewrite equation (3.3.2) as

$$\psi_i + \sum_{j=1}^{N} B_{ij}^* \psi_j = \psi_{s_i} \tag{3.3.3}$$

where

$$B_{ij}^* = \frac{1}{4\pi} \int_{\Omega} \tilde{\chi} \nabla v_j . \nabla \left(\frac{1}{R_i'}\right) d\Omega_{\underline{r}'} \tag{3.3.4}$$

and this in turn can be written as

$$\sum_{j=1}^{N} B_{ij} \psi_j = \psi_{s_i}, \qquad 1 \leqslant i \leqslant N \tag{3.3.5}$$

with

$$B_{ij} = \begin{cases} B_{ij}^* & i \neq j \\ 1 + B_{ii}^* & i = j. \end{cases}$$

Calculation of the diagonal terms

Returning to the integral equation (3.3.1) we see that $\psi \equiv \psi_s \equiv 1$ provides an exact solution of this equation. Thus, by using the fact that $\sum_{j=1}^{N} v_j = 1$ (and hence $\sum_{j=1}^{N} \nabla v_j = \underline{0}$), and noting that $\psi = 1$ can be exactly represented by our basis function approximation, we see that

$$\underline{\psi} = [1\ 1\ \ldots\ 1]^T \text{ and } \underline{\psi}_s = [1\ 1\ \ldots\ 1]^T$$

provide an exact solution to equation (3.3.2). Then, from equation (3.3.5) we have that

$$\sum_{j=1}^{N} B_{ij} = 1, \qquad 1 \leqslant i \leqslant N,$$

and hence the diagonal terms of the matrix may be calculated as

$$B_{ii} = 1 - \sum_{j \neq i} B_{ij} = 1 - \sum_{j \neq i} B_{ij}^{*}. \tag{3.3.6}$$

A result of this kind is particularly useful in the case of formulation III of the integral equation since it is possible to remove all reference to the 'solid angle term', $c(\underline{r})$, from the numerical scheme. After collocation, formulation III leads to the linear system

$$K\underline{\psi} = \underline{\psi}_s, \qquad K = D + K^{*}$$

where D is a diagonal matrix with entries $(1 + c(\underline{r}_i)\chi_i)$ and the i-j th entry of K* is given by

$$K_{ij}^{*} = \frac{1}{4\pi} \int_{\partial\Omega} \tilde{\chi}\, v_j\, \nabla\left(\frac{1}{R_i'}\right).\underline{\hat{n}}\, dS_{\underline{r}'}$$

$$- \frac{1}{4\pi} \int_{\Omega} v_j\, \nabla\tilde{\chi}.\nabla\left(\frac{1}{R_i'}\right) d\Omega_{\underline{r}'} .$$

Using the same analysis as for formulation I, it is easy to show that

$$\sum_{j=1}^{N} K_{ij} = 1$$

and hence, since

$$K_{ij} = \begin{cases} K_{ij}^* & i \neq j \\ 1 + c_i\chi_i + K_{ii}^* & i = j \end{cases}$$

we have

$$K_{i1} = 1 - \sum_{j\neq i} K_{ij} = 1 - \sum_{j\neq i} K_{ij}^*$$

3.4 Complete System of Equations

We now have (M + N) equations for the (M + N) unknowns, namely

$$\left.\begin{aligned} B(\underline{\chi})\underline{\psi} &= \underline{\psi}_s \\ \underline{\chi} &= \underline{F}(\underline{\psi}) \end{aligned}\right\} \qquad (3.4.1)$$

where $\underline{\chi} = (\chi_1\ \chi_2\ \ldots\ \chi_M)^T$,

$\underline{\psi} = (\psi_1\ \psi_2\ \ldots\ \psi_N)^T$,

$\underline{\psi}_s$ is a vector containing the values of the source potential at the nodes $\underline{r}_i^{(\psi)}$, $1 \leqslant i \leqslant N$, and

$$F_k(\underline{\psi}) = \bar{\chi}(H_k^{av}), \qquad 1 \leqslant k \leqslant M.$$

3.5 Solution of the Non-linear System

To solve the non-linear system of equations (3.4.1), a simple iterative scheme was proposed. A scheme of this kind was suggested by Armstrong et al. [1978].

Guess $\underline{\chi}^{(o)}$

$n = 1,2,\ldots$ until convergence

$$B(\underline{\chi}^{n-1})\underline{\psi}^{(n)} = \underline{\psi}_s$$

$$\underline{\chi}^{(n)} = \underline{F}(\underline{\psi}^{(n)})$$

This scheme seems to converge quite rapidly (10 iterations or less) on coarse grids. However, as the mesh is refined the convergence rate slows down and eventually the scheme becomes impractical. In an attempt to speed up the convergence rate we tried to extrapolate the results by assuming that each component of $\underline{\chi}$ satisfies

$$\chi^{(\infty)} = \chi^{(n)} + \alpha\beta^n$$

on the n-th iteration. The extrapolated values $\chi^{(\infty)}$ could then be checked by doing one further iteration. This modified iterative scheme improved the convergence rate at some nodes, but at other nodes did not appear to make a significant difference. Hence, we were led to examine a more sophisticated non-linear solver.

If we return to the non-linear system (3.4.1), we see that it can be written as a system of M non-linear functions f_i in M variables, namely

$$\underline{f}(\underline{\chi}) = \underline{0}$$

where

$$\underline{f}(\underline{\chi}) = \underline{\chi} - \underline{F}(\underline{\psi}) = \underline{0}$$

and $\underline{\psi}$ is the solution of $B(\underline{\chi})\underline{\psi} = \underline{\psi}_s$. The NAG library provides four subroutines for solving this type of problem, all of which are based on the Powell hybrid method [1970]. We have found it expedient to use a routine which requires the user to supply an initial approximation to the Jacobian, since this can reduce computational costs significantly. Details of the numerical differentiation are given later in this chapter.

The choice of the initial guess $\underline{\chi}^{(o)}$ seems to be unimportant in the sense that both the simple iterative scheme and the Powell method converge even if $\underline{\chi}^{(o)}$ is far from the solution. However, it is wise to have a good initial guess, where possible, for reasons of economy. We interpolated the results from a coarser grid to provide these starting values; alternatively, it may be possible to choose $\underline{\chi}^{(o)}$ by extrapolating the results obtained from several previous grids.

It is well known that integral equation methods yield full, unsymmetric matrices in general, and hence the cost of solving the linear system

$$B(\underline{\chi})\underline{\psi} = \underline{\psi}_s$$

may be quite high. We have compared two codes which use essentially

the same algorithm. The first is a NAG library routine which uses Crout's method with partial pivoting. The second code uses Gaussian elimination with row prenormalization and partial pivoting. It can be shown that the two methods are more or less equivalent, with the same operations carried out, but in a different order (see, for example, Forsythe and Moler [1967], Stewart [1973]). However, comparative timings of the two routines on the Cray-1 have shown that the Gaussian elimination routine performs up to 35 times faster than the NAG routine, and this ratio improves as the order of the matrix increases. Crout's method is only preferable to Gaussian elimination on a machine which can accumulate the inner products in double precision, as this reduces the effects of rounding errors, and it may be this fact which makes the NAG routine so costly (double precision calculations are twenty times more expensive than single precision on the Cray-1 and also inhibit vectorization). However, we have not experienced any noticeable rounding errors by using the Gaussian elimination solver. It should be noted that, in general, Gaussian elimination type routines are optimal for serial computers, and cannot easily be vectorized on parallel machines since the algorithms are recursive. (A recurrence is a sequence of evaluations in which the latest term in the sequence depends on one or more of the previously computed terms.) Currently there is a lot of interest in the development of vector algorithms for tridiagonal systems (see, for example, Hockney and Jesshope [1981], Jordan [1982], Kershaw [1982]). However, as far as general linear systems are concerned, the author does not know of any codes which have been fully vectorized on the Cray.

3.6 Evaluation of the Integrals

A typical off-diagonal entry of the linear system (3.3.5) is given by

$$B_{ij}^{*} = \frac{1}{4\pi} \sum_{k=1}^{M} \chi_k \int_{\Omega} \omega_k \nabla v_j . \nabla\left(\frac{1}{R_i'}\right) \, d\Omega_{\underline{r}'}$$

With the basis functions v_j and ω_k defined in terms of the shape functions as outlined in section 3.1, the integral over the whole domain can be expressed as a linear combination of integrals over each volume element. A typical volume integral is thus

$$V_{JK}(\underline{r}) = \int_{e} L_K(\underline{\xi}^e(\underline{r}')) \nabla Q_J(\underline{\xi}^e(\underline{r}')) . \nabla\left(\frac{1}{R_i'}\right) \, d\Omega_{\underline{r}'} \qquad (3.6.1)$$

where J and K are local node numbers; that is, global node j is given by the pair (e,J), j being the J-th node of volume element e, and similarly for k. Of course, the relation between global nodes and the (volume element, local node) pairs is one-to-many.

We have considered two approaches for the evaluation of integrals of the kind (3.6.1).

After a simple change of variables it is possible to rewrite $V_{JK}(\underline{r})$ as a linear combination of integrals, almost all of which can be evaluated analytically without <u>too</u> much difficulty. (The remainder can be evaluated by a combination of analytic and quadrature techniques.)

By transforming the origin to the field point $\underline{r}_i$ (i.e. by putting $\underline{R} = (X,Y,Z) = \underline{r}' - \underline{r}_i$) and denoting the limits of the new region by

$$A \leqslant X \leqslant B$$

$$C \leqslant Y \leqslant D$$

$$E \leqslant Z \leqslant F$$

we get

$$V_{JK}(\underline{r}) = \int_A^B dX \int_C^D dY \int_E^F \frac{L_K(\underline{\xi}^e(\underline{r}'(\underline{R})))\nabla\, Q_J(\underline{\xi}^e(\underline{r}'(\underline{R}))).\underline{R}}{R^3}\, dZ$$

where $\underline{r}'(\underline{R}) = \underline{R} + \underline{r}_i$, $\underline{\xi}^e(\underline{r}'(\underline{R})) = T^{-1}(\underline{R} - (\underline{k} - \underline{r}'))$ and $R = (X^2 + Y^2 + Z^2)^{1/2}$.

The linear and quadratic shape functions were defined in section 3.1 for the reference volume element $-1 \leqslant \xi,\eta,\zeta \leqslant 1$, and after applying the linear transformation $\underline{\xi}^e(\underline{r}'(\underline{R})) = T^{-1}(\underline{R} - (\underline{k} - \underline{r}'))$ the shape functions can easily be expanded as polynomials in X, Y and Z. Then

$$Q_J(\underline{\xi}^e(\underline{r}'(\underline{R}))) = a_0 + a_1X + a_2Y + a_3Z + a_4XY + a_5YZ + a_6ZX$$

$$+ a_7X^2 + a_8Y^2 + a_9Z^2 + a_{10}XYZ + a_{11}X^2Y + a_{12}ZX^2 + a_{13}XY^2$$

$$+ a_{14}Y^2Z + a_{15}Z^2X + a_{16}YZ^2 + a_{17}X^2YZ + a_{18}XY^2Z + a_{19}XYZ^2$$

and

$$L_K(\underline{\xi}^e(\underline{r}'(\underline{R}))) = b_0 + b_1X + b_2Y + b_3Z + b_4XY + b_5YZ$$

$$+ b_6ZX + b_7XYZ$$

where strictly $a_i \equiv a_i^{(J)}(A,B,C,D,E,F)$ and $b_i \equiv b_i^{(K)}(A,B,C,D,E,F)$. It follows that

$$V_{JK} = \sum_{i=1}^{53} f_i(\underline{a},\underline{b})\, I_i(A,B,C,D,E,F) \tag{3.6.2}$$

where

$$I_i(A,B,C,D,E,F) = \int_A^B dX \int_C^D dY \int_E^F \frac{X^{p_i} Y^{q_i} Z^{r_i}}{(X^2 + Y^2 + Z^2)^{3/2}}\, dZ,$$

$$\underline{a} = (a_0^{(J)}, a_1^{(J)}, \ldots, a_{19}^{(J)})^T,$$

$$\underline{b} = (b_0^{(K)}, b_1^{(K)}, \ldots, b_7^{(K)})^T,$$

$f_i(\underline{a},\underline{b})$ is the coefficient of $X^{p_i} Y^{q_i} Z^{r_i}$ in the expansion of the product $L_K \nabla Q_J . \underline{R}$,

and p_i, q_i and r_i, $1 \leqslant i \leqslant 53$, satisfy

$$\left.\begin{aligned} &1 \leqslant p_i, q_i, r_i \leqslant 3 \\ &1 \leqslant p_i+q_i,\ q_i+r_i,\ r_i+p_i \leqslant 5 \\ &1 \leqslant p_i+q_i+r_i \leqslant 7 \end{aligned}\right\} \tag{3.6.3}$$

Almost all of the integrals $I_i(A,B,C,D,E,F)$ occurring in (3.6.2) can be evaluated by referring to standard tables of integrals (for example, Dwight, 1961). In the remaining integrals some terms are difficult to integrate analytically in the third variable and in

these cases Gaussian quadrature was used. It was found that these terms are well-behaved so that a low order quadrature is sufficient. Thus, the accurate computation of V_{JK} would appear to present no great difficulty. However, the thinness of the plate causes some computational problems:

If we suppose that the X and Y integrations are performed first, with indefinite integral $G_i(X,Y,Z)$, then the i-th integral in (3.6.2) becomes

$$\int_E^F \{G_i(B,D,Z) - G_i(A,D,Z) - G_i(B,C,Z) + G_i(A,C,Z)\}\, dZ.$$

Now it is clear that if

$$\int_E^F G_i(X^*,Y^*,Z)\, dZ = [H_i(X^*,Y^*,Z)]_E^F ,$$

$$X^*,Y^* \text{ fixed,}$$

and the function H_i does not vary much over the range $E \leqslant Z \leqslant F$, then this will result in the subtraction of two nearly equal numbers. In fact, it was discovered that in some cases up to 14 places of accuracy were being lost, and this obviously causes trouble on a machine which works to 14 significant figures in single precision. One possible solution is to use double precision for these calculations. However, this would be extremely expensive and so a method combining analytic and quadrature techniques was devised:

Returning to equation (3.6.2), we see that a typical integral may be rewritten as

$$I_i(A,B,C,D,E,F) = \int_E^F Z^{r_i} \left\{ \int_A^B dX \int_C^D \frac{X^{p_i} Y^{q_i}}{(X^2+Y^2+Z^2)^{3/2}} \, dY \right\} dZ.$$

The X and Y integrations can be performed analytically, since they present no cancellation problems, and the resulting function varies slowly with Z. Thus a high accuracy can be obtained by using a low order Gaussian quadrature for the Z-integration. The analytic formulae for these integrals are given in the appendix to this chapter.

Note

Collie [1976] proposes an alternative approach for the analytic evaluation of the type of integrals appearing in equation (3.6.1). It is shown that the integrals over a volume element (which in the general case is a polyhedron) can be reduced to surface and line integrals over the faces and edges of the element; the analytic formulae are given for the case when the magnetization $\underline{M}$ (= $-\chi\nabla\psi$) is a linear function of the coordinates of the element. At present it is unclear whether the cancellation problems we encountered would occur if we adopted this strategy and it would certainly be interesting to compare the accuracy and computational cost of the two approaches.

Surface Integrals

In the case when χ is constant (or $\tilde{\chi}$ is taken to be piece-wise constant for non-linear problems) it is preferable to use formulation III of the integral equation as this necessitates the evaluation of surface integrals only. Using the same notation as before, a typical contribution from surface element s is given by

$$S = \int_s \frac{Q_J(\underline{\xi}^e(\underline{r}'))\underline{R}_i' \cdot \hat{\underline{n}}}{R_i'^3} \, dS_{\underline{r}'}.$$

However, because of the simple geometry of the plate

$\underline{R}_i'.\hat{\underline{n}}$ = d = perpendicular distance of the collocation point from the element,

and therefore

$$S = d \int_s \frac{Q_J(\underline{\xi}^e(\underline{r}'))}{(x_1^2 + x_2^2 + d^2)^{3/2}} \, dx_1 \, dx_2 \qquad (3.6.4)$$

where s lies in the (x_1,x_2)-plane. Hence S = 0 if the collocation point lies in the same plane as the element, and in all other cases the integrand of S is never singular. This led us to try standard Gaussian quadrature for the evaluation of (3.6.4). This proved to be satisfactory for {X = constant} and {Y = constant} elements, but because of the thinness of the plate the integrand can become <u>almost</u> singular for {Z = constant} elements, and this causes obvious numerical difficulties. In these cases the quadratic shape functions can be expanded as polynomials in X and Y as before, and the integrals can be evaluated analytically.

<u>Notes</u>

(i) In section 3.3 we observed that the diagonal entries of the linear system (3.3.5) can be calculated from

$$B_{ii} = 1 - \sum_{j \neq i} B_{ij}^*, \qquad 1 \leqslant i \leqslant N$$

(with the corresponding result for linear problems). We have used this relation in all our calculations.

(ii) For the volume integrals, product Gaussian quadrature in all three variables would not appear to be sufficient because of the singularity in the integrand when the collocation point belongs to the element (although the worst possible case, when node J coincides with the collocation point, can be avoided by the use of (i) above). However, it may be that special quadrature formulae could be derived.

3.7 Calculation of the Source Potential

It now remains to evaluate the right hand side of the linear system (3.3.5). To do this we need to calculate the potential due to a source of three coaxial solenoids. An algorithm which uses elliptic integrals to compute the field of axially symmetric magnetic systems is given in the paper by Garrett [1965]. The potential can then be obtained by numerical integration.

The equations given by Garrett refer to a field ring of cylindrical radius ρ which passes through the field point, and a coaxial source ring of radius a. The axial separation of the field ring and the source ring is x. The origin is taken to lie in the plane of the field point, so that x is positive when the source is to the right. The simplest source is a circular current loop. In our case, the magnet windings can be modelled as cylindrical current sheets (ideal solenoids), and the field of an ideal solenoid is obtained by integrating the field of a current loop along the axis. Garrett notes that only the coordinates of the end circles of the solenoid appear in the definite integral, which thus contains two terms of

opposite sign. Hence it is convenient to ignore the physical distributed currents of the winding and to attribute the entire field to these two source rings, which are of identical absolute strength but are of opposite sign. The positive sign belongs to the right end of a positive current sheet. The source strength of a loop is Ni, where N is the turn count and the sign depends only on the current i. The equations are written for single positive sources of unit turn count, the field from a system of sources being obtained by algebraic summation. The system of sources resulting from the configuration of three coaxial solenoids is indicated in figure 3.1.

The axial and radial components of the solenoid field for each source are given by

$$B_x(x,\rho) = \frac{10^{-7} ixck}{\rho} \left[K + \frac{a - \rho}{2a}(\Pi - K)\right] \qquad (3.7.1)$$

$$B_\rho(x,\rho) = \frac{10^{-7} ir_1}{\rho} [2(K - E) - k^2 K] \qquad (3.7.2)$$

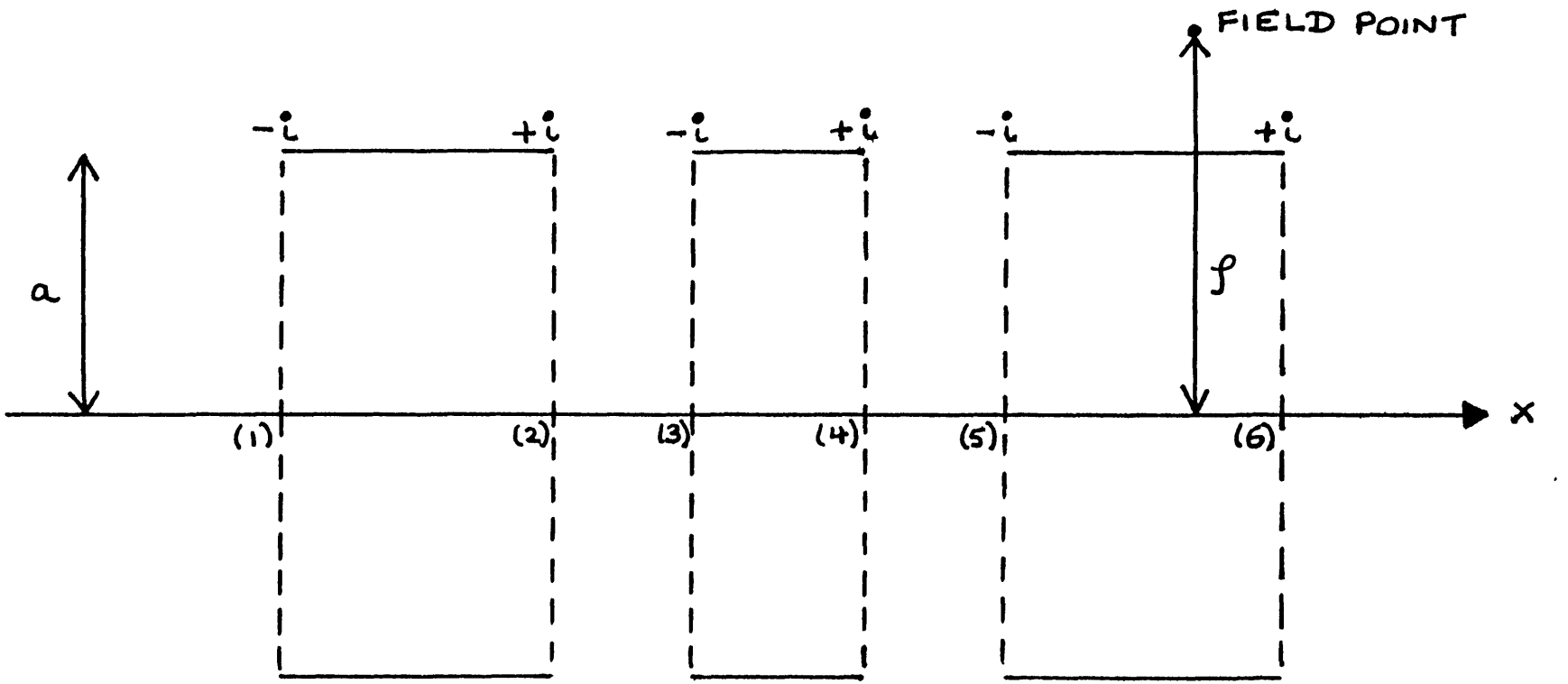
where

$$r_1^2 = (a + \rho)^2 + x^2$$

$$k^2 = \frac{4a\rho}{r_1^2}$$

$$c^2 = \frac{4a\rho}{(a + \rho)^2} \quad .$$

K, E and Π are complete elliptic integrals to modulus k of the 1st, 2nd and 3rd kind respectively; the parameter of Π is $-c^2$.



$a = 0.5061$ m

$i = 3421250$ Am^{-1}

Fig. 3.1. System of sources resulting from 3 coaxial solenoids.

The integrals K and E may be computed from the Hastings approximations [Hastings, 1955]. However, since Π is also required, Garrett suggests an iterative method for computing Π in which K and E emerge as by-products, and we have therefore used this method.

Once we have obtained the components of the field in the axial and radial directions by applying equations (3.7.1) and (3.7.2) to all six sources, it is a simple matter to resolve the radial component of the field, B_ρ, into the y and z components B_y and B_z:

If the coordinates of the field point are given by (x_F, y_F, z_F) then

$$B_y = \frac{y_F}{\rho} B_\rho$$

and

$$B_z = \frac{z_F}{\rho} B_\rho,$$

where, of course, $\rho = \sqrt{y_F^2 + z_F^2}$.

Thus, we are able to calculate the field due to the source of three solenoids at any point in space. However, we need to integrate the field to obtain the source potential ψ_s.

Let $\underline{r}_P$ and $\underline{r}_Q$ be any two points in Ω_c (the 'cut' space). Then

$$\int_{\underline{r}_P}^{\underline{r}_Q} \underline{H}.\ \underline{ds} = -\int_{\underline{r}_P}^{\underline{r}_Q} \nabla\psi_s.\underline{ds} = \psi_s(\underline{r}_P) - \psi_s(\underline{r}_Q),$$

where the line integral is along any path lying entirely in Ω_c. Thus the potential at any point $\underline{r}_Q$ in Ω_c is given by

$$\psi_s(\underline{r}_Q) = \psi_s(\underline{r}_P) - \int_{\underline{r}_P}^{\underline{r}_Q} \underline{H}_s.\ \underline{ds}.$$

If we now take $\underline{r}_P = (x_P, y_P, z_P)$ to be any point such that $x_P = 0$, then $\psi_s(\underline{r}_P) = 0$ and hence

$$\psi_s(\underline{r}_Q) = - \int_{\underline{r}_P}^{\underline{r}_Q} \underline{H}_s . \underline{ds} = \frac{-1}{\mu_0} \int_{\underline{r}_P}^{\underline{r}_Q} \underline{B}_s . \underline{ds}$$

For simplicity, define the path joining $\underline{r}_P$ and $\underline{r}_Q$ to be a straight line. Then

$$\psi_s(\underline{r}_Q) = - \frac{1}{\mu_0} \int_0^1 \underline{B}_s(\underline{s}(t)) . (\underline{r}_Q - \underline{r}_P) \, dt,$$

where $\underline{s}(t) = \underline{r}_P + t(\underline{r}_Q - \underline{r}_P)$,

and this integral can be evaluated using standard Gaussian quadrature techniques.

3.8 Recovery of Fields

Once approximations to ψ and χ have been obtained there are several different methods which can be used to compute an approximation to the field $\underline{H}$ at any point $\underline{r}$ in Ω_c:

(i) The integral equation for ψ can be differentiated to give an integral equation for $\underline{H}$. Thus in the case of formulation I we obtain

$$\underline{H}(\underline{r}) = \frac{1}{4\pi} \nabla \int_\Omega \chi(\underline{r}') \nabla\psi(\underline{r}') . \nabla(\frac{1}{R'}) \, d\Omega_{\underline{r}'} - \nabla\psi_s(\underline{r}), \quad \underline{r} \in \Omega_c. \quad (3.8.1)$$

For points outside the domain Ω the gradient in (3.8.1) can be taken under the integral sign, and so the field integral equation becomes

$$\underline{H}(\underline{r}) = \frac{1}{4\pi} \int_{\Omega} \chi(\underline{r}') \left[\frac{\nabla\psi(\underline{r}')}{(R')^3} - 3 \frac{\nabla\psi\,(\underline{r}').\underline{R}'}{(R')^5} \underline{R}' \right] d\Omega_{\underline{r}'} - \nabla\psi_s(\underline{r}) ,$$

$$\underline{r} \in \Omega_c - \bar{\Omega} \qquad (3.8.2)$$

This is not true for points lying in the domain Ω, since this would lead to divergent integrals (the proof of this is given in Arsenin [1968], for example).

(ii) The potential at any point $\underline{r} \in \Omega_c$ can be computed from the integral equation (2.6.9) and thus the field can be obtained by numerical differentiation. For example, if $\underline{H} = (H_x, H_y, H_z)$,

$$H_x(x,y,z) \simeq - \frac{\psi(x + h,y,z) - \psi(x - h,y,z)}{2h}$$

Alternatively, the integral equation for ψ can be used to compute ψ at the 20 nodes of a "small" volume element defined by $(x\pm h, y\pm h, z\pm h)$, and these nodal values can be interpolated using the 20-node shape functions. This can then be differentiated analytically to give an approximation to the field at (x,y,z).

(iii) Inside the iron region Ω the basis function representation of ψ can be differentiated analytically, i.e.

$$\underline{H}(\underline{r}) = - \sum_j \psi_j \nabla v_j(\underline{r}),$$

with the limitation that this expression is not defined at inter-element boundaries.

3.9 Evaluation of the Field Integral Equation

The integral equation for $\underline{H}$ is evaluated in a similar manner to the integral equation for ψ. If we substitute the approximations for ψ and χ, given by

$$\tilde{\psi}(\underline{r}) = \sum_{j=1}^{N} \psi_j \, v_j(\underline{r})$$

$$\tilde{\chi}(\underline{r}) = \sum_{k=1}^{M} \chi_k \, \omega_k(\underline{r}),$$

into equation (3.8.2), we obtain

$$\underline{H}(\underline{r}) = \frac{1}{4\pi} \sum_{j=1}^{N} \psi_j \sum_{k=1}^{M} \chi_k \int_{\Omega} \omega_k(\underline{r}') \left[\frac{\nabla v_j(\underline{r}')}{(R')^3} - \frac{3\nabla v_j(\underline{r}').\underline{R}'\underline{R}'}{(R')^5} \right] d\Omega_{\underline{r}'}$$

$$- \nabla\psi_s(\underline{r}), \quad R' = |\underline{r}' - \underline{r}|$$

and thus a typical field integral is given by

$$\int_{\Omega} \omega_k(\underline{r}') \left[\frac{\nabla v_j(\underline{r}')}{(R')^3} - \frac{3\nabla v_j(\underline{r}').\underline{R}' \; \underline{R}'}{(R')^5} \right] d\Omega_{\underline{r}'} \qquad (3.9.1)$$

Now, if we transform the origin to the field point and expand the shape functions as polynomials in X, Y and Z, with coefficients $\underline{a}$ and $\underline{b}$, as before, (3.9.1) becomes

$$\underline{V}_{JK}(\underline{r}) = -3 \sum_{i=1}^{53} \underline{g}_i^{(1)}(\underline{a},\underline{b}) \int_A^B dX \int_C^D dY \int_E^F \frac{X^{p_i^{(1)}} Y^{q_i^{(1)}} Z^{r_i^{(1)}}}{(X^2+Y^2+Z^2)^{5/2}} dZ$$

$$+ \sum_{j=1}^{39} \underline{g}_j^{(2)}(\underline{a},\underline{b}) \int_A^B dX \int_C^D dY \int_E^F \frac{X^{p_j^{(2)}} Y^{q_j^{(2)}} Z^{r_j^{(2)}}}{(X^2+Y^2+Z^2)^{3/2}} dZ \qquad (3.9.2)$$

where

$\underline{g}_i^{(k)}(\underline{a},\underline{b})$, k = 1,2, give the coefficients of $X^{p_i^{(k)}} Y^{q_i^{(k)}} Z^{r_i^{(k)}}$ in the expansions of the products $L_K \nabla Q_J . \underline{R}'\underline{R}'$ and $L_K \nabla Q_J$ respectively, $p_i^{(1)}$, $q_i^{(1)}$, $r_i^{(1)}$, $1 \leqslant i \leqslant 53$, satisfy

$$\left.\begin{aligned} &0 \leqslant p_i^{(1)}, q_i^{(1)}, r_i^{(1)} \leqslant 4 \\ &1 \leqslant p_i^{(1)} + q_i^{(1)},\ q_i^{(1)} + r_i^{(1)},\ r_i^{(1)} + p_i^{(1)} \leqslant 6 \\ &2 \leqslant p_i^{(1)} + q_i^{(1)} + r_i^{(1)} \leqslant 8 \end{aligned}\right\} \qquad (3.9.3)$$

and $p_j^{(2)}$, $q_j^{(2)}$, $r_j^{(2)}$, $1 \leqslant j \leqslant 39$, satisfy

$$\left.\begin{aligned} &0 \leqslant p_j^{(2)}, q_j^{(2)}, r_j^{(2)} \leqslant 3 \\ &0 \leqslant p_j^{(2)} + q_j^{(2)},\ q_j^{(2)} + r_j^{(2)},\ r_j^{(2)} + p_j^{(2)} \leqslant 5 \\ &0 \leqslant p_j^{(2)} + q_j^{(2)} + r_j^{(2)} \leqslant 6 \end{aligned}\right\} \qquad (3.9.4)$$

The integrals appearing in equation (3.9.2) can be evaluated using a mixture of analytic and quadrature techniques, as outlined in section 3.6 and in the appendix to this chapter.

3.10 Economy

It is clear that there are inherent symmetries in the problem which should be exploited in order to make the numerical scheme as efficient as possible. The scalar potential ψ possesses the same symmetries as the source potential; that is, ψ is anti-symmetric about $x = 0$ and symmetric about $y = 0$, which of course implies that $\psi = 0$ on $x = 0$. It follows that the susceptibility χ is symmetric about $x = 0$ and $y = 0$, since χ is a function of $|\nabla\psi|$. Thus, it is only necessary to define the unknown χ's in the region β, defined by

$$\beta = \{(x,y) : x \geqslant 0,\ y \geqslant 0\},$$

which we shall refer to as the 'basic' region. The unknown ψ's need only to be defined in the region β^-, where $\beta^- = \{(x,y) : x > 0,\ y \geqslant 0\}$. Taking these symmetries into account reduces the number of degrees of freedom for a particular mesh to approximately a quarter of the original number.

A further substantial saving can be made by noticing that the volume integrals V_{JK}, defined by

$$V_{JK}(\underline{r}) = \int_e L_K(\underline{\xi}^e(\underline{r}'))\ \nabla Q_J(\underline{\xi}^e(\underline{r}')).\nabla\left(\frac{1}{R_i'}\right)\ d\Omega_{\underline{r}'},$$

depend only on the relative position of the volume element e and the collocation point $\underline{r}_i$, and not on their actual position in space. Therefore, if a standard finite element assembly process is used many of the integrals will be repeatedly calculated, and the computational cost will rise accordingly. To avoid this, we have used

a scheme which calculates contributions from a reference volume element and a 'relative' collocation point and then adds these contributions into all the appropriate places in the matrix. We shall outline our scheme for the 2-D case; the generalization to 3-D is straightforward.

In 2-dimensions, let n_x and n_y be the number of elements in the x and y directions respectively, and let the dimensions of the plate be $2\ell_x$ by $2\ell_y$. Define

$$\Delta x = \frac{\ell_x}{2n_x}, \qquad \Delta y = \frac{\ell_y}{2n_y}$$

and define a reference element by

$$-\ell_x \leqslant x \leqslant -\ell_x + 2\Delta x$$

$$-\ell_y \leqslant y \leqslant -\ell_y + 2\Delta y$$

(see figure 3.2). Then the 'relative' collocation points with respect to this reference element are given by

$$\underline{x}_{\underline{k}} = (k_1\Delta x, k_2\Delta y),$$

with the index $\underline{k}$ defined by

$$\underline{k} = \{(k_1,k_2) : -2n_x + 1 \leqslant k_1 \leqslant 2n_x,\ -2n_y + 1 \leqslant k_2 \leqslant 2n_y,$$

$$\text{mod}\,(k_1,2) + \text{mod}\,(k_2, 2) \leqslant 1\}.$$

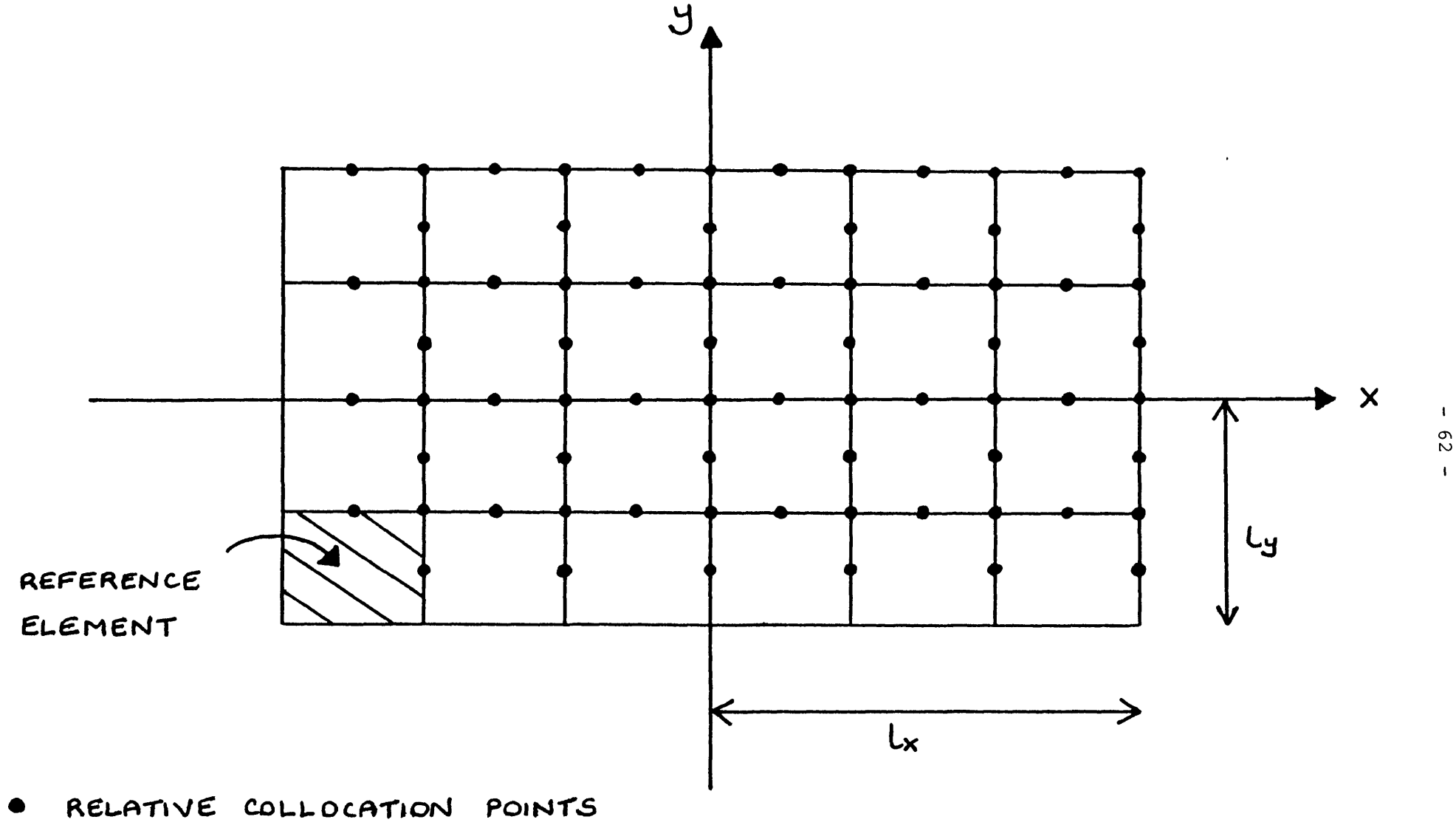


Fig. 3.2. Reference element and relative collocation points for economy scheme in 2D.

Once the matrix of integrals for a 'relative' collocation point with respect to the reference element has been calculated, the next step is to add in the results at all relevant positions in the matrix B. This is done by moving the relative collocation point, and hence the reference element, systematically through the basic region (so that the 'relative' collocation point becomes an actual collocation point) and then reflecting the element, where possible, about the collocation point. In this way one generates all possible (element, collocation point) combinations. If we denote the collocation points by $\underline{k}'$, where

$$\underline{k}' = \{(k_1', k_2') : 0 \leqslant k_1' \leqslant 2n_x,\ 0 \leqslant k_2' \leqslant 2n_y,$$

$$\text{mod}\ (k_1', 2) + \text{mod}\ (k_2', 2) \leqslant 1\ \}$$

then the centre of the transformed element is given by

$$[k_1' - (k_1 + 2n_x - 1),\ k_2' - (k_2 + 2n_y - 1)].$$

The symmetry operations which may be applied to the element are denoted by

$$\underline{S} = (I,\ R_x(\underline{k}'),\ R_y(\underline{k}'),\ R_{xy}(\underline{k}')),$$

where we have used the notation $S_2 = R_x(\underline{k}')$ to denote reflection about $x = k_1'\Delta x$, for example. The matrix of integrals for this (element, collocation point) combination is then added into the

matrix B. Thus an outline of the code to set up the matrix B for a 2-dimensional problem is as follows:

$k_1 = (-2n_x + 1)(1)(2n_x)$ } gives 'relative' collocation point w.r.t. reference element

Define $k_1'f = \begin{cases} 0 & k_1 \text{ even} \\ 1 & k_1 \text{ odd} \end{cases}$

$k_2 = (-2n_y + 1)(1)(2n_y)$

Define $k_2'f = \begin{cases} 0 & k_2 \text{ even} \\ 1 & k_2 \text{ odd} \end{cases}$

If $(\{\text{mod}(k_1,2) + \text{mod}(k_2,2)\} \leqslant 1)$ then:

Calculate matrix of integrals

$k_1' = (k_1'f)(2)(2n_x - k_1'f)$ } move relative collocation point through basic region

$k_2' = (k_2'f)(2)(2n_y - k_2'f)$

$e_1 = k_1' - (k_1 + 2n_x - 1)$ } centre of transformed element

$e_2 = k_2' - (k_2 + 2n_y - 1)$

$i = 1, 4$ } apply symmetry operations to element

$\underline{e}^{(i)} = [S_i(\underline{k}')]\underline{e}$

If reflected element lies in the plate, add in the matrix of integrals to the appropriate places in the matrix B

endif

It should be noted that this 'economy scheme' applies equally well to the recovery of exterior potentials, if these are to be calculated at a grid of points compatible with the discretization. We have used a scheme which incorporates essentially the same ideas, but adds in the contributions using an alternative loop structure. An economy scheme could also be applied to the recovery of fields using the field integral equation (3.8.1), although we did not have time to implement this.

3.11 Some Computational Aspects

The problem we are solving is necessarily 3-dimensional and the numerical method we have chosen gives rise to full, non-symmetric linear systems of equations. These two factors indicate that storage requirements and computational costs may be quite high, particularly as the mesh is refined.

The code used in this project was developed and tested on the CDC Cyber 855 at Imperial College, but most of the production runs have been done on the Cray 1-S at the University of London Computer Centre. Use of the Cray 1-S led us to re-examine our code to see whether some attempt at vectorization could be made, in order to make efficient use of the resources available to us. Since our code was already written and tested by the time the University of London Computer Centre acquired the Cray-1 we decided not to re-structure the program completely, but rather to analyse the existing inner do-loops to see whether they could easily be vectorized. This was possible in a number of cases, notably in the Gaussian quadrature

routines used in the field calculation. We appreciate that further savings could probably be made if we had more time to consider this problem.

Use of Direct Access Storage

If we return to the calculation of a typical entry of the linear system, B_{ij}, where

$$B_{ij} = \begin{cases} B_{ij}^* & i \neq j \\ 1 + B_{ii}^* & i = j \end{cases}$$

and

$$B_{ij}^* = \frac{1}{4\pi} \sum_{k=1}^{M} \chi_k \int_{\Omega} \omega_k \nabla v_j . \nabla \left(\frac{1}{R_i'}\right) \, d\Omega_{\underline{r}'},$$

we see that the integrals are independent of $\{\chi_k\}$ and hence can be set up once and for all before the non-linear solver is called. Therefore, we are essentially storing a 3-dimensional array I(i,j,k), given by

$$I(i,j,k) = \int_{\Omega} \omega_k \nabla v_j . \nabla \left(\frac{1}{R_i'}\right) \, d\Omega_{\underline{r}'},$$

$$1 \leqslant i,j \leqslant N, \quad 1 \leqslant k \leqslant M,$$

which is reformulated as a 2-dimensional array for each update of the $\{\chi_k\}$. We have used a FORTRAN direct access file to store the 3-dimensional array, with the first index of the array used as the record number to which the 2-D array I(.,j,k), $1 \leqslant j \leqslant N$, $1 \leqslant k \leqslant M$, is written. We shall use the notation $D^{(i)}(j,k)$ to

denote the array stored under record number i; that is, for fixed i,

$$I(i,j,k) = D^{(i)}(j,k) \qquad 1 \leqslant j \leqslant N,$$
$$1 \leqslant k \leqslant M.$$

Thus, we may write the entries of the matrix $B(\underline{\chi})$ as

$$\left.\begin{aligned} B_{ij} &= \frac{1}{4\pi} \sum_{k=1}^{M} \chi_k \, D^{(i)}(j,k) \\ B_{ii} &= 1 - \frac{1}{4\pi} \sum_{k=1}^{M} \chi_k \, D^{(i)}(i,k) \end{aligned}\right\} \qquad (3.11.1)$$

where

$$D^{(i)}(i,k) = \sum_{j \neq i} I(i,j,k),$$

since we have exploited the fact that the diagonal terms can be calculated in terms of the other entries in the row (see section 3.3).

As we shall see in the next section, the form of the $\{B_{ij}\}$ in (3.11.1) can be exploited in the calculation of the Jacobian.

3.12 Approximation of the Jacobian

In section 3.5 we showed that the non-linear system can be written as

$$\underline{f}(\underline{\chi}) \equiv \underline{\chi} - \underline{F}(\underline{\psi}) = \underline{0} \qquad (3.12.1)$$

where $\underline{\psi}$ is the solution of

$$B(\underline{\chi})\underline{\psi} = \underline{\psi}_s \tag{3.12.2}$$

and

$$F_i(\underline{\psi}) = \bar{\chi}(H_i^{av}), \quad 1 \leqslant i \leqslant M.$$

If we use a quasi-Newton method to solve this system we need to be able to compute an initial approximation to the Jacobian $J(\underline{f};\underline{\chi})$. In general, one has to compute the Jacobian using finite differences; for example, the j-th column of the Jacobian

$$\left(\frac{\partial \underline{f}}{\partial \chi_j}\right) = \left(\frac{\partial f_1}{\partial \chi_j}, \frac{\partial f_2}{\partial \chi_j}, \ldots, \frac{\partial f_M}{\partial \chi_j}\right)^T$$

can be approximated as

$$\frac{\partial \underline{f}}{\partial \chi_j} = \frac{\underline{f}(\underline{\chi}^{(\varepsilon,j)}) - \underline{f}(\underline{\chi})}{\varepsilon \chi_j}$$

where $\underline{\chi}^{(\varepsilon,j)} = \underline{\chi} + \varepsilon\chi_j\underline{e}^{(j)}$, $\underline{e}^{(j)}$ being the j-th unit vector. ε is chosen to be optimal in some sense; that is, to be "small", but not so small as to induce cancellation problems. It should be observed that this scaled finite difference breaks down if $\chi_j = 0$. However, this possibility does not arise in the problem we have considered.

Note that if we apply this method directly to the non-linear system defined by (3.12.1) it requires (M+1) solves of the linear

system (3.12.2), and this becomes extremely costly as the mesh is refined. We have exploited the form of the matrix B to reduce this cost.

To calculate $\underline{f}(\underline{\chi}^{(\varepsilon,j)})$ we need to evaluate

$$B(\underline{\chi}^{(\varepsilon,j)})\underline{\psi} = \underline{\psi}_s. \tag{3.12.3}$$

Using equation (3.11.1) it is easy to show that for any two vectors $\underline{a}$ and $\underline{b}$ of length M,

$$B(\underline{a} + \underline{b}) = B(\underline{a}) + B(\underline{b}) - I$$

and hence we can write equation (3.12.3) as

$$B(\underline{\chi})\underline{\psi} = \underline{\psi}_s - [B(\varepsilon\chi_j\underline{e}^{(j)}) - I]\underline{\psi}$$

$$= \underline{\psi}_s - \varepsilon\chi_j A^{(j)}\underline{\psi}, \tag{3.12.4}$$

where the entries of the NxN matrix $A^{(j)}$ are given by

$$A_{k\ell}^{(j)} = \begin{cases} \frac{1}{4\pi} D^{(k)}(\ell,j) & k \neq \ell \\ \frac{-1}{4\pi} D^{(k)}(k,j) & k = \ell \end{cases}$$

This suggests the following iterative scheme:
Take $\underline{\psi}^{(o)}$ to be the solution of $B(\underline{\chi})\underline{\psi} = \underline{\psi}_s$, and define $\underline{\psi}^{(p)}$, $p \geq 1$, by

$$B(\underline{\chi})\underline{\psi}^{(p)} = \underline{\psi}_s - \varepsilon\chi_j A^{(j)}\,\underline{\psi}^{(p-1)} \tag{3.12.5}$$

If the LU decomposition is preserved when $\underline{\psi}^{(o)}$ is calculated, then the solution of the linear system (3.12.5) at each iteration can be carried out very cheaply.

The iterative scheme can be written as

$$\underline{\psi}^{(p)} = G\,\underline{\psi}^{(p-1)} + \underline{b} \qquad (3.12.6)$$

where G, the iteration matrix, is given by

$$G = -\varepsilon\chi_j\,(B(\underline{\chi}))^{-1}\,A^{(j)}.$$

Hence, the spectral radius of G, $\rho(G)$, is

$$\varepsilon\chi_j\rho((B(\underline{\chi}))^{-1}\,A^{(j)})$$

and, consequently, provided ε is sufficiently small, the iterations will converge rapidly. In practice we have found that with $\varepsilon = 10^{-5}$ 3 or 4 iterations are sufficient. It should be noted that ε also has to satisfy the conditions of the finite difference approximation; that is, ε is "small" but not so small that cancellation problems arise.

Thus our algorithm for computing an approximation to the Jacobian at $\underline{\chi}$ is as follows:

Solve $B(\underline{\chi})\underline{\psi} = \underline{\psi}_s$ (keep $\underline{\psi}$ and LU decomposition)

Evaluate $\underline{F}(\underline{\psi})$

$j = 1,2,\ldots,M$

$\underline{\psi}^{(o)} = \underline{\psi}$

$p = 1,2,\ldots$

Solve $B(\underline{\chi})\underline{\psi}^{(p)} = \underline{\psi}_s - \varepsilon\chi_j A^{(j)}\underline{\psi}^{(p-1)}$ using the LU decomposition

Let the final iterate be $\underline{\psi}^*$

j-th column of Jacobian =

$$\frac{1}{\varepsilon\chi_j}\left[\varepsilon\chi_j \underline{e}^{(j)} - \underline{F}(\underline{\psi}^*) + \underline{F}(\underline{\psi})\right]$$

It should be noted that this scheme requires only one LU decomposition to be performed.

Appendix A.3: Evaluation of the Volume Integrals by Analytic and Quadrature Techniques

We have shown that the volume integrals which occur in both the potential and field integral equations can be expressed as a linear combination of integrals of the form

$$I_i(A,B,C,D,E,F) = \int_A^B dX \int_C^D dY \int_E^F \frac{X^{p_i} Y^{q_i} Z^{r_i}}{(X^2+Y^2+Z^2)^{k/2}} \, dZ \qquad (A.3.1)$$

where $k = 3$ or 5, and the index i and corresponding integer powers p_i, q_i, r_i are defined by equations (3.6.3), (3.9.3) or (3.9.4) as appropriate. The X and Y integrations are performed analytically, and the final Z-integration is evaluated by quadrature techniques. Thus equation (A.3.1) is rewritten as

$$I_i(A,B,C,D,E,F) = \int_E^F Z^{r_i} \left\{ \int_A^B dX \int_C^D \frac{X^{p_i} Y^{q_i}}{(X^2+Y^2+Z^2)^{k/2}} \, dY \right\} dZ \qquad (A.3.2)$$

and the first step is to establish analytic formulae for the inner (x,y) integrations. For the case $k = 3$, which occurs in both the potential and field integral equations, there are 9 distinct integrals to be evaluated analytically. If we define

$$J_{m,j}(A,B,C,D,Z) = \int_A^B dX \int_C^D \frac{X^{\alpha(m,j)} Y^{\beta(m,j)}}{(X^2 + Y^2 + Z^2)^{3/2}} \, dY \qquad (A.3.3)$$

where $m = m(i)$, $j = j(i)$

$$\alpha(m,j) = (1-j)P_m + jQ_m = \begin{cases} P_m & j = 0 \\ Q_m & j = 1 \end{cases}$$

$$\beta(m,j) = (1 - j)Q_m + jP_m = \begin{cases} Q_m & j = 0 \\ P_m & j = 1 \end{cases}$$

and P_m and Q_m are given in Table A.1, then equation (A.3.2) becomes

$$I_i(A,B,C,D,E,F) = \int_E^F Z^{r_i} J_{m,j}(A,B,C,D,Z)\, dZ.$$

Of course, the values of P_m and Q_m in Table A.1 represent the 9 distinct integrals to be evaluated.

The case k = 5, which only occurs in the field integral equation, gives 13 integrals to be evaluated analytically; these are defined by the powers P_m and Q_m given in Table A.2.

m	P_m	Q_m
1	0	0
2	0	1
3	0	2
4	0	3
5	1	1
6	1	2
7	1	3
8	2	2
9	2	3

Table A.1

m	P_m	Q_m
1	0	0
2	0	1
3	0	2
4	0	3
5	0	4
6	1	1
7	1	2
8	1	3
9	1	4
10	2	2
11	2	3
12	2	4
13	3	3

Table A.2

We present here the analytic formulae for the case k = 3. The integrals for the case k = 5 can be evaluated in a similar manner.

Without loss of generality take j = 0 in equation (A.3.3) and define $J_m^*(A,B,C,D,Z) = J_{m,0}(A,B,C,D,Z)$. Then

$$J_m^*(A,B,C,D,Z) = \int_A^B dX \int_C^D \frac{X^{P_m} Y^{Q_m}\, dY}{(X^2+Y^2+Z^2)^{3/2}}, \qquad (A.3.4)$$

$$1 \leq m \leq 9,$$

and thus J_m^* represents the 9 different integrals to be evaluated.

It is convenient to write the integrals J_m^* (A,B,C,D,Z) in terms of the following one-dimensional integrals, $F_i(x,y,z)$, where y and z are fixed and $1 \leqslant i \leqslant 10$:

$$F_1(x,y,z) = \int \frac{dx}{(x^2 + y^2 + z^2)^{1/2}}$$

$$= \log (x + r)$$

$$F_2(x,y,z) = \int \frac{x\, dx}{(x^2 + y^2 + z^2)^{1/2}}$$

$$= r$$

$$F_3(x,y,z) = \int \frac{x^2\, dx}{(x^2 + y^2 + z^2)^{1/2}}$$

$$= \frac{xr}{2} - \frac{(y^2 + z^2)}{2} \log (x + r)$$

$$F_4(x,y,z) = \int \frac{x^3\, dx}{(x^2 + y^2 + z^2)^{1/2}}$$

$$= \frac{r^3}{3} - (y^2 + z^2)r$$

$$F_5(x,y,z) = \int \frac{x^4\, dx}{(x^2 + y^2 + z^2)^{1/2}}$$

$$= \frac{x^3 r}{4} - \frac{3}{8} (y^2 + z^2)xr + \frac{3}{8} (y^2 + z^2)^2 \log (x + r)$$

$$F_6(x,y,z) = \int (x^2 + y^2 + z^2)^{1/2}\, dx$$

$$= \frac{1}{2} \{xr + (y^2 + z^2) \log (x + r)\}$$

$$F_7(x,y,z) = \int x^2(x^2 + y^2 + z^2)^{1/2}\, dx$$

$$= \frac{xr^3}{4} - \frac{(y^2 + z^2)xr}{8} - \frac{(y^2 + z^2)^2}{8} \log (x + r)$$

$$F_8(x,y,z) = \int \log (y + (x^2 + y^2 + z^2)^{1/2})\, dx$$

$$= x \log (y + r) + y \log (x + r) - x + 2z\vartheta \quad .$$

$$F_9(x,y,z) = \int x^2 \log (y + (x^2 + y^2 + z^2)^{1/2})\, dx$$

$$= \frac{1}{3} \{x^3 (\log (y + r) - \frac{1}{3})$$

$$- \frac{y}{2} (y^2 + 3z^2) \log (x + r) + x(z^2 + \frac{yr}{2}) - 2z^3\vartheta\}$$

$$F_{10}(x,y,z) = \int \frac{dx}{(x^2 + z^2)(x^2 + y^2 + z^2)^{1/2}}$$

$$= \left|\frac{1}{yz}\right| \tan^{-1} \left(\frac{v}{(1 + (\frac{z}{y})^2 - v^2)^{1/2}} \right)$$

where $r = (x^2 + y^2 + z^2)^{1/2}$

$$\varphi = \frac{1}{2} \tan^{-1} \left(\frac{x}{(y^2 + z^2)^{1/2}}\right)$$

$$\vartheta = \tan^{-1}\left\{ \frac{[(y^2 + z^2)^{1/2} - y] \tan \varphi}{z} \right\}$$

$$v = \frac{x}{(x^2 + z^2)^{1/2}} \quad .$$

Then

$$J_1^*(A,B,C,D,Z) = D\{F_{10}(B,D,Z) - F_{10}(A,D,Z)\}$$

$$- C\{F_{10}(B,C,Z) - F_{10}(A,C,Z)\}$$

$$J_2^*(A,B,C,D,Z) = F_1(B,C,Z) - F_1(A,C,Z)$$

$$- F_1(B,D,Z) + F_1(A,D,Z)$$

$$J_3^*(A,B,C,D,Z) = C\{F_1(B,C,Z) - F_1(A,C,Z)\}$$

$$- D\{F_1(B,D,Z) - F_1(A,D,Z)\}$$

$$+ F_8(B,D,Z) - F_8(A,D,Z) - F_8(B,C,Z) + F_8(A,C,Z)$$

$$J_4^*(A,B,C,D,Z) = F_6(B,D,Z) - F_6(A,D,Z)$$

$$- F_6(B,C,Z) + F_6(A,C,Z)$$

$$+ F_3(B,D,Z) - F_3(A,D,Z) - F_3(B,C,Z) + F_3(A,C,Z)$$

$$+ Z^2\{F_1(B,D,Z) - F_1(A,D,Z) - F_1(B,C,Z) + F_1(A,C,Z)\}$$

$$J_5^*(A,B,C,D,Z) = F_2(B,C,Z) - F_2(A,C,Z) - F_2(B,D,Z) + F_2(A,D,Z)$$

$$J_6^*(A,B,C,D,Z) = F_3(D,A,Z) - F_3(C,A,Z) - F_3(D,B,Z) + F_3(C,B,Z)$$

$$J_7^*(A,B,C,D,Z) = F_4(D,A,Z) - F_4(C,A,Z) - F_4(D,B,Z) + F_4(C,B,Z)$$

$$J_8^*(A,B,C,D,Z) = C\{F_3(B,C,Z) - F_3(A,C,Z)\}$$

$$- D\{F_3(B,D,Z) - F_3(A,D,Z)\}$$

$$+ F_9(B,D,Z) - F_9(A,D,Z) - F_9(B,C,Z) + F_9(A,C,Z) .$$

$$J_9^*(A,B,C,D,Z) = F_7(B,D,Z) - F_7(A,D,Z) - F_7(B,C,Z) + F_7(A,C,Z)$$

$$+ F_5(B,D,Z) - F_5(A,D,Z) - F_5(B,C,Z) + F_5(A,C,Z)$$

$$+ Z^2\{F_3(B,D,Z) - F_3(A,D,Z) - F_3(B,C,Z) + F_3(A,C,Z)\}.$$

Obviously, the case when j = 1 follows trivially since

$$J_{m,0}(A,B,C,D,Z) = J_{m,1}(C,D,A,B,Z),$$

$$1 \leqslant m \leqslant 9.$$

Thus only the Z-integration remains to be done, and for the most part standard Gaussian quadrature is used. However, special care must be taken if the integrand ($= Z^{r_i} J_{m,j}(A,B,C,D,Z)$) contains a logarithmic term and either E or F is zero, or nearly zero. In this case $I_i(A,B,C,D,E,F)$ may contain terms of the form

$$\int_E^F Z^{r_i+n} \log Z \, dZ, \quad n \geqslant 0,$$

for which standard Gaussian quadrature will not be sufficient.

This problem can be overcome either by evaluating the log term analytically or by using log-weighted Gaussian quadrature.

Note

The analytic integrals given here are also relevant to the {Z = constant} surface integrals which arise when formulation III of the integral equation is used.

CHAPTER 4: RESULTS AND CONCLUDING REMARKS

4.1 (ψ,χ) Calculation

Three different choices of shape function for χ have been considered. Following the work of Armstrong et al. [1978] we originally took $\tilde{\chi}$ to be piecewise constant, i.e. the susceptibility is assumed to be constant within each volume element. This scheme has the advantage that if formulation III of the integral equation is used, then only surface integrals need to be evaluated (although the integration is over all surfaces of the volume elements). However, first indications were that this scheme would require a large number of elements to obtain a reasonable level of convergence, and this led us to consider a higher order approximation for χ. In fact, we took a linear approximation for χ and assumed that $\tilde{\chi}$ was continuous across element interfaces.

The plate was subdivided into a regular grid and this enabled us to use the economy scheme outlined in Chapter 3. If we had used a graded mesh, with smaller elements near the corners of the plate, for example, then the economy scheme would not have been possible. We denote the discretization by (n_x,n_y,n_z), where n_x is the number of elements in the x-direction of the basic region, and similarly for n_y and n_z. Since the x and y dimensions of the plate were taken to be equal, for convenience and simplicity we also took $n_x = n_y = N$. (In this way a further saving could have been made since our economy scheme was developed for rectangular, rather than square, elements in the xy-plane.) For smaller values

of N (up to 3 or 4) the discretization in the z-direction was found to be important, in the sense that for fixed N, $n_z > 1$ was needed in order to obtain 4 significant figures of agreement in the values of ψ at the common nodes. However, for larger N, $n_z = 1$ was sufficient to obtain agreement to 4 significant figures at nodal ψ values and 2 or 3 significant figures for the nodal χ's.

For a fixed mesh, the nodal values of ψ seemed to converge more rapidly than the nodal χ values. A possible explanation for this is that we took quadratic elements to represent ψ whereas χ was only represented by linear elements. This would indicate that faster convergence might have been obtained if we had chosen quadratic elements for both ψ and χ. The results of our calculations are shown in figures 4.1(a) - 4.1(j) for some typical nodes. Clearly, it is necessary to obtain good approximations to ψ and χ if we want to use these values to compute an approximation to the field.

Computational costs for three-dimensional problems are always high, and can escalate rapidly as the mesh is refined. Thus, refining the grid beyond a certain threshold is not feasible. There are two main stages in the method we have used:

(i) the assembly process to set up the matrix of integral contributions on the FORTRAN direct access file;

(ii) reformulation of the matrix B and solution of the non-linear system.

In Table 4.2 we show the comparative Cray timings for different grids; N indicates the discretization (= (N,N,1)).

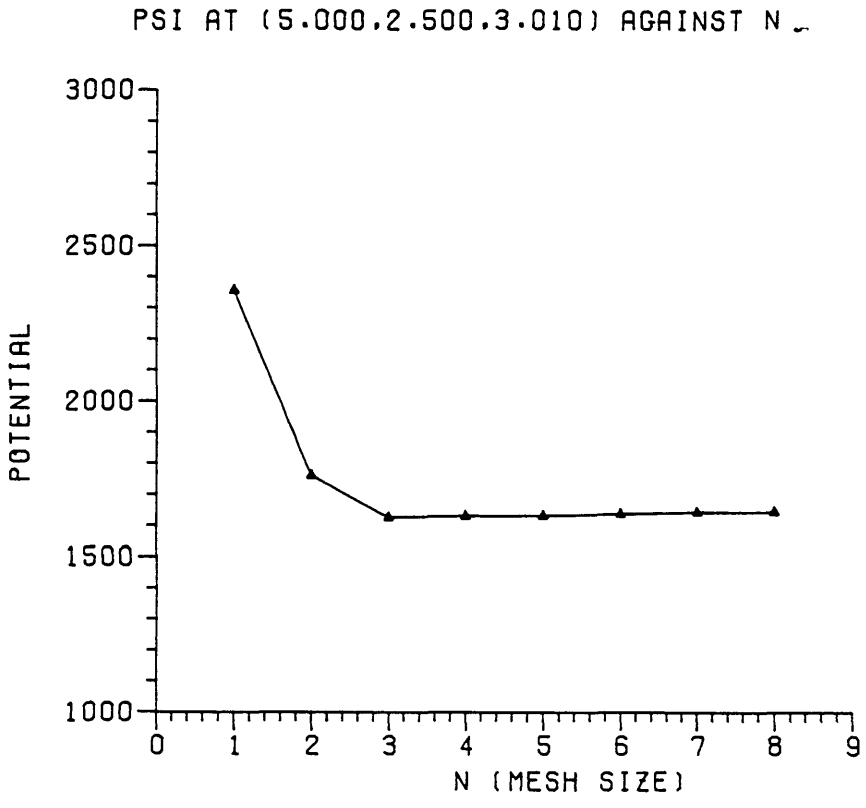


Fig. 4.1(a).

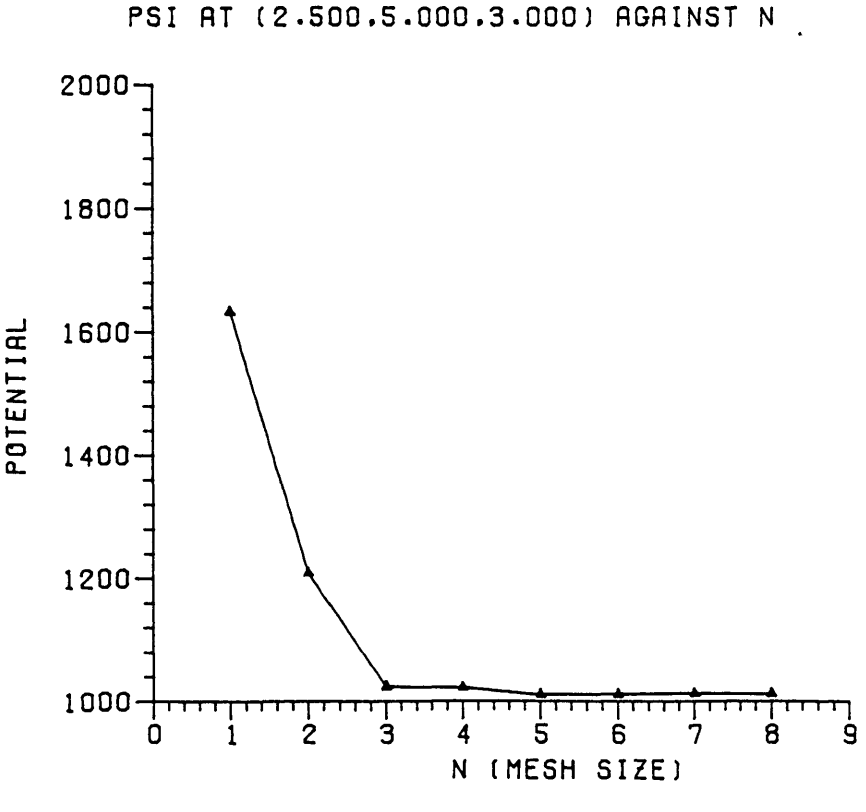


Fig. 4.1(b).

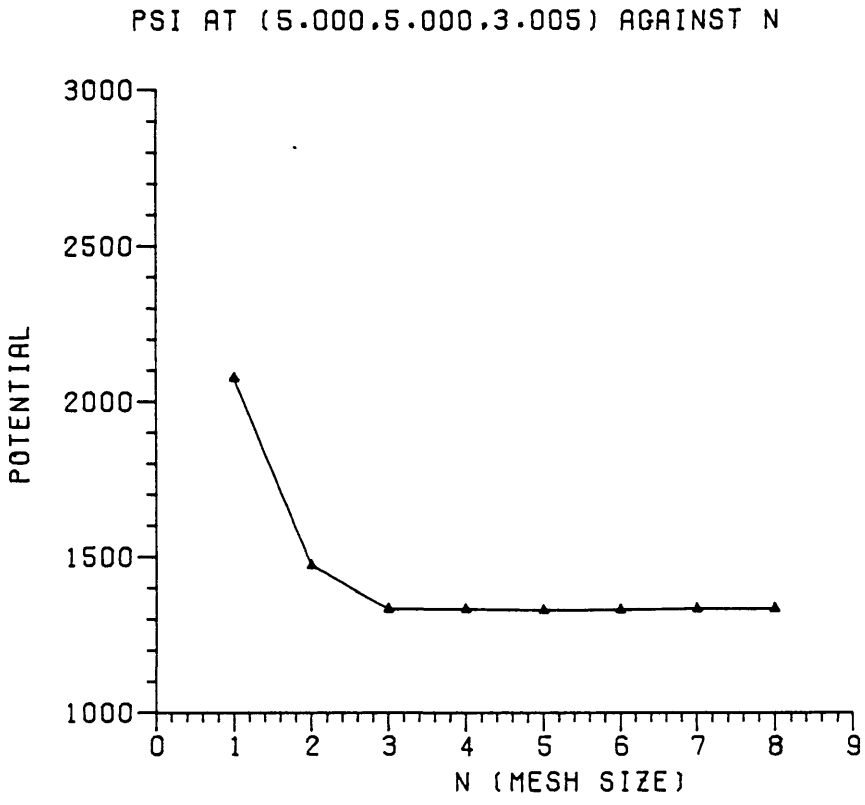


Fig. 4.1(c).

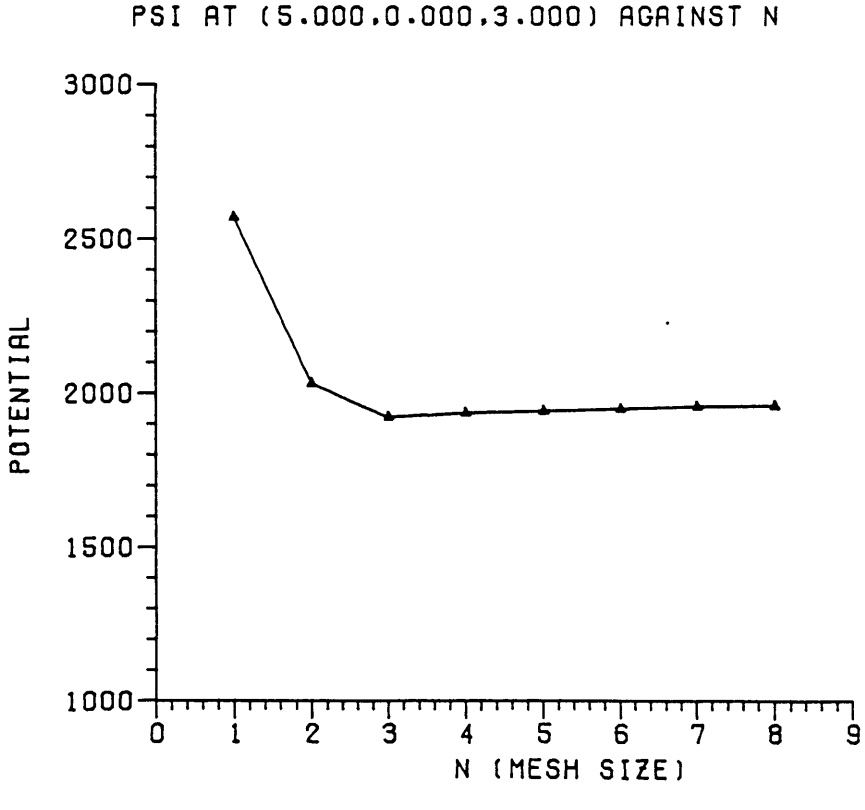


Fig. 4.1(d).

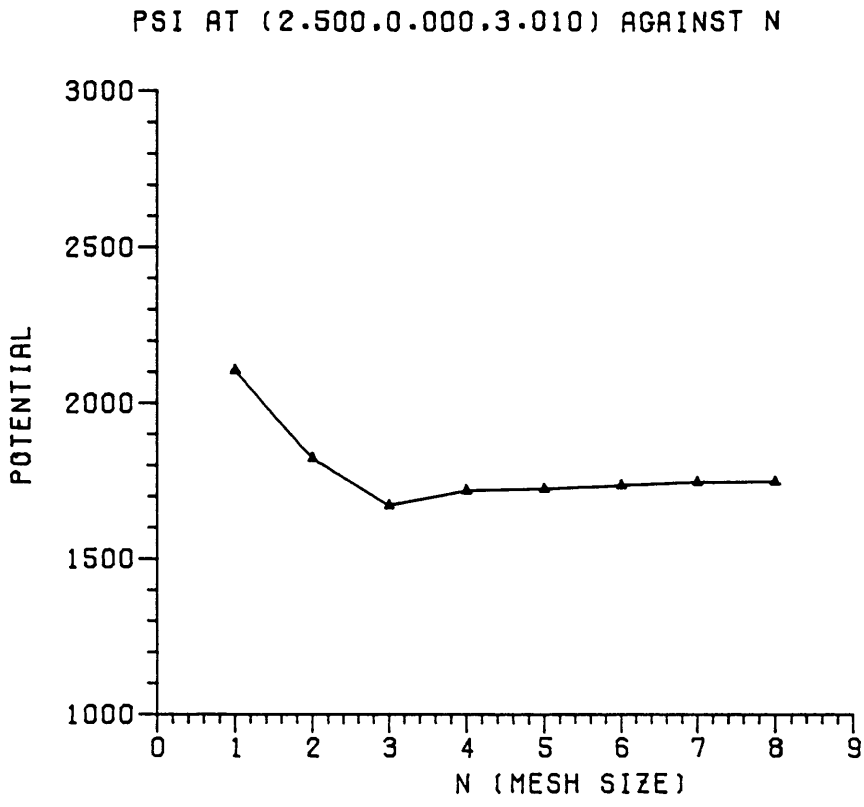


Fig. 4.1(e).

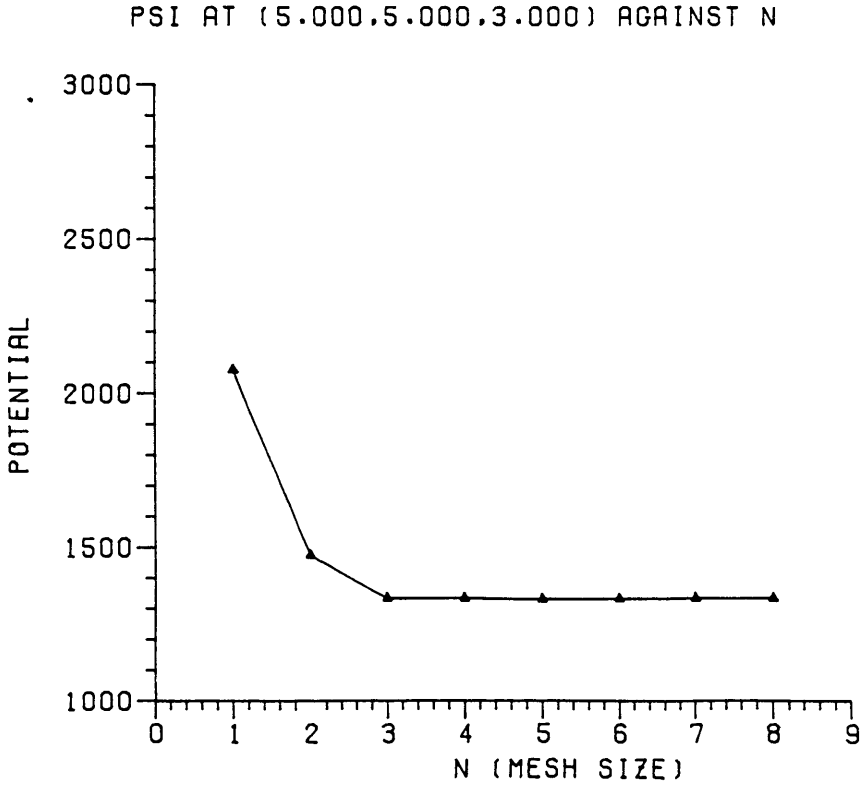


Fig. 4.1(f).

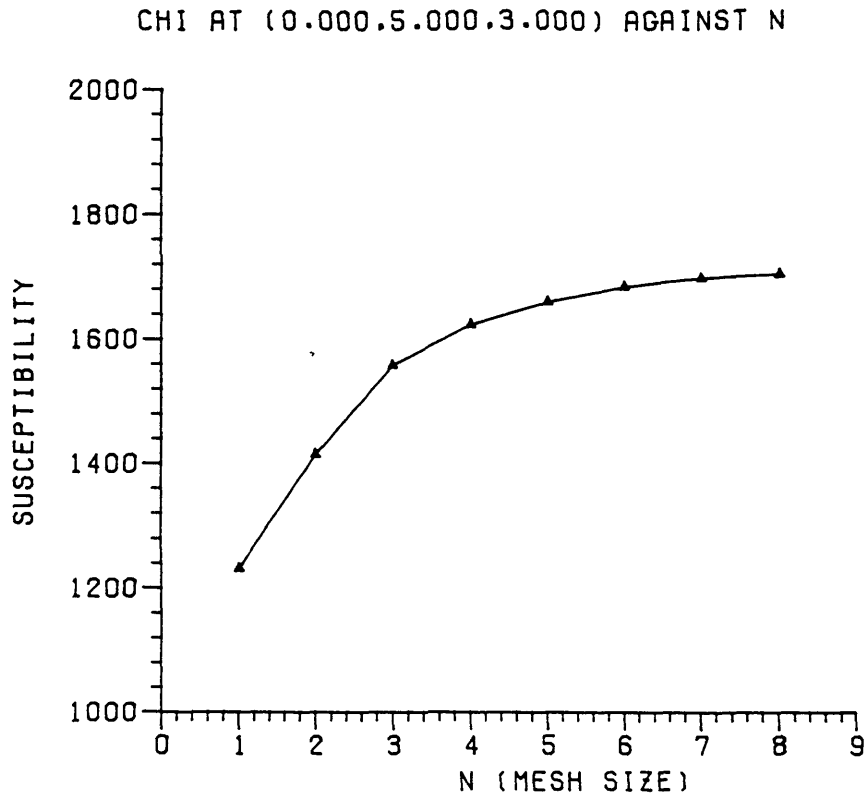


Fig. 4.1(g).

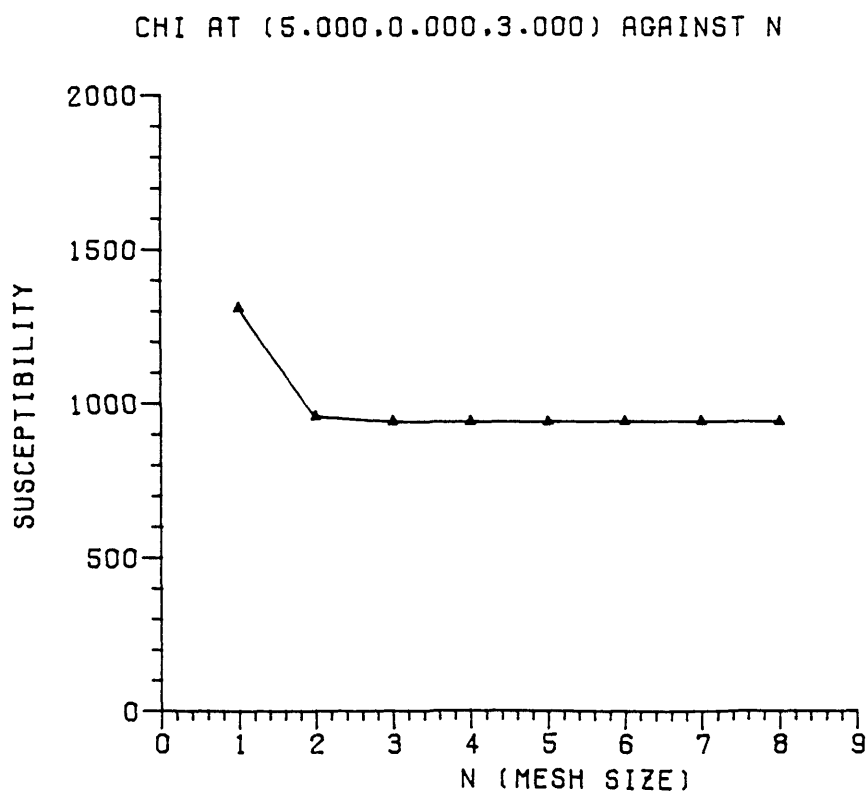


Fig. 4.1(h).

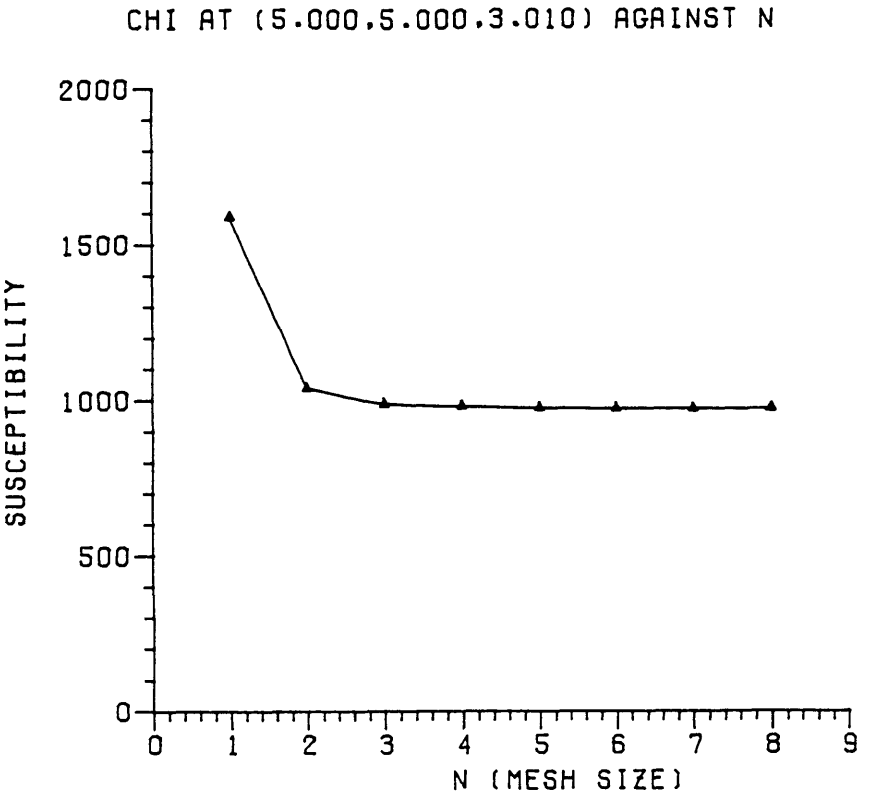


Fig. 4.1(i).

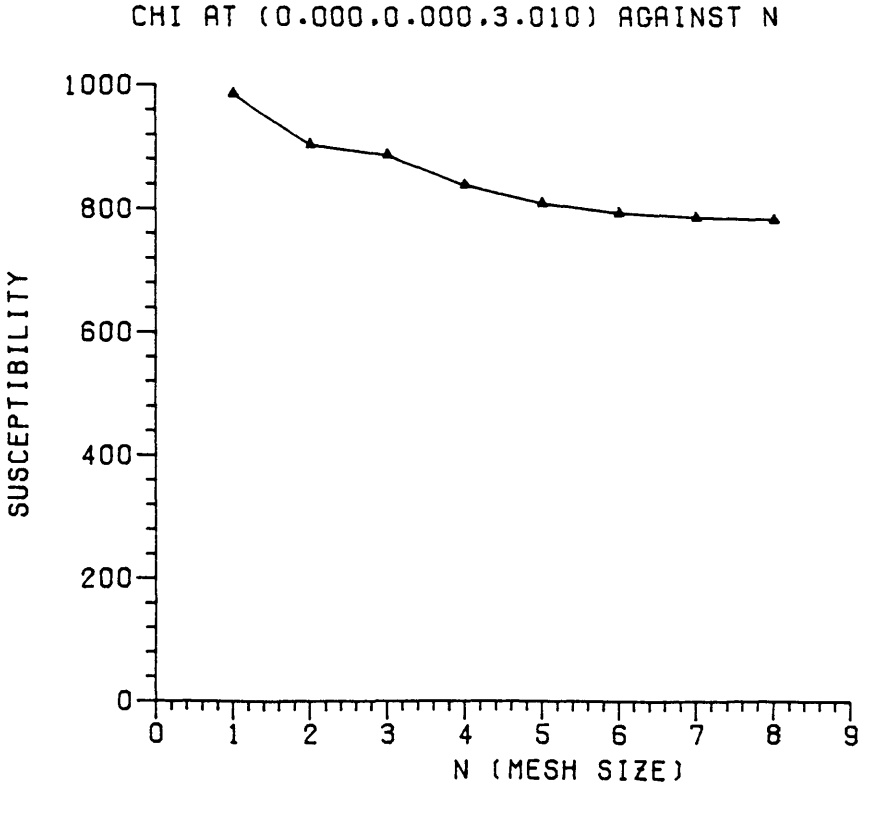


Fig. 4.1(j).

N	SIZE OF MATRIX	SIZE OF NON-LINEAR SYSTEM	SET-UP TIME (SECONDS)	NON-LINEAR SOLVE TIME (SECONDS)	SET-UP TIME / SOLVE TIME
1	12	8	1.39	.034	40.9
2	38	18	6.52	.366	17.8
3	78	32	17.2	1.18	14.6
4	132	50	37.8	7.44	5.08
5	200	72	76.8	26.0	2.95
6	282	98	157.	102. *	-
7	378	128	330.	220. *	-
8	488	162	688.	398.	1.73

Table 4.2: CRAY TIMINGS

These timings are illustrated by figure 4.3.

The set-up time has remained the dominant factor throughout these calculations although the ratio of set-up time to solve time decreases as the mesh is refined. Since the dominant factor in the first stage of the method is the evaluation of the integrals, it would be interesting to compare our mixed analytic and quadrature scheme with the entirely analytic scheme of Collie [1976] in terms of both accuracy and computational cost. By choosing a higher order

---

* Note: A slightly different strategy was used in these cases, and these timings could have been improved.

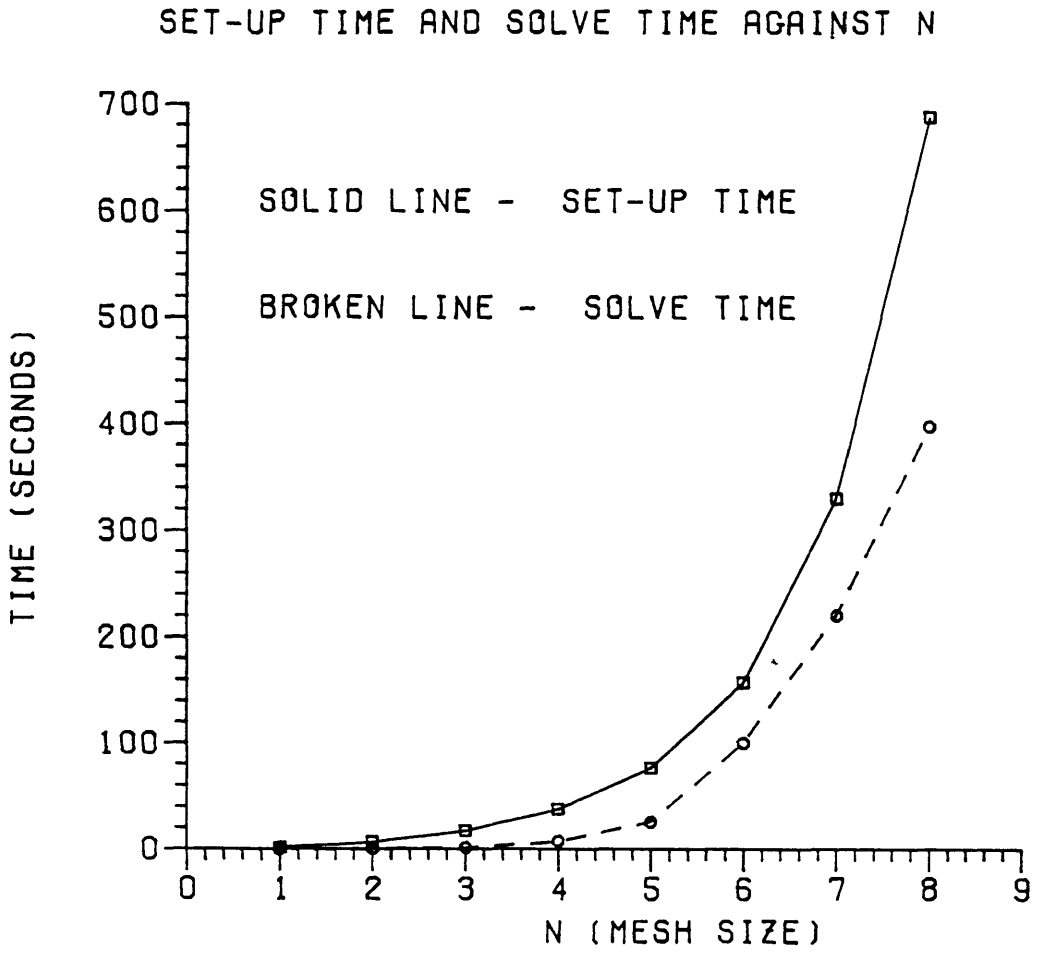


Fig. 4.3. Graph of Cray timings against N,

when the mesh size is (N,N,1).

approximation for χ it may be possible to improve the rate of convergence, but at the same time the cost of setting up the matrix would increase, as would the size and solution cost of the non-linear system. We used the NAG subroutine C05PBF to solve the non-linear system, and Table 4.4 illustrates the number of function evaluations required by the routine for various grids. (The grids are defined by (N,N,n_z).) It is interesting to note that the number of function evaluations required did not increase as the mesh was refined.

n_z \ N	1	2	3	4	5	6	7	8
1	8	10	8	9	11	8	-	9
2	12	7	6	5	7			
3	13	7	6	5				
4	13	7	11					
5	13							

Table 4.4: Number of function evaluations required by C05PBF for grids (N,N,n_z).

One way of giving additional flexibility to $\tilde{\chi}$ without substantially increasing the set-up time is to choose $\tilde{\chi}$ to be linear over each volume element but not necessarily continuous across element interfaces. This is the third possibility we considered. However, limited experiments using this approximation gave no indication that this would significantly improve the rate of convergence.

4.2 Recovery of Fields

In Chapter 3 we outlined possible methods for recovering the field (equivalently the flux density) in free space. We have chosen to use the integral equation for $\underline{H}$ (equation (3.8.2)). Simkin and Trowbridge [1980] have noted that not only is the recovery of fields expensive, but the computed values of the field close to the surface of the magnetic material are strongly affected by the discretization. We have found that while this last remark is true, the computed fields on the z-axis exhibit smooth, if somewhat slow, convergence (figure 4.5). Elsewhere the convergence is not smooth, although reasonable accuracy is apparently obtained some distance from the plate. This is illustrated by figures 4.6(a),(b) and 4.7(a),(b),(c). The smooth convergence of the field at points on the z-axis could perhaps be attributed to the special symmetry properties that these points possess with respect to the plate. The graphs of these fields against N (figure 4.5) indicate that it might be possible to use extrapolation to obtain the converged value. We tried two different extrapolation formulae:

$$\text{(i)} \qquad x_N = x_\infty + \alpha\beta^N;$$

$$\text{(ii)} \qquad x_N = x_\infty + \gamma h^p, \; h \equiv \frac{1}{N},$$

where the grid is defined by (N,N,1) and $x \equiv B_z$. The results of these extrapolations, using the computed fields obtained from grids defined by N = 6,7,8 are shown in Table 4.8.

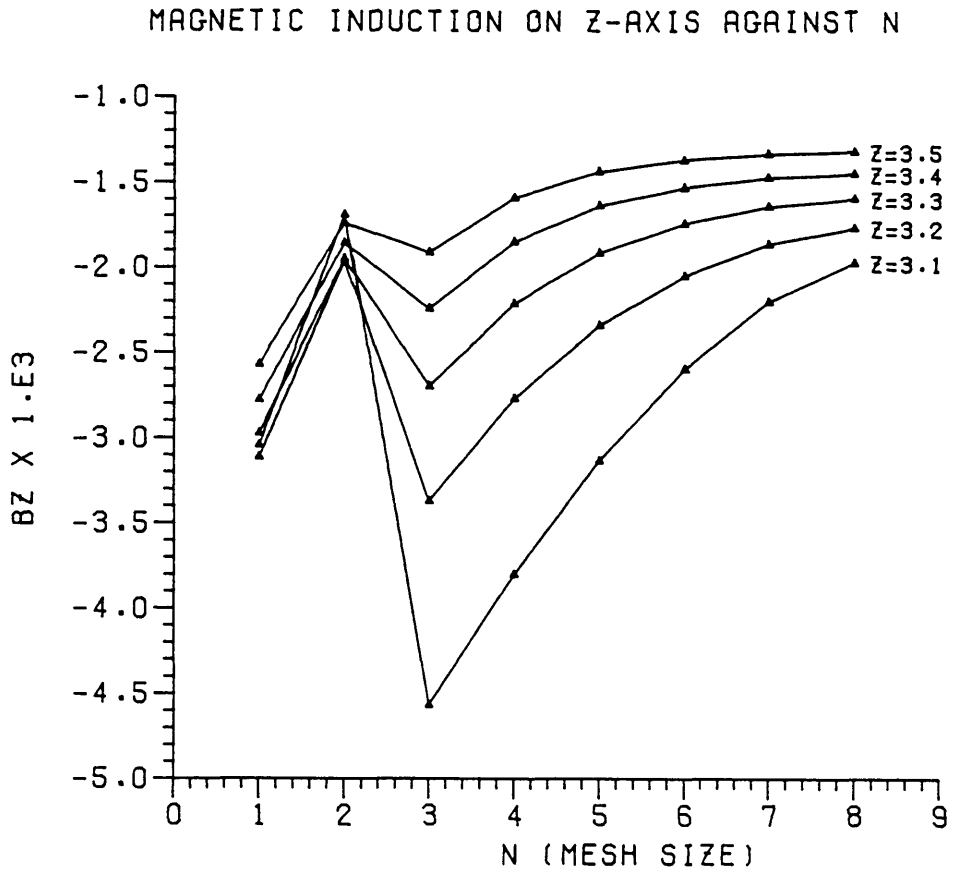

MAGNETIC INDUCTION ON Z-AXIS AGAINST N
BZ X 1.E3
-1.0
-1.5
-2.0
-2.5
-3.0
-3.5
-4.0
-4.5
-5.0
0
1
2
3
4
5
6
7
8
9
N (MESH SIZE)
Z=3.5
Z=3.4
Z=3.3
Z=3.2
Z=3.1

Fig. 4.5.

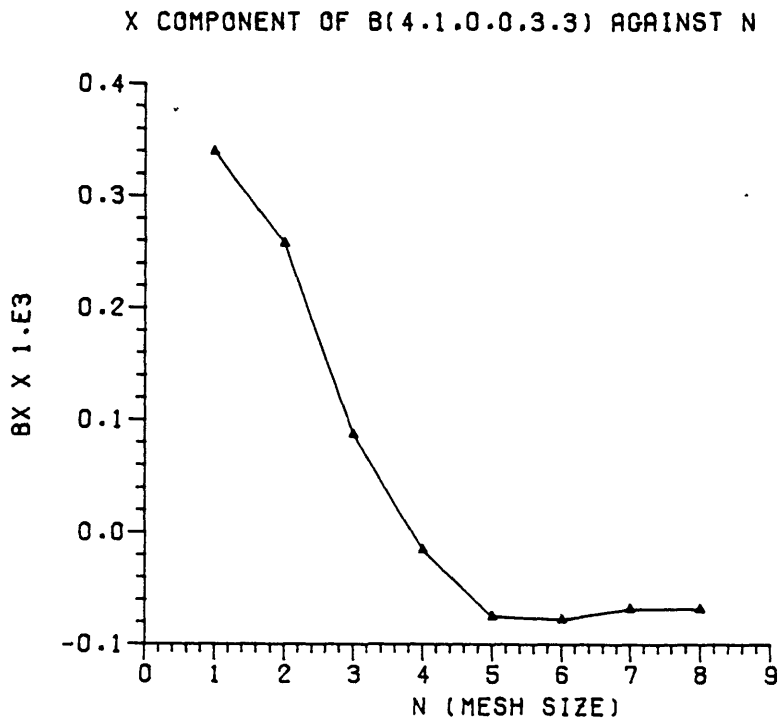


Fig. 4.6(a).

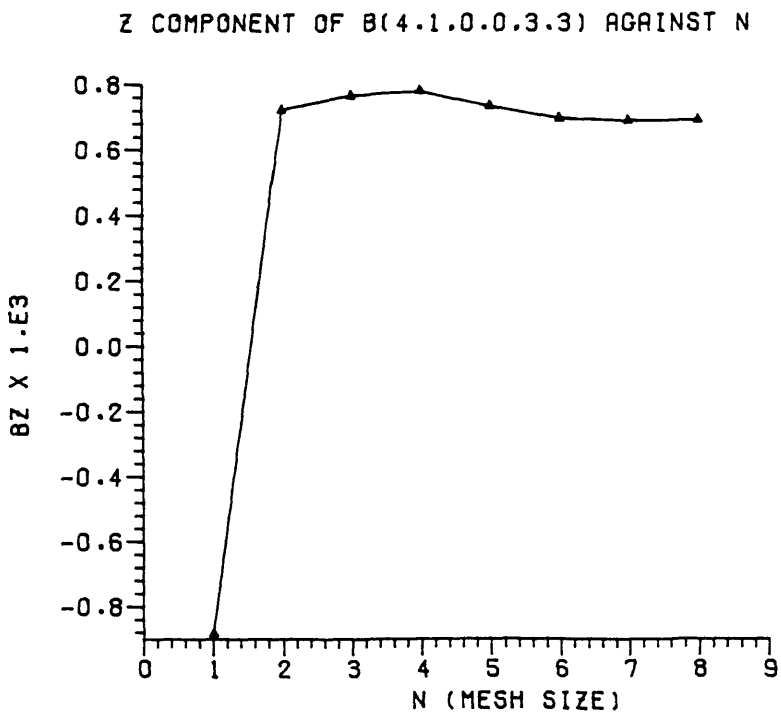


Fig. 4.6(b).

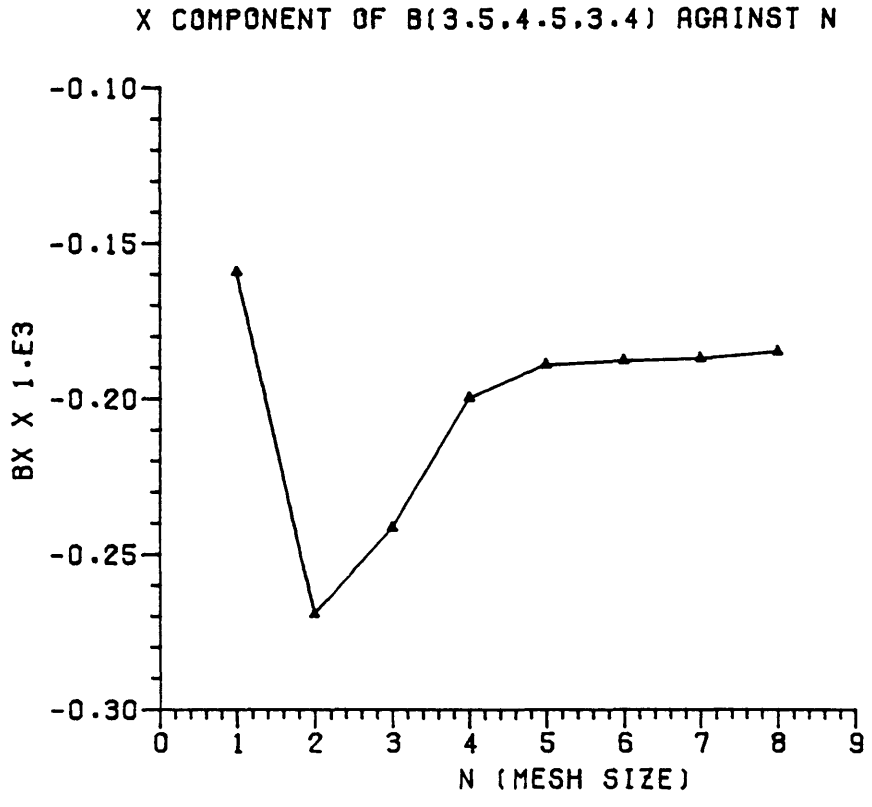


Fig. 4.7(a).

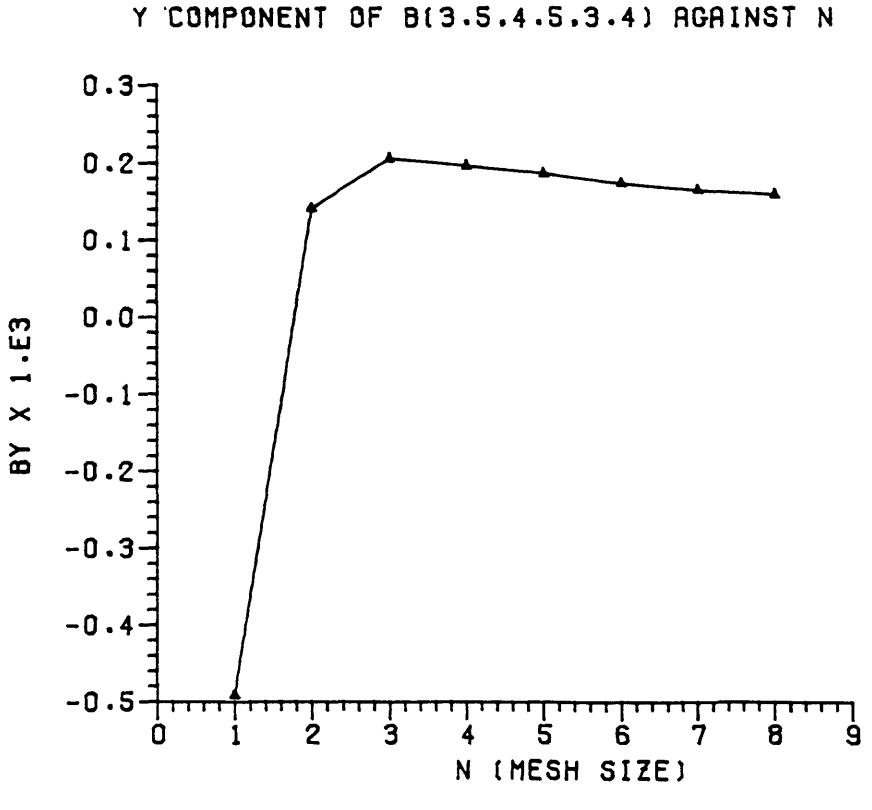


Fig. 4.7(b).

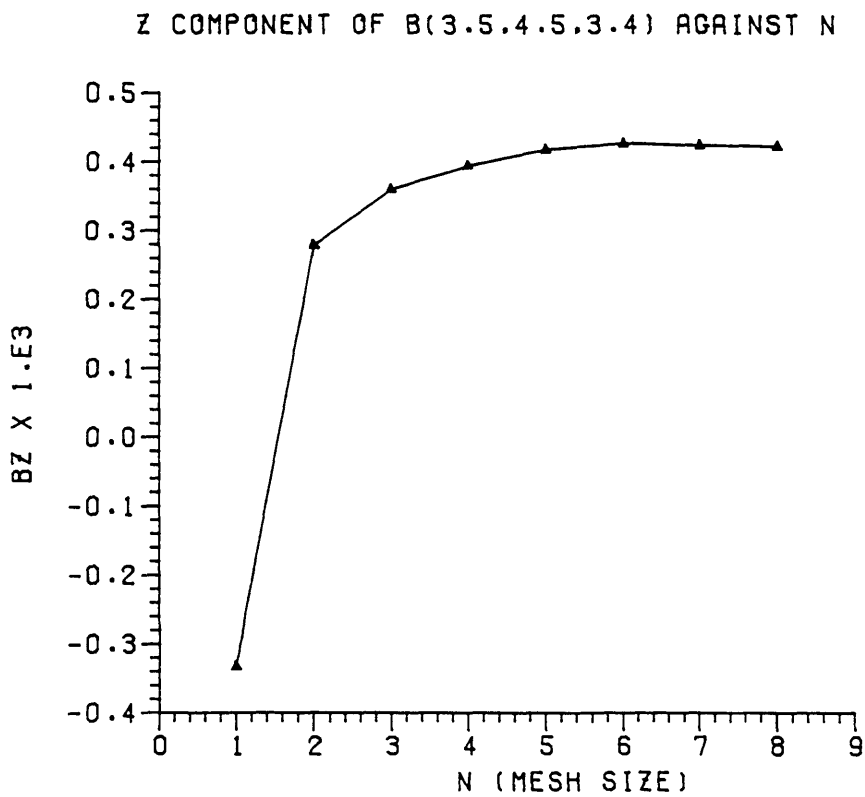

Z COMPONENT OF B(3.5,4.5,3.4) AGAINST N
BZ X 1.E3
0.5
0.4
0.3
0.2
0.1
0.0
-0.1
-0.2
-0.3
-0.4
0
1
2
3
4
5
6
7
8
9
N (MESH SIZE)

Fig. 4.7(c).

z	B_z computed on (8,8,1) grid	$x_\infty^{(i)}$	$x_\infty^{(ii)}$
3.1	- .198 E-2	- .166 E-2	- .146 E-2
3.2	- .177 E-2	- .167 E-2	- .162 E-2
3.3	- .160 E-2	- .156 E-2	- .155 E-2
3.4	- .145 E-2	- .143 E-2	- .143 E-2
3.5	- .132 E-2	- .131 E-2	- .131 E-2

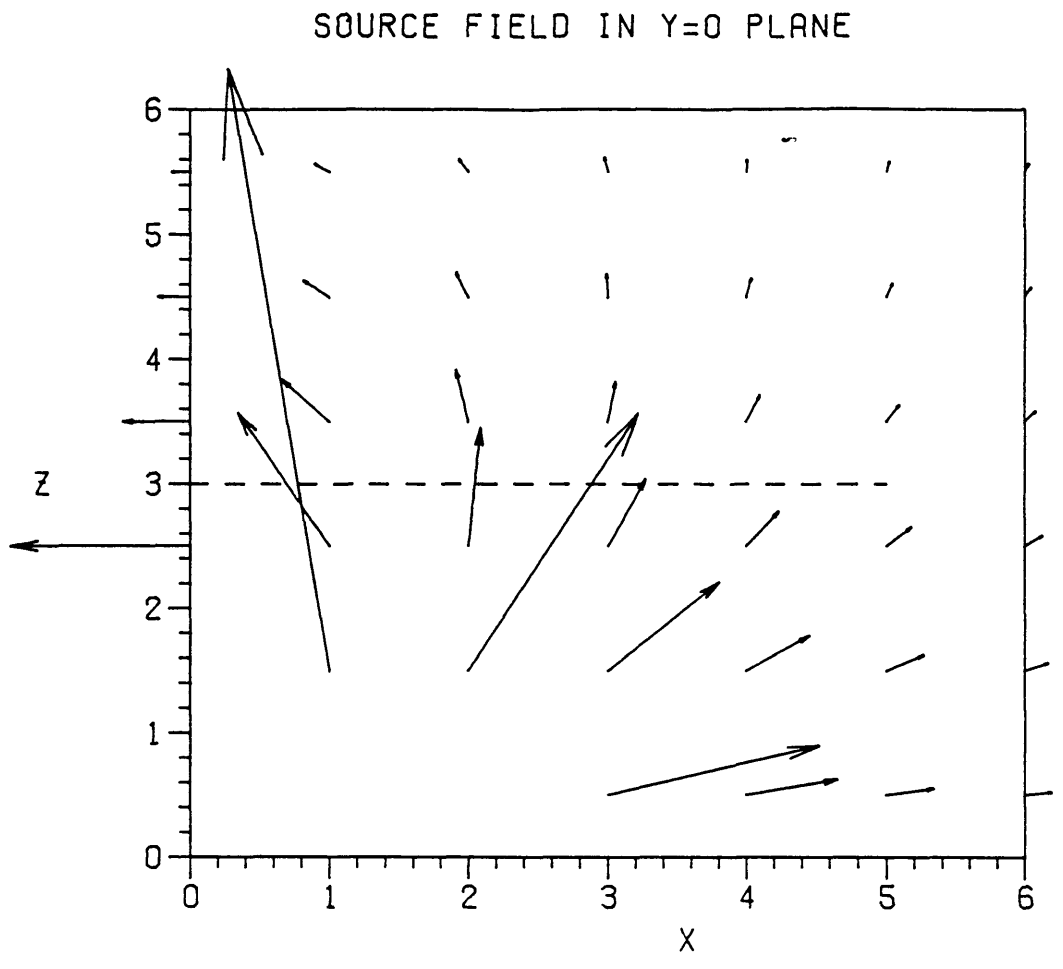
Table 4.8. $|\underline{B}|$ on the z-axis (computed on (8,8,1) grid) compared with extrapolated values.

Clearly, there are still problems with the fields near to the surface of the plate, since there is no reason to prefer one extrapolation formula to the other.

The overall effect of introducing the magnetic shield is shown by figures 4.9 and 4.10, which illustrate the source field and the resultant field in the $\{y = 0\}$ plane. The resultant fields shown in figures 4.9 and 4.10 were calculated using $\tilde{\psi}$ and $\tilde{\chi}$ from the finest mesh we used (= (8,8,1)), and are sufficiently far from the plate to be regarded as 'converged' values. These figures clearly indicate a reduction in the field strength due to the introduction of the plate.

4.3 Conclusion

We have applied the boundary integral equation method to a problem of practical interest in magnetostatics. However, the numerical



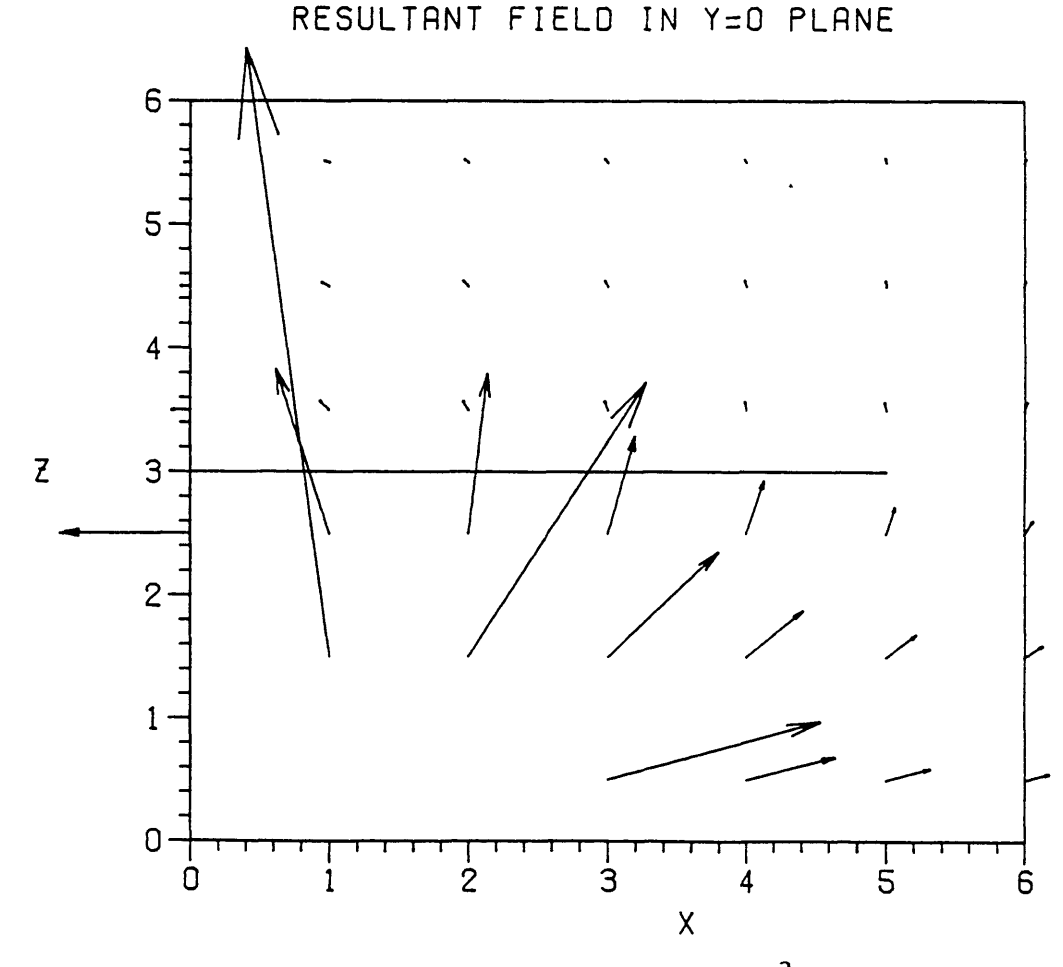
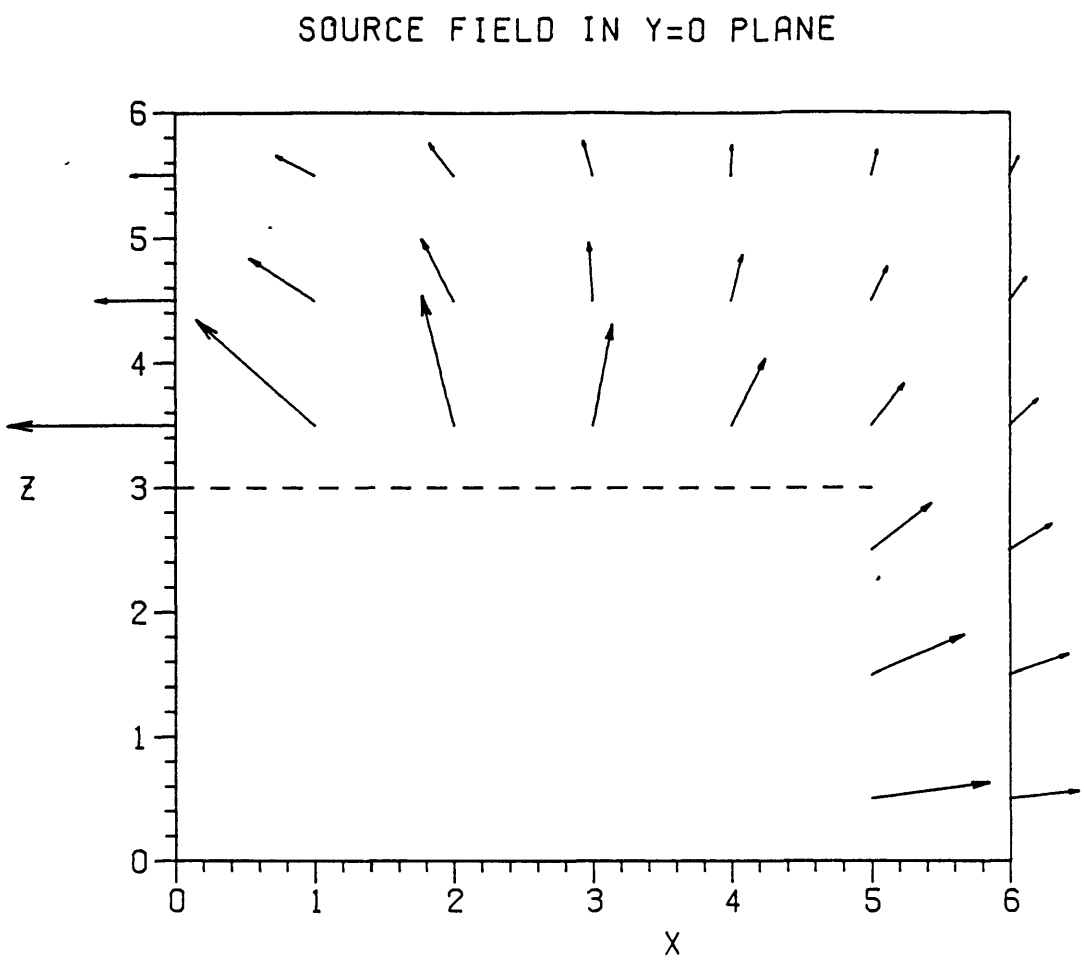


Fig. 4.9. (Scale: 1 cm ~ 5.5 x 10^{-3} Tesla).



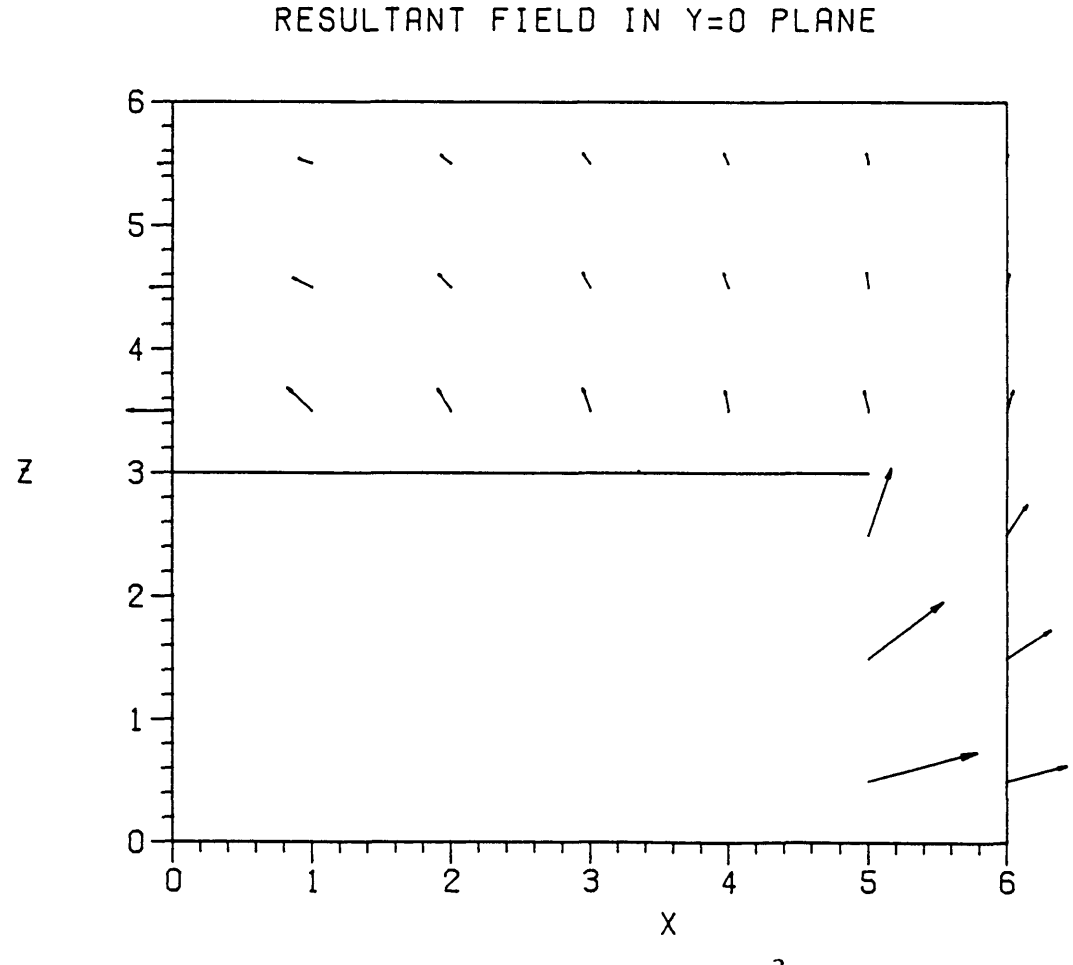


Fig. 4.10. (Scale: 1 cm ~ 2.2 x 10^{-3} Tesla).

techniques we have used are applicable to a wide range of linear and non-linear problems.

Our results for the magnetic screening problem indicate that whilst acceptable convergence can be obtained for the nodal ψ's and χ's, the computed fields confirm the observations of Simkin and Trowbridge [1980] in that they depend on the discretization and are inaccurate near the surface of the plate. However, away from the surface of the plate the fields show some signs of convergence as the mesh is refined, and we might expect the fields computed from the (8,8,1) grid to be reasonably accurate.

Our calculations have indicated that the maximum field strength is on or near the z-axis. Whilst we acknowledge that the field calculations are not accurate near the surface of the plate, we can nevertheless say with some confidence that the maximum value of $|\underline{B}|$ above the plate is greater than 10^{-3} Tesla, which is the required tolerance level. Thus, it would seem that this particular plate of magnetic material would not form a suitable shield.

We recall that one of the main objectives of this work was to determine a screen which would provide adequate shielding for the magnetic scanner. We have seen that the plate used in these calculations (low carbon mild steel of dimensions 10 x 10 x .01 metres, placed at a distance of 3 metres from the magnet centre) would not be sufficient, and this suggests the following ideas for future work:

(i) Vary the dimensions of the rectangular plate, or possibly introduce several layers of metal. This presents a practical (structural) problem - the volume of metal required may be too heavy to be feasible in an existing building.

(ii) Investigate the effect of varying the distance of the plate from the magnet centre, although this will obviously be limited by the size of the room.

(iii) Investigate the effect of varying the shape of the plate. We took a rectangular plate for simplicity and this fact enabled us to evaluate some of the integrals analytically. For curved elements isoparametrics would probably need to be used and the methods for evaluating the integrals would have to be reconsidered. It is possible that special quadrature formulae would be required.

(iv) Choice of magnetic material. We have only considered low-carbon mild steel; it may be that another metal is to be preferred.

Clearly, the choice of formulation (integral or differential) and method of solution (e.g. collocation or weighted-residual) could be important in terms of accuracy and computing costs. In this thesis we have used collocation for the numerical solution of the integral equation (3.2.1). Recent work by Armstrong, Simkin and Trowbridge [1983] has indicated that a Galerkin weighted-residual scheme may give significant improvements in accuracy over collocation methods, for a given amount of computation. However, the results presented in their paper are for linear problems only, and it remains to be seen whether this applies equally to non-linear problems.

CHAPTER 5: PERCOLATION IN GENTLY SLOPING BEACHES

5.1 Introduction

Many problems in applied mathematics can be modelled as ordinary or partial differential equations in domains where part or all of the boundary is to be determined as the solution. Depending on whether the boundary is stationary or moving, these problems are usually referred to as free or moving boundary problems. An example of this type of problem is the flow of liquids and gases in porous media; in particular, the problem of a rectangular dam between two reservoirs has been covered extensively in the literature (see, for example, Elliott and Ockendon [1982]).

In this chapter we apply the boundary integral equation method to a study of percolation in gently sloping beaches. An asymptotic formulation of this problem is given in the paper by Aitchison, Elliott and Ockendon [1983].

5.2 The Model Problem

In this work we assume that the free boundary between the saturated and dry parts of the porous medium (the beach) and the beach surface are nearly in the same horizontal line. If y is the coordinate vertically upwards, then the beach surface is

$$y = 1 + \varepsilon G(x),$$

where $G = O(1)$. The base of the region ($y = 0$) is assumed to be impermeable. The model used by Aitchison, Elliott and Ockendon

has been made dimensionless by referring lengths to a typical beach depth d_0, pressure to $\rho g d_0$ and time to $\frac{\mu}{k\rho g}$, where k is the permeability of the medium, and ρ and μ are the density and viscosity of the liquid respectively. The free boundary is written as

$$y = 1 + \varepsilon F(x,t),$$

where, of course, $F \leqslant G$.

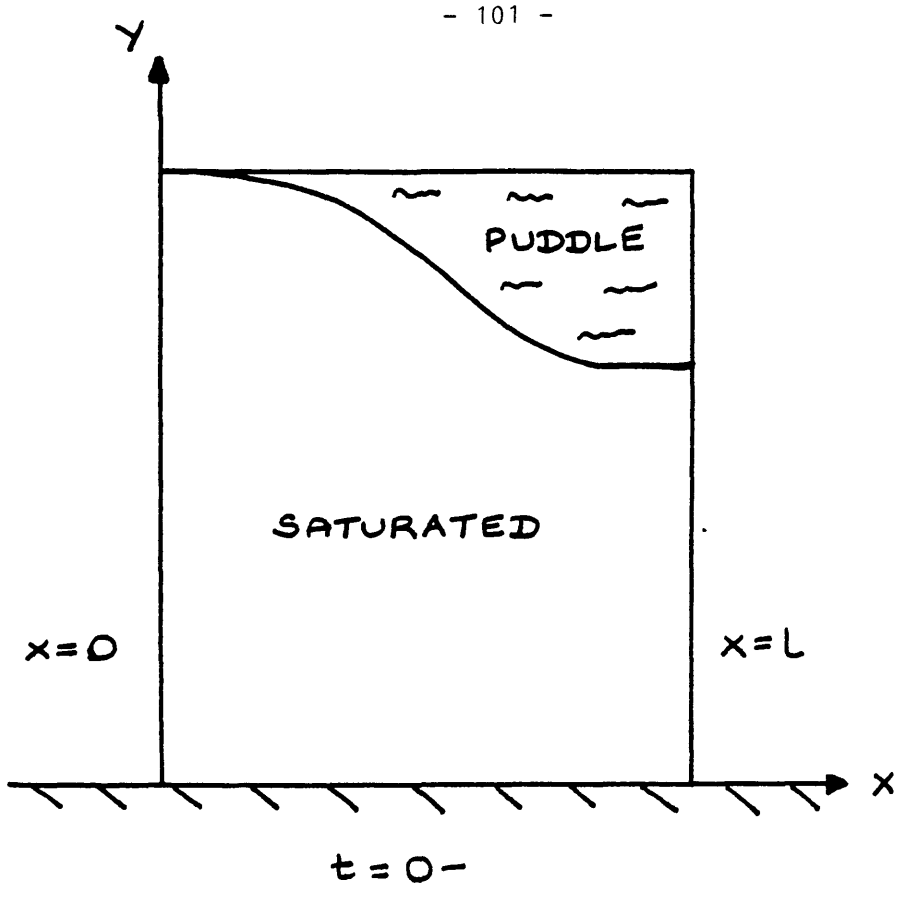
We consider the case when the beach is a sandbank, the height of which is an even periodic function of x, with period 2ℓ. We suppose that the tide flows in the z-direction and that initially the water just covers the sandbank, forming a puddle. By assuming that the percolation time $\frac{\mu}{k\rho g}$ is much longer than the time scale of the ebb, the puddle is, in effect, removed instantaneously. Thus, the initial free boundary lies on the beach surface, i.e.

$$F(x,0) = G(x).$$

We calculate the position of the free boundary F(x,t) for times $t > 0$. Clearly, there is no flux across $x = 0$ and $x = \ell$ and thus we need only consider the region $0 \leqslant x \leqslant \ell$ (Figure 5.1).

5.3 An Asymptotic Formulation

As mentioned previously, an asymptotic formulation of the unsteady problem described in section 5.2 is given in the paper by Aitchison, Elliott and Ockendon [1983]. This enables us to write the problem as:



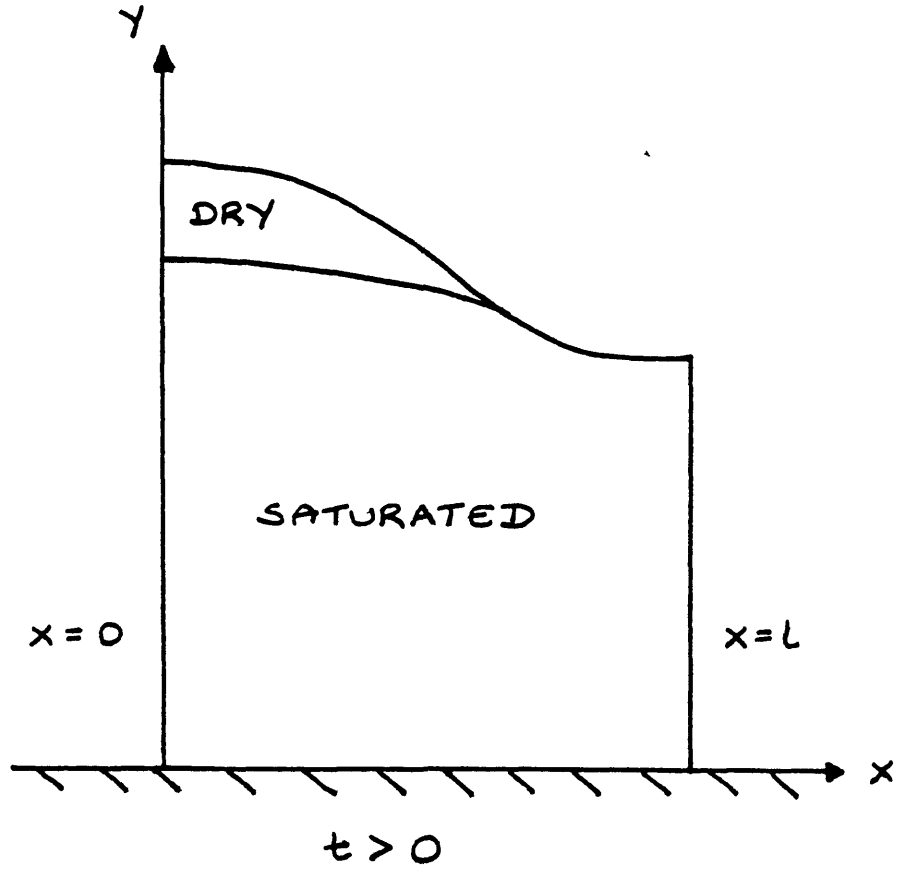


Fig. 5.1. Symmetrical sandbank.

(P): Find u such that

$$\left.\begin{aligned} &\nabla^2 u = 0 \quad \text{in } \Omega \\ &u \leqslant G,\ \frac{\partial u}{\partial t} + \frac{\partial u}{\partial y} \leqslant 0,\quad \left(\frac{\partial u}{\partial t} + \frac{\partial u}{\partial y}\right)(u-G) = 0 \text{ on } \Gamma \\ &\frac{\partial u}{\partial y} = 0 \text{ on } y = -1,\ 0 \leqslant x \leqslant 1 \\ &\frac{\partial u}{\partial x} = 0 \text{ on } x = 0,1 \quad -1 \leqslant y \leqslant 0 \end{aligned}\right\}$$

where

$$\Omega = \{(x,y) : 0 \leqslant x \leqslant 1, \quad -1 \leqslant y \leqslant 0\}$$

and

$$\Gamma = \{(x,y) : 0 \leqslant x \leqslant 1, \quad y = 0\}.$$

The conditions on Γ are known as a linear complementarity system of boundary conditions.

5.4 An Explicit Scheme

The time derivative in the linear complementarity boundary conditions can be replaced by either a forward or backward finite difference, leading to either an implicit or an explicit scheme. We have chosen to use an explicit scheme:

Define $u_\Gamma^0 = G_\Gamma$

and find u_Γ^{n+1} such that

$$u_\Gamma^{n+1} = \min\left(\{ u_\Gamma^n - \Delta t. \frac{\partial u_\Gamma^n}{\partial y}\}, G_\Gamma\right).$$

Thus, at each time step the problem reduces to solving Laplace's equation in the domain Ω, with Dirichlet boundary conditions on Γ and homogeneous Neumann boundary conditions on the other three sides.

In the remaining sections of this chapter we outline how this problem can be solved using the boundary integral equation method, and present results for the beach $G(x) = \cos \pi x$.

5.5 The Boundary Integral Equation

A version of the boundary integral equation method which is suitable for elliptic boundary value problems is described in the paper by Xanthis, Bernal and Atkinson [1981]. The formulation is also given here for completeness.

Let Ω denote a bounded open region in $\mathbb{R}^2$, with boundary $\partial\Omega$ and let

$$\partial\Omega = \overline{\partial\Omega_1 \cup \partial\Omega_2}$$

where

$$\partial\Omega_1 \cap \partial\Omega_2 = \varphi.$$

Further, let $u(\underline{x})$ satisfy

$$\nabla^2 u = 0 \quad \text{in } \Omega \tag{5.5.1}$$

$$u = \bar{u} \text{ on } \partial\Omega_1 \tag{5.5.2}$$

$$\frac{\partial u}{\partial n} = \bar{t} \text{ on } \partial\Omega_2 \tag{5.5.3}$$

where $\bar{u}$ and $\bar{t}$ are given functions, and $\frac{\partial u}{\partial n}$ is the outward normal derivative of u.

Let $\underline{x} \in \partial\Omega$ and define $\omega(\underline{x},\varepsilon)$ as the disc of radius ε centred at $\underline{x}$, i.e.

$$\omega(\underline{x},\varepsilon) \equiv \{\underline{y} : |\underline{x} - \underline{y}| \leqslant \varepsilon\} .$$

Further, define $\Omega(\underline{x},\varepsilon)$ as the region obtained from Ω by deleting the region $\omega(\underline{x},\varepsilon) \cap \Omega$. Let $\partial\Omega(\underline{x},\varepsilon)$ be the boundary of $\Omega(\underline{x},\varepsilon)$ (see figure 5.2). If we take

$$v(\underline{x},\underline{y}) = \frac{1}{2\pi} \ln \left(\frac{1}{r}\right), \text{ where } r = |\underline{x} - \underline{y}|$$

then u and v are both harmonic in $\Omega(\underline{x},\varepsilon)$ and so by Green's third identity (see Appendix A.5) we have

$$\int_{\partial\Omega(\underline{x},\varepsilon)} \{u \frac{\partial v}{\partial n} - v \frac{\partial u}{\partial n}\} \, dS = 0. \qquad (5.5.4)$$

On taking the limit $\varepsilon \to 0$ in (5.5.4), then, provided

$$\lim_{\varepsilon \to 0} \varepsilon \ln \varepsilon \int_{\partial\omega \cap \Omega} \frac{\partial u}{\partial n} \, dS = 0, \qquad (5.5.5)$$

we obtain

$$\oint [u(\underline{y}) - u(\underline{x})] \frac{\partial v}{\partial n} \, dS_{\underline{y}} = \oint v \frac{\partial u}{\partial n} \, dS_{\underline{y}} \qquad (5.5.6)$$

$$\forall \underline{x} \in \partial\Omega$$

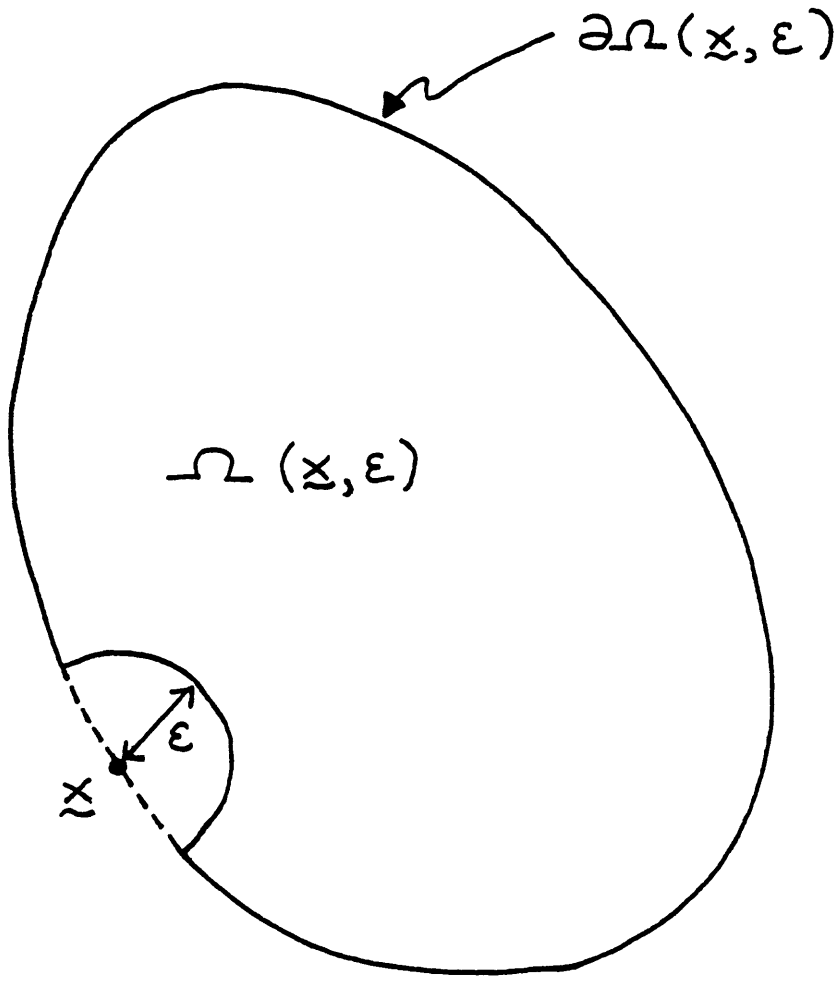


Fig. 5.2. The region $\Omega(\underline{x},\varepsilon)$.

where

$$\int f(\underline{x},\underline{y})\, dS_{\underline{y}} = \lim_{\epsilon \to 0} \int_{\partial\Omega \cap \partial\Omega(\underline{x},\epsilon)} f(\underline{x},\underline{y})\, dS_{\underline{y}}.$$

Note that condition (5.5.5) is satisfied if $|\nabla u(\underline{x})|$ is bounded for $\underline{x} \in \Omega$.

If we now let $U(\underline{x},\underline{y}) \equiv v(\underline{x},\underline{y})$ for $\underline{y} \in \partial\Omega$, and let

$$T(\underline{x},\underline{y}) \equiv \nabla_{\underline{y}}\, v(\underline{x},\underline{y}).\underline{n}(\underline{y})$$

where $\underline{n}(\underline{y})$ is the outward unit normal at $\underline{y}$, then (5.5.6) can be written as

$$\int T(\underline{x},\underline{y})\, [u(\underline{y}) - u(\underline{x})]\, dS_{\underline{y}} = \int U(\underline{x},\underline{y})\, \frac{\partial u}{\partial n}(\underline{y})\, dS_{\underline{y}}, \qquad (5.5.7)$$

$$\forall \underline{x} \in \partial\Omega$$

In a similar fashion one can obtain an integral equation valid for $\underline{x} \in \Omega$, namely

$$u(\underline{x}) + \int_{\partial\Omega} T(\underline{x},\underline{y}) u(\underline{y})\, dS_{\underline{y}} = \int_{\partial\Omega} U(\underline{x},\underline{y})\, \frac{\partial u}{\partial n}(\underline{y})\, dS_{\underline{y}} \qquad (5.5.8)$$

Using the boundary integral equation (5.5.7) and the boundary conditions (5.5.2) and (5.5.3) one can obtain approximations to u and $\frac{\partial u}{\partial n}$ on the boundary $\partial\Omega$, and then use equation (5.5.8) to compute an approximation to u at any interior point of Ω.

5.6 Discretization and Solution Methods

For the percolation problem the region Ω is defined by

$$\Omega \equiv \{(x,y) : 0 \leqslant x \leqslant 1, \quad -1 \leqslant y \leqslant 0\},$$

with Dirichlet boundary conditions on $\partial\Omega_1$, where

$$\partial\Omega_1 \equiv \Gamma = \{(x,y) : 0 \leqslant x \leqslant 1, \quad y = 0\}$$

and homogeneous Neumann boundary conditions on the remaining three sides.

The boundary $\partial\Omega$ is sub-divided into elements and we assume that the elements and nodes are numbered anti-clockwise from the point (1,0). In this work, quadratic elements have been used. We define n to be the total number of nodes and q the number of nodes on Γ (see figure 5.3).

We now assume an approximate solution to the boundary integral equation (5.5.7) of the form

$$\left.\begin{aligned} \tilde{u}(\underline{x}) &= \sum_{\ell=1}^{n} u_\ell \, v_\ell^{(u)}(\underline{x}) \\ \tilde{t}(\underline{x}) &= \sum_{m=1}^{n'} t_m \, v_m^{(t)}(\underline{x}) \end{aligned}\right\} \qquad (5.6.1)$$

where $v_\ell^{(u)}$ and $v_m^{(t)}$ are computationally convenient functions which reflect the behaviour of u and t ($\equiv \frac{\partial u}{\partial n}$) as far as possible. In particular, since u is continuous throughout the domain Ω, whereas t may have discontinuities (for example, at corners), it seems sensible

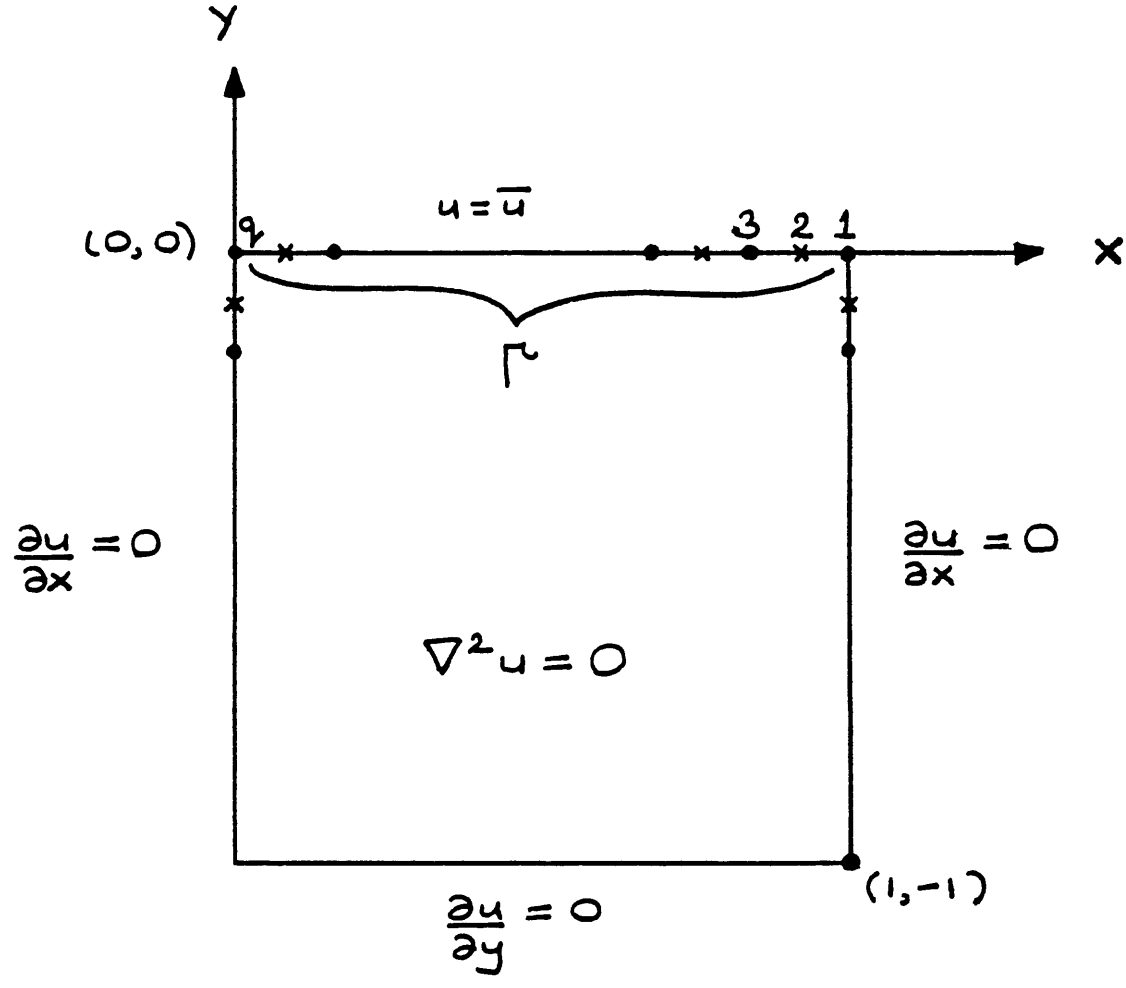


Fig. 5.3. Diagram of the region Ω, showing the discretization and node-numbering on Γ.

to choose the $v^{(u)}$'s to be continuous and the $v^{(t)}$'s such that one can represent functions with discontinuities at selected points on the boundary. Further discussion on the choice of approximating functions is given later.

On substituting the expressions for $\tilde{u}$ and $\tilde{t}$ into the integral equation (5.5.7) one obtains

$$\sum_{\ell=1}^{n} u_\ell \int T(\underline{x},\underline{y})[v_\ell^{(u)}(\underline{y}) - v_\ell^{(u)}(\underline{x})]\, dS_{\underline{y}}$$

$$= \sum_{m=1}^{n'} t_m \int U(\underline{x},\underline{y})\, v_m^{(t)}(\underline{y})\, dS_{\underline{y}}. \qquad (5.6.2)$$

Of course, (5.6.2) will not be satisfied exactly for all $\underline{x} \in \partial\Omega$. However, if we demand that (5.6.2) is satisfied exactly at the nodes $\underline{x}^{(k)}$, $k = 1,2,\ldots,n$, then we have

$$\left.\begin{aligned} &\sum_{\ell=1}^{n} T_{k\ell}\, u_\ell = \sum_{m=1}^{n'} U_{km}\, t_m \qquad k = 1,2,\ldots,n \\ &\text{where} \\ &T_{k\ell} \equiv \int T(\underline{x}^{(k)},\underline{y})\, [v_\ell^{(u)}(\underline{y}) - v_\ell^{(u)}(\underline{x}^{(k)})]\, dS_{\underline{y}} \\ &U_{km} \equiv \int U(\underline{x}^{(k)},\underline{y})\, v_m^{(t)}(\underline{y})\, dS_{\underline{y}} \end{aligned}\right\} \qquad (5.6.3)$$

i.e. n linear equations for (n + n') unknowns. We now show that the remaining n' equations can be obtained from the boundary conditions. Returning to figure 5.3 we see that it would be sensible to assume

that $\frac{\partial u}{\partial n}$ is continuous at all nodes except (1,0) and (0,0), i.e. nodes 1 and q. Therefore, we define n', the number of t unknowns, as

$$n' = n + 2,$$

and thus the total number of unknowns becomes 2n + 2. However, there are q Dirichlet boundary conditions and (n - q + 2) Neumann boundary conditions which give us the additional (n + 2) equations.

5.7 Choice of Approximating Functions

It is often necessary in boundary integral equation methods to define an approximation to the boundary $\partial\Omega$. However, in this case the boundary is particularly simple and each element can be represented parametrically by

$$\underline{x}^e(\xi) = (x^e(\xi), y^e(\xi)) \qquad \xi \in [0,1].$$

If we now define

$$v_\ell^{(u)}(\underline{x}(\xi)) = \begin{cases} 0 & \text{unless } \underline{x} \text{ belongs to an element having } \ell \text{ as a node} \\ N_j(\xi) & \text{when } \underline{x} \in e \text{ and } \ell \text{ is the j-th node of e} \end{cases}$$

where the $N_j(\xi)$, $1 \leqslant j \leqslant 3$, are the quadratic Lagrangian polynomials, it follows that

$$\left.\begin{array}{ll} \text{(i)} & v_k^{(u)}(\underline{x}_\ell) = \delta_{k\ell} \quad \text{(and hence } \tilde{u}(x_\ell) = u_\ell\text{)}; \\ \text{(ii)} & \{v_k^{(u)}\} \text{ are continuous, piecewise polynomial and have compact support;} \\ \text{(iii)} & \sum_\ell v_\ell^{(u)}(\underline{x}) = 1. \end{array}\right\} \qquad (5.7.1)$$

The basis functions $v_\ell^{(t)}(\underline{x}(\xi))$ can be defined in an analogous fashion, although we now relax the continuity condition at nodes 1 and q. Thus we define

$$v_\ell^{(t)}(\underline{x}(\xi)) \equiv v_\ell^{(u)}(\underline{x}(\xi)), \quad \ell \neq 1, \quad \ell \neq q,$$

and in order to allow t to be discontinuous at node q we define

$$v_{q_1}^{(t)}(\underline{x}(\xi)) = \begin{cases} v_q^{(u)}(\underline{x}(\xi)) & \underline{x} \in \Gamma \\ 0 & \text{otherwise} \end{cases}$$

and

$$v_{q_2}^{(t)}(\underline{x}(\xi)) = \begin{cases} 0 & \underline{x} \in \Gamma \\ v_q^{(u)}(\underline{x}(\xi)) & \text{otherwise} \end{cases}$$

The discontinuity in t at node 1 is dealt with in a similar manner.

5.8 Final System of Equations

Equation (5.6.3) can be written in matrix notation as

$$T\underline{u} = U\underline{t}$$

or

$$\underset{q}{\overset{\longleftrightarrow}{}} \quad \underset{n-q}{\overset{\longleftrightarrow}{}}$$

$$n\updownarrow\left[\begin{array}{c|c} T^{(1)} & T^{(2)} \end{array}\right] \begin{bmatrix} \underline{u}^{(1)} \\ \hline \underline{u}^{(2)} \end{bmatrix} \begin{matrix} \updownarrow q \\ \updownarrow n-q \end{matrix}$$

$$= n\updownarrow\left[\begin{array}{c|c} U^{(1)} & U^{(2)} \end{array}\right] \begin{bmatrix} \underline{t}^{(1)} \\ \hline \underline{t}^{(2)} \end{bmatrix} \begin{matrix} \updownarrow q \\ \updownarrow n+2-q \end{matrix} \qquad (5.8.1)$$

Substituting the known boundary conditions ($\underline{u}^{(1)} = \bar{\underline{u}}^{(1)}$, $\underline{t}^{(2)} = \underline{0}$) into (5.8.1) gives the linear system

$$n\updownarrow\left[\begin{array}{c|c} T^{(2)} & -U^{(1)} \end{array}\right] \begin{bmatrix} \underline{u}^{(2)} \\ \hline \underline{t}^{(1)} \end{bmatrix} \begin{matrix} \updownarrow n-q \\ \updownarrow q \end{matrix} = \underset{nx1}{\left[-T^{(1)}\bar{\underline{u}}^{(1)}\right]} \qquad (5.8.2)$$

to be solved for $[\underline{u}^{(2)^T} \; \underline{t}^{(1)^T}]$.

5.9 Evaluation of the Integrals

In the program to compute the unknowns from equation (5.8.2) an element-by-element assembly process similar to that of standard finite element calculations is used. The integrals over each element are evaluated using appropriate Gaussian quadrature formulae. [Tables of Gaussian quadrature points and weights are given in Stroud and Secrest, 1966.]

On element e the contribution to $U_{km(e,j)}$ is

$$\int_0^1 U(\underline{x}^{(k)}, \underline{x}^e(\xi))\, N_j(\xi)\, \frac{dS^e(\xi)}{d\xi}\, d\xi \qquad (5.9.1)$$

where

$$\frac{dS^e(\xi)}{d\xi} = \left| \frac{d\underline{x}^e(\xi)}{d\xi} \right|$$

and

$$U(\underline{x},\underline{y}) = \frac{1}{2\pi} \ln \left(\frac{1}{r}\right), \quad r = |\underline{x} - \underline{y}|.$$

If $k \notin e$ then the integral in (5.9.1) is well-behaved and can be evaluated using standard Gaussian quadrature. However, if k is a node of element e then

$$\underline{x}^{(k)} = \underline{x}^e(\xi^*), \quad \text{for some } \xi^* \in [0,1].$$

Let

$$I^* = -\frac{1}{2\pi} \int_0^1 \ln |\underline{x}^e(\xi^*) - \underline{x}^e(\xi)|\, f(\xi)\, d\xi\,, \qquad (5.9.2)$$

$$f(\xi) = N_j(\xi)\, \frac{dS^e(\xi)}{d\xi}.$$

Then I^* will have a logarithmic singularity at $\xi = \xi^*$. However, the singularity can be "subtracted out" by rewriting (5.9.2) as

$$I^* = -\frac{1}{2\pi} \int_0^1 \ln \left| \frac{\underline{x}^e(\xi^*) - \underline{x}(\xi)}{\xi^* - \xi} \right| f(\xi)\, d\xi$$

$$-\frac{1}{2\pi} \int_0^1 \ln |\xi^* - \xi|\, f(\xi)\, d\xi \qquad (5.9.3)$$

[see, for example, Hsiao, Kopp and Wendland, 1980]. The first integral in (5.9.3) is regular, since

$$\lim_{\xi \to \xi^*} \left| \frac{\underline{x}(\xi^*) - \underline{x}(\xi)}{\xi^* - \xi} \right| = |\underline{x}'(\xi^*)|$$

and, after a simple change of variables, the second integral can be evaluated using a combination of standard and log Gaussian quadrature.

The problem of singularities does not arise in the calculation of the integrals $T_{k\ell}$, if one notices that $\underline{u} = \{\text{constant}\}$ and $\underline{t} = \underline{0}$ provide an exact solution of the integral equation (5.5.7). This, together with (5.7.1), implies that

$$\sum_{\ell} T_{k\ell} = 0$$

and hence T_{kk} can be computed as

$$- \sum_{\ell \neq k} T_{k\ell} \ .$$

If $\ell = (e,j) \neq k$, then the contribution to $T_{k(e,j)}$ is

$$\int_0^1 T(\underline{x}^{(k)}, \underline{x}^{(e)}(\xi))\ N_j(\xi)\ \frac{dS(\xi)}{d\xi}\ d\xi$$

and this is evaluated using standard Gaussian quadrature.

5.10 Time-Stepping Algorithm

For a particular discretization, the algorithm for the time-stepping problem is therefore

define time-step Δt

set initial Dirichlet boundary condition:

$\{\underline{u}\}_i = \{G_\Gamma\}_i$, $i = 1,2,\ldots,q$

set up B.I.E. matrix and find its LU decomposition

time-stepping loop (N)

solve B.I.E. system for $\underline{u}_N^{(2)}$, $\underline{t}_N^{(1)}$

update Dirichlet boundary condition:

$\{\underline{u}_{N+1}^{(1)}\}_i = \min(\{\underline{G}_\Gamma\}_i, \{\underline{u}_N^{(1)} - \Delta t.\underline{t}_N^{(1)}\}_i)$

The free boundary at time step N is given by $\underline{u}_{N+1}^{(1)}$.

It should be noted that the B.I.E. matrix $[T^{(2)} - U^{(1)}]$ is independent of time and is therefore set up once and for all at the start of the program. The LU decomposition of the matrix was found by calling a NAG library routine which uses Gaussian elimination with partial pivoting.

5.11 Results

The method described in the previous sections of this chapter was used to obtain results for the beach $G(x) = \cos \pi x$, $0 \leqslant x \leqslant 1$.

For a fixed mesh size h ($\equiv 1/N$, where N is the number of elements on each arc) it is first necessary to establish a stability criterion for the explicit time-stepping algorithm. A criterion of the form

$$\Delta t \leqslant Ch^p$$

was assumed, and it was found experimentally that $p \sim 1$. This agrees with the theoretical result given by Aitchison, Elliott and Ockendon [1983] although their result is for linear finite elements in the domain and we have used quadratic elements on the boundary. Having found a stability criterion it is then necessary to show the convergence of the numerical scheme as the mesh is refined. It was found that 4 elements per side was sufficient to obtain agreement to 2 decimal places. The results of our calculations for times $0 \leqslant t \leqslant 1$ are shown in figure 5.4(a) and these agree closely with those presented by Aitchison, Elliott and Ockendon. Figure 5.4(b) indicates the result of taking a time step which does not satisfy the stability criterion.

5.12 Conclusion

We have presented an application of the boundary integral equation method to a free boundary problem, and our results agree closely with those obtained by Aitchison, Elliott and Ockendon using the

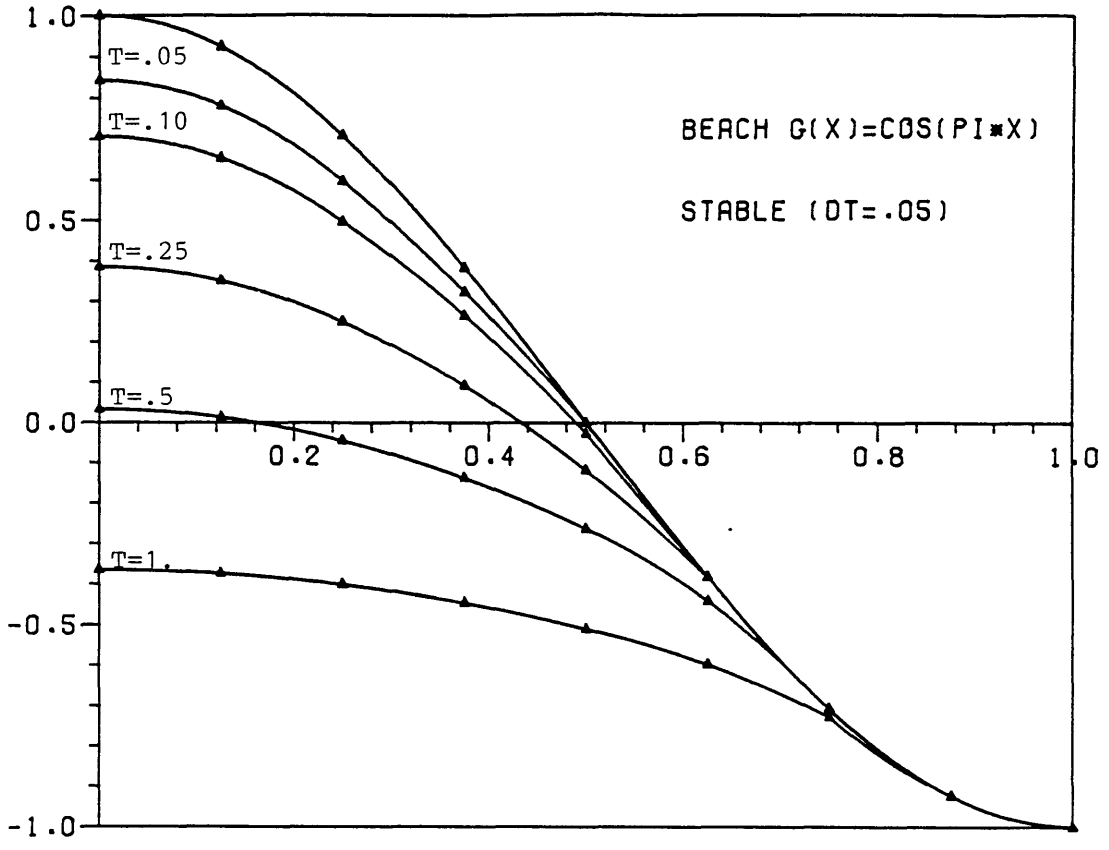


Fig. 5.4(a). F(x,t) when G(x) = cos πx, $0 \leqslant t \leqslant 1$.

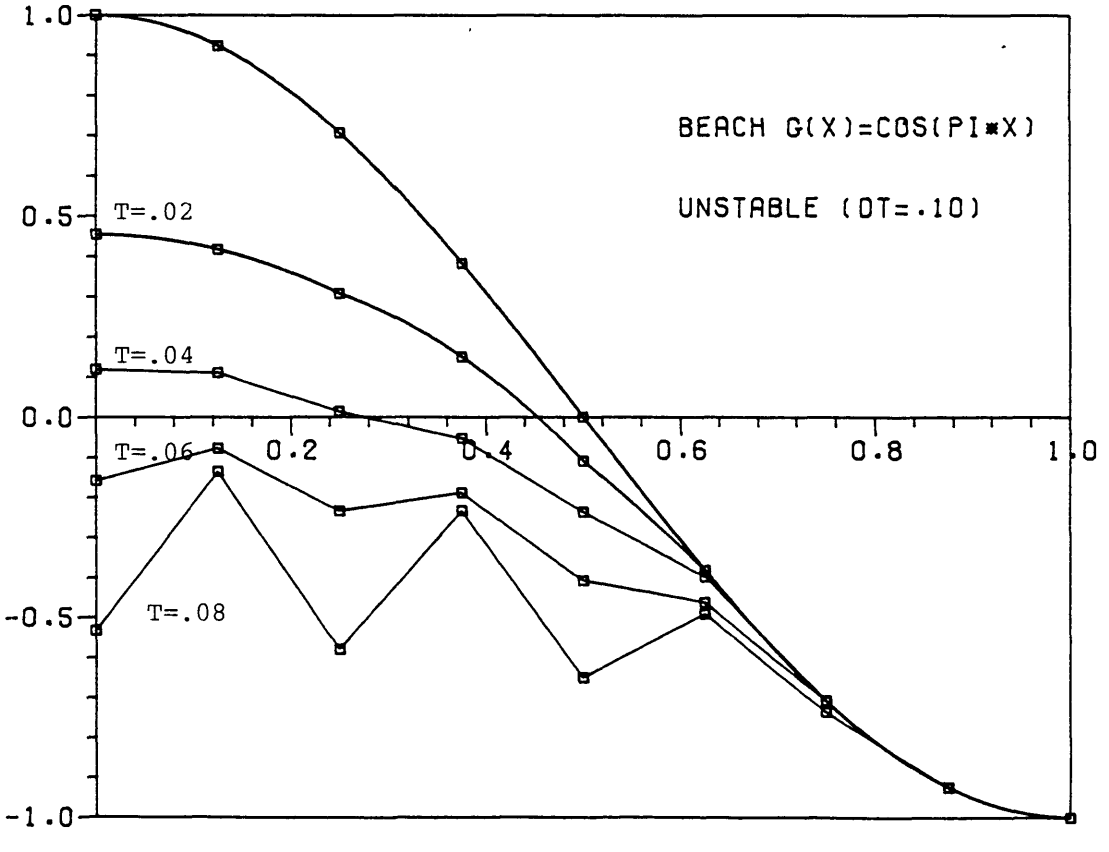


Fig. 5.4(b). F(x,t) when G(x) = cos πx
and stability criterion is not satisfied.

finite element method. No attempt has been made to analyse theoretically the stability or convergence of our method, but we have observed that the stability criterion given in the paper by Aitchison, Elliott and Ockendon applies.

We have not been able to make a detailed comparison of the computational effort of the two methods, but we believe that the usual advantages of the boundary integral equation method are relevant, for example:

(i) only the boundary of the region needs to be discretized, thus reducing the number of unknowns for a given mesh size;

(ii) the dimension of the problem is reduced by one, yielding 1-D integrals as opposed to 2-D integrals with the finite element method.

Appendix A.5: Derivation of Green's 3rd Identity

Let Ω denote a bounded open region in $\mathbb{R}^2$, with boundary $\partial\Omega$ and let u and v be continuous functions with continuous 1st and 2nd derivatives inside and on $\partial\Omega$. Further, suppose that u and v are harmonic in $\bar{\Omega}$. Then

$$\int_{\Omega} \nabla.(u\nabla v)d\Omega = \int_{\Omega} \{\nabla u.\nabla v + u\nabla^2 v\}\, d\Omega$$

$$= \int_{\partial\Omega} u \frac{\partial v}{\partial n}\, dS \quad \text{by the Gauss divergence theorem.}$$

Interchanging u and v,

$$\int_{\Omega} \{\nabla u.\nabla v + v\nabla^2 u\}\, d\Omega = \int_{\partial\Omega} v \frac{\partial u}{\partial n}\, dS$$

and hence

$$\int_{\partial\Omega} \left(u \frac{\partial v}{\partial n} - v \frac{\partial u}{\partial n}\right) dS = 0.$$

REFERENCES

Aitchison, J.M., Elliott, C.M., Ockendon, J.R.:
Percolation in gently sloping beaches. IMA Journal of Applied Mathematics, 30, pp. 269-287, 1983

Armstrong, A.G.A.M., Collie, C.J., Diserens, N.J., Newman, M.J., Simkin, J., Trowbridge, C.W.:
New developments in the magnet design computer program GFUN. Rutherford Laboratory, RL-75-066, 1975.

Armstrong, A.G.A.M., Collie, C.J., Simkin, J., Trowbridge, C.W.:
The solution of 3D magnetostatic problems using scalar potentials. Proceedings of COMPUMAG conference, Grenoble, 1978. (Also Rutherford Laboratory, RL-78-088, 1978).

Armstrong, A.G.A.M., Simkin, J., Trowbridge, C.W.:
The Galerkin method of weighted residuals applied to the restricted magnetostatic scalar-potential boundary-integral equation in three dimensions. (COMPUMAG-Genoa) IEEE Trans. MAG-19, No. 6, pp. 2329-2332, 1983.

Arsenin, V.Ya.: Basic equations and special functions of mathematical physics. Iliffe Books Ltd., 1968.

Collie, C.J.: Magnetic fields and potentials of linearly varying current or magnetization in a plane-bounded region. Proceedings of COMPUMAG conference, Oxford, 1976. (Also Rutherford Laboratory, RL-76-037).

Dwight, H.B.: Tables of integrals and other mathematical data. Macmillan, 1961.

Elliott, C.M. and Ockendon, J.R.: Weak and variational methods for moving boundary problems. Pitman, 1982.

Forsythe, G.E. and Moler, C.B.: Computer solution of linear algebraic systems. Prentice-Hall, 1967.

Garrett, M.W.: An elliptic integral computer package for magnetic fields, forces, and mutual inductances of axisymmetric systems, and a versatile line-tracing routine. Oak Ridge National Laboratory Report, ORNL-3575, 1965.

Graffi, D.: Nonlinear partial differential equations in physical problems. Pitman, 1980.

Hastings, C.: Approximations for digital computers. Princeton University Press, 1955.

Hockney, R.W. and Jesshope, C.R.: Parallel computers. Adam Hilger Ltd., 1981.

Hsiao, G.C., Kopp, P., Wendland, W.L.: A Galerkin collocation method for some integral equations of the first kind. Computing, 25, pp. 89-130, 1980.

Jordan, T.L.: A guide to parallel computation and some Cray-1 experiences. In Parallel Computations, Ed. Garry Rodrigue, Academic Press, 1982.

Kellogg, O.D.: Foundations of potential theory. Dover, 1953.

Kershaw, D.: Solution of single tridiagonal linear systems and vectorization of the ICCG algorithm on the Cray-1. In Parallel Computations, Ed. Garry Rodrigue, Academic Press, 1982.

Powell, M.J.D.: A hybrid method for non-linear algebraic equations. In: Numerical Methods for Non-linear Algebraic Equations. Ed. P.Rabinowitz, Gordon and Breach, 1970.

Pugh, E.M., and Pugh, E.W. Principles of Electricity and Magnetism. Addison-Wesley, 1970.

Reitz, J.R. and Milford, F.J.: Foundations of Electromagnetic Theory. Addison-Wesley, 1967.

Silvester, P.P. and Ferrari, R.L.: Finite Elements for Electrical Engineers. C.U.P., 1983.

Simkin, J.: A comparison of integral and differential equation solutions for field problems. (COMPUMAG-Chicago) IEEE Trans. MAG-18, No. 2, pp. 401-405, 1982. (Also Rutherford Laboratory, RL-81-076, 1981).

Simkin, J., Trowbridge, C.W.: Magnetostatic fields computed using an integral equation derived from Green's theorems. Proceedings of COMPUMAG conference, Oxford, 1976. (Also Rutherford Laboratory, RL-76-041, 1976).

Simkin, J., Trowbridge, C.W.: On the use of the total scalar potential in the numerical solution of field problems in electromagnetics. IJNME, 14, pp. 423-440, 1979.

Simkin, J., Trowbridge, C.W.: Three-dimensional nonlinear electromagnetic field computations, using scalar potentials. IEE PROC., Vol. 127, Pt. B, No. 6, pp. 368-374, 1980.

Stewart, G.W.: Introduction to Matrix Computations. Academic Press, 1973.

Stratton, J.A.: Electromagnetic Theory. McGraw-Hill, 1941.

Stroud, A.H. and Secrest, D.: Gaussian quadrature formulae. Prentice Hall, 1966.

Trowbridge, C.W.: Applications of integral equation methods for the numerical solution of magnetostatic and eddy current problems. Rutherford Laboratory, RL-76-071, 1976.

Vladimirov, V.S.: Equations of Mathematical Physics. Marcel Dekker, Inc., 1971.

Xanthis, L.S., Bernal, M.J.M., Atkinson, C.: The treatment of singularities in the calculation of stress intensity factors using the boundary integral equation method. Comp. Methods in Appl. Mech. & Eng., 26, pp. 285-304 (1981).

Zienkiewicz, O.C.: The finite element method in engineering science. McGraw Hill, 1971.

Zienkiewicz, O.C., Kelly, D.W., Bettess, P.: The coupling of the finite element method and boundary solution procedures. IJNME, 11, pp. 355-375, 1977.